NASA CR-72906
PWA-4145

FINAL REPORT

THE EFFECT OF DESIGN AND OPERATING FACTORS ON LIFE AND PERFORMANCE OF MATRIX FUEL CELLS

by

K. O. Wood and W. F. Bell

PRATT & WHITNEY AIRCRAFT
South Windsor Engineering Facility
Box 109, Governors Highway
South Windsor, Connecticut 06074

prepared for

NATIONAL AERONAUTICS AND SPACE ADMINISTRATION

February 28, 1971

CONTRACT NAS 3-13229

NASA Lewis Research Center
Cleveland, Ohio
Dr. Robert E. Post, Project Manager
Direct Energy Conversion Division

NOTICE

This report was prepared as an account of Government-sponsored work. Neither the United States, nor the National Aeronautics and Space Administration (NASA), nor any person acting on behalf of NASA:

A) Makes any warranty or representation, expressed or implied, with respect to the accuracy, completeness, or usefulness of the information contained in this report, or that the use of any information, apparatus, method, or process disclosed in this report may not infringe privately-owned rights; or

B) Assumes any liabilities with respect to the use of, or for damages resulting from the use of, any information, apparatus, method or process disclosed in this report.

As used above, "person acting on behalf of NASA" includes any employee or contractor of NASA, or employee of such contractor, to the extent that such employee or contractor of NASA or employee of such contractor prepares, disseminates, or provides access to any information pursuant to his employment or contract with NASA, or his employment with such contractor.

NASA CR- 72906
PWA-4145

THE EFFECT OF DESIGN AND OPERATING FACTORS ON LIFE AND PERFORMANCE OF MATRIX FUEL CELLS

by

K. O. Wood and W. F. Bell

PRATT & WHITNEY AIRCRAFT

prepared for

NATIONAL AERONAUTICS AND SPACE ADMINISTRATION

NASA Lewis Research Center
Contract NAS 3-13229
Dr. Robert E. Post, Project Manager

FOREWORD

The work described herein was done at the South Windsor Engineering Facility, Pratt & Whitney Aircraft, from July 1969 to December 1970 under NASA Contract NAS3-13229. This work was initially performed under the management of Dr. Lawrence Thaller and was completed with Dr. Robert E. Post, Direct Energy Conversion Division, NASA-Lewis Research Center, as Project Manager.

TABLE OF CONTENTS

ILLUSTRATIONS

LIST OF ILLUSTRATIONS (Cont'd)

LIST OF ILLUSTRATIONS (Cont'd)

LIST OF ILLUSTRATIONS (Cont'd)

LIST OF TABLES

ABSTRACT

The effect of design and operating factors on the performance and life of alkaline electrolyte, hydrogen/oxygen, matrix fuel cells was investigated. Full size single cells were operated on a simulated space shuttle load profile and were refurbished by flushing with fresh electrolyte to extend their useful life. This program provides a data base for the design of fuel cells with a one year operating life. Cell life of over 6400 hours at a potential of 0.945 volts with no net voltage decay was demonstrated while operating at a temperature of 176°F (80°C) and a current density of 75 amps/ft^2 (80.7 MA/CM^2).

I. SUMMARY

Ten powerplant size cells were tested on a simulated space shuttle load profile including shutdown and storage on nitrogen for one day each week. A total of 18,250 hours of operation were accumulated on these cells.

One cell has accumulated over 6400 load hours and 38 startups with an electrolyte change at 5000 hours. A high power density cell run in conjunction with this program has accumulated over 6000 hours and 29 startups without changing the electrolyte. Both of these long life cells are operating at an average current density of 75 amps/ft^2 (80.7 MA/CM^2) and a maximum oxygen electrode temperature of 176°F (80°C). These cells are still on test with no net voltage decay to date.

The primary cause of performance degradation is electrolyte volume loss. Carbonation of the electrolyte is the major cause of volume loss. Cell electrolyte carbonation data and materials corrosion tests have shown that the glass fiber and epoxy cell frame contributes significantly to electrolyte carbonation. Low operating temperature reduces frame corrosion and increases cell life. A change to a more inert cell frame material should also improve cell life.

An important factor investigated in this program is the effect of reactant contaminants on cell life. Both cells discussed above use oxygen with a hydrocarbon content of 6 to 10 ppm. This is the contamination level expected from propulsion grade reactants. In addition, the first cell discussed above has been operated with 4 ppm of carbon dioxide added to the oxygen supply which is well above the level expected in the spacecraft reactants. Both of these impurities can of course be scrubbed from the supply gas if longer cell life is required.

Each cell test included refurbishment of the cell by flushing it with fresh electrolyte. This procedure was similar to that which would be used for refurbishing the cell stack in a fuel cell system. These refurbishments were generally successful in restoring performance and extending operating life by as much as a factor of two.

A regression analysis performed on the data obtained in the program indicates that low current density is a major factor in achieving long life with low voltage decay. This is because the voltage loss due to a given amount of cell degradation is proportional to current density.

Potassium titanate matrix material was used in five of the cells tested. These cells experienced rapid voltage decay due to anode poisoning. It is suspected that a reaction occurred between the PKT and the silver plating used in the electrodes. A high power density cell using gold plating on the electrodes in place of the conventional silver plating has not experienced rapid decay indicating that the use of gold eliminates the anode poisoning problem.

II. INTRODUCTION

The NASA Space Shuttlecraft requires an electrical power system capable of multiple mission operation with high reliability and high performance. This single cell test program was to provide a data base for the design of long life cells for the space shuttle application. The tests were run using a simulated shuttle load profile so that the data generated was relevant to the shuttle application. The cell used is the 0.5 square foot (464.65 CM^2) hydrogen-oxygen matrix cell used in the PC8B-3 and PC8B-4 powerplants for space applications. This cell is similar in principle, although much improved in detail, to the matrix cell in the PC8A-2 powerplant operated at NASA LeRC. The basic characteristics of the PC8B cell have already been established in over one million hours of testing on approximately 3500 cells. A fractional factorial test program was designed to allow objective evaluation of the effect of the following factors on cell life and electrochemical performance with a reasonable program duration:

- Maximum oxygen electrode temperature at average load
- Carbon dioxide level in oxygen
- Matrix thickness
- Average current density
- Matrix material

The cell tests were run on automated test stands. Control and alarm consoles continuously monitor operating conditions and protect the cells against stand or cell malfunction. Data was recorded every hour by a computerized Automatic Data Acquisition and Recording System.

Previous experience has shown that cells which have decayed because of electrolyte degradation can have their performance restored by flushing with fresh electrolyte. This refurbishment procedure was successfully performed on a PC8A-2 cell stack at the Lewis Research Center and on single cells at Pratt & Whitney Aircraft. This refurbishment procedure was included as part of each cell test in this program to evaluate its effect on cell life and performance.

III CELLS TESTED

A. CELL DESIGN

Cell Mechanical Design Features and Materials

A schematic of the Pratt & Whitney Aircraft matrix cell is shown in Figure 1, and a picture of the major elements in Figure 2. Each cell consists of one unitized electrode assembly and two coolant plates (housings) to confine and distribute reactant gases and coolant. The cell features (1) a unitized electrode assembly which eliminates interelectrode seals and minimizes the possibility of error during stack assembly and (2) a cell housing with an integrally molded seal to eliminate soldered joints between coolant plates and to prevent seal extrusion when the cell stack is compressed.

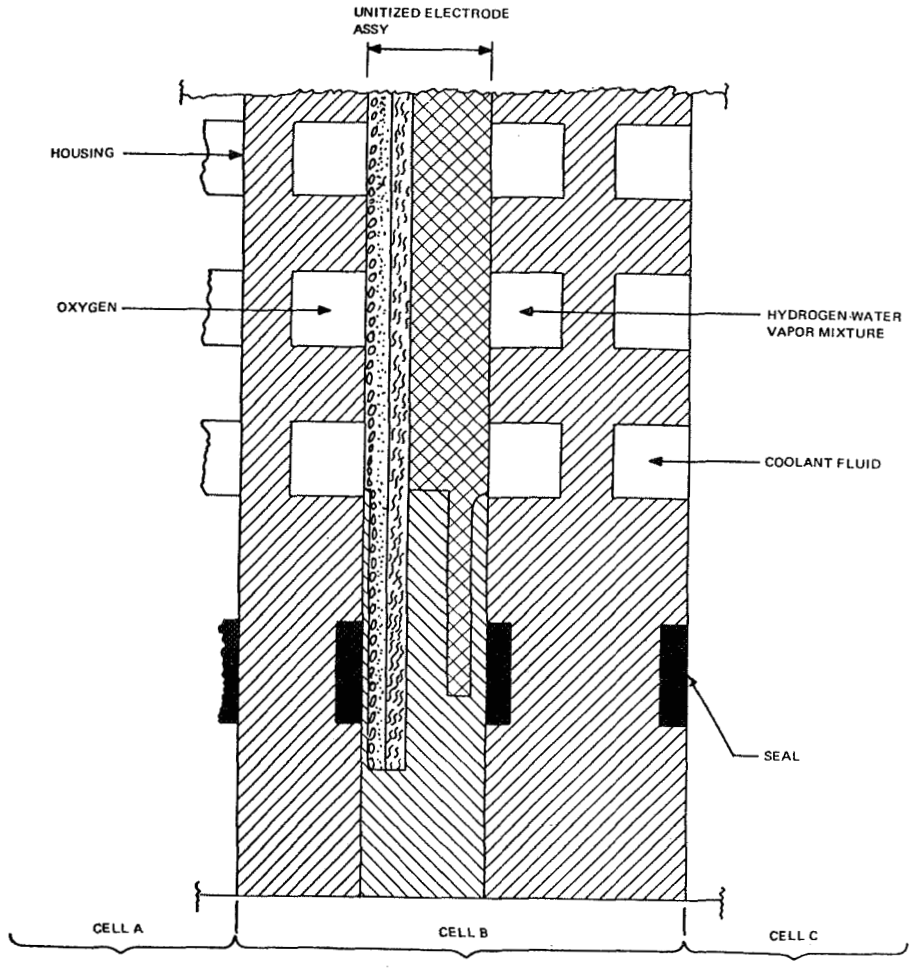

Figure 1 Pratt & Whitney Aircraft Matrix Cell Assembly

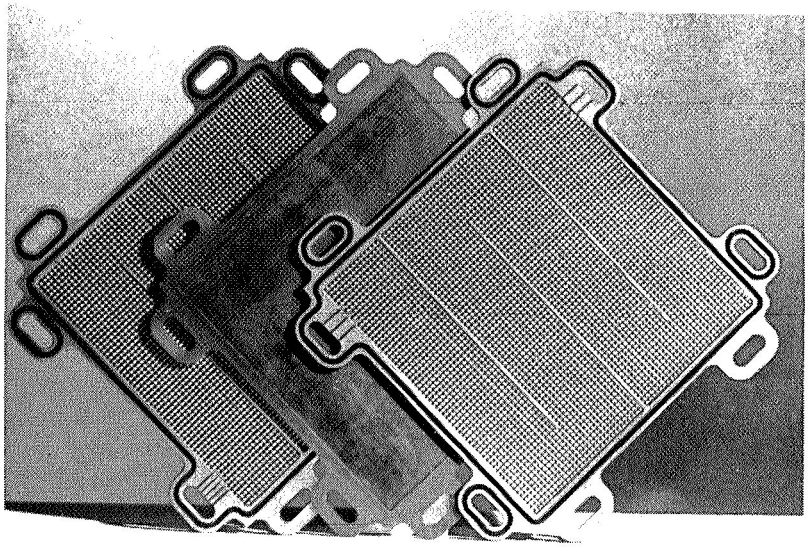

Figure 2 Pratt & Whitney Aircraft Matrix Cell Parts

The unitized electrode assembly, Figure 3, is a molded assembly consisting of the anode, cathode, porous matrix, and a non-conducting support frame. Electrolyte is contained in the matrix of the unitized electrode assembly.

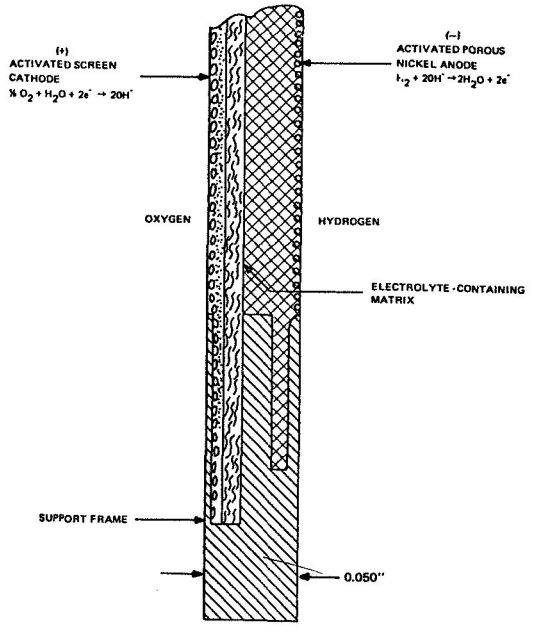

Figure 3 Unitized Electrode Assembly

The support frame serves as an integral part of the cell stack internal manifolding system, provides positive electrical insulation of the electrodes, eliminates edge seals and holds the electrodes rigidly in place. This construction results in a minimum of variation in performance from cell-to-cell.

The cell housing provides for the distribution and containment of both reactant gases and coolant fluid, supports the unitized electrode assembly, ensures stack rigidity and provides the path for conducting current from cell-to-cell. It consists of two nickel-plated magnesium plates, the oxygen plate and the hydrogen plate. They are specially contoured for distribution and sealing of reactant gas and coolant fluids. Magnesium was chosen for its low density, good chemical milling characteristics, and good electrical and thermal conductivity. A special nickel-plating process provides corrosion resistance. The plates are manufactured by sequential chemical milling, machining, and plating operations. Rubber seals are molded in place as the final operation.

The oxygen plate supports the screen cathode of the unitized electrode assembly with the multiple pin and rib pattern illustrated in Figure 4.

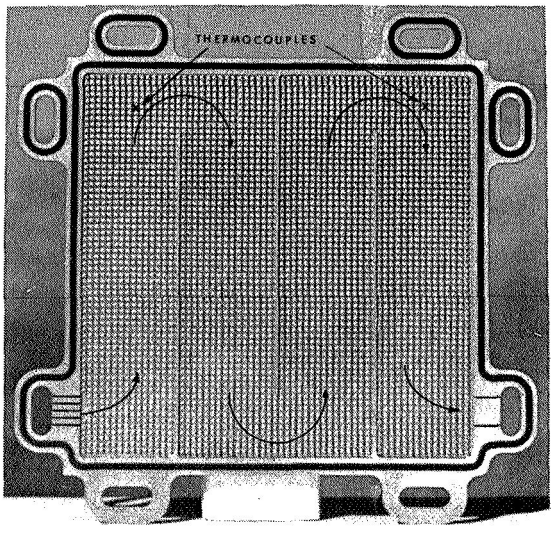

Figure 4 Oxygen Plate

The ribs provide a positive flow path for purging of residual contaminants in the reactants. The metering slots at the cell inlet and exit are sized to control the distribution of reactant gases from cell-to-cell. The flow path has been selected to bring the cool, dry oxygen reactant gas in a counter flow pattern with the hydrogen and liquid coolant to minimize temperature and electrolyte concentration variations. The pins and ribs also provide a low resistance path for electrical current from the cathode to the adjacent cell.

The opposite side of the oxygen plate is a flush surface which serves as one side of the intercell coolant cavity.

The hydrogen plate, Figure 5, supports the sintered hydrogen electrode of the unitized electrode assembly with a multiple pin and rib pattern similar to that on the oxygen electrode. A pattern similar to the oxygen electrode provides cell rigidity and a rigid cell assembly. The multiple pin pattern provides good contact with the electrode sinter for low internal resistance.

The rib pattern provides for circulation of the hydrogen-water vapor mixture in an actual powerplant. The metering ports at the inlet and exit of the gas housing are designed to provide uniform flow distribution from cell-to-cell within the stack assembly with minimum pressure drop.

The opposite side of the hydrogen cooling plate is contoured with the same rib-pin pattern to provide coolant passages for control of stack temperature. The inlet ports of the coolant cavity reduce the coolant pressure to a level slightly below the cell reactant pressures to obtain good electrical contact between adjacent cell housings.

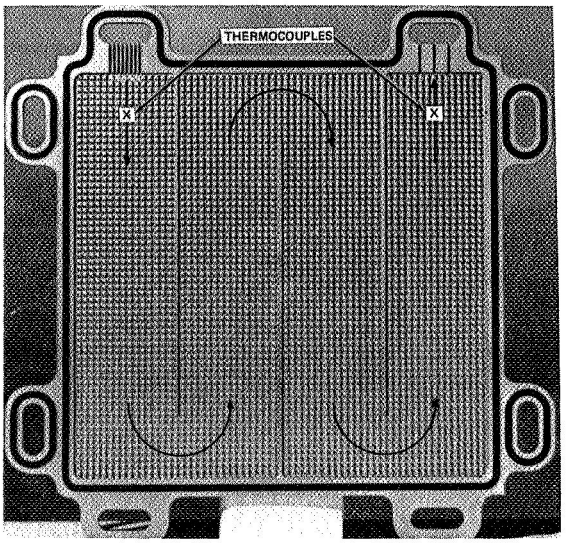

Figure 5 Hydrogen Plate

The flow path for the wet hydrogen parallels the coolant fluid flow path to match the lower temperature at the inlet with the dryer hydrogen stream at the inlet, and the higher temperature at the exit with the wetter hydrogen stream at the exit. This approach provides for uniform evaporation of water from the entire surface of the hydrogen electrode and reduces the range of electrolyte concentration which a cell must tolerate over its range of operating conditions.

Cell Electrochemical Design Features and Materials

The cells tested were of the standard powerplant design described below with the only modification being the use of a different matrix material and thickness in certain tests.

An important factor in obtaining good cell endurance is wide "tolerance" to electrolyte volume change, i.e., cell performance should not vary significantly with changes of the volume of electrolyte in the cell. The Pratt & Whitney Aircraft matrix cell achieves this objective by use of a sintered hydrogen electrode which acts as a reservoir to accommodate electrolyte change, a catalyzed screen cathode and a thin asbestos matrix to minimize the volume of electrolyte in the cell.

The matrix is made of 0.010" (0.254 MM) thick fuel cell grade asbestos. This matrix is used in all PC8A, PC8B, PC9, and PC10 powerplants. This use of a thin matrix minimizes the inventory of electrolyte in the cell when the cell operates over a range of loads and the cell concentration changes. The volume variation of the electrolyte is also minimized. Consequently, there is a minimum movement of the electrolyte-gas interface within the hydrogen electrode. This in turn minimizes the variation of cell performance with concentration variation. An added benefit of the thin matrix is lower cell internal resistance. Because the Pratt & Whitney Aircraft matrix cell powerplant uses a "coupled" regulator to maintain a controlled pressure differential across each cell under all operating conditions, the matrix never experiences more than approximately a 2 psi (0.1406 Kg/CM^2) pressure differential. The pressure differential capability of the 0.010 inch (0.254 MM) thick asbestos matrix is over 20 psi (1.406 Kg/CM^2).

The oxygen electrode, Figure 6, consists of a silver-plated, fine-mesh nickel screen embedded in a porous Teflon structure activated with a platinum-palladium catalyst. The catalyst loading is 10 mg/cm^2. The catalyst agglomerates provide a reaction site for the reduction of oxygen at the gas/electrolyte interface. The Teflon provides non-wetting pores for the transport of oxygen gas to the reaction sites. The screen serves as a structural support, a current collector, and provides a low resistance path for electron flow from the cell housing to the reaction sites. The same oxygen electrode structure, the catalyst, and catalyst loading are used in the PC8A, PC8B, PC9, and PC10 powerplants.

The hydrogen electrode, Figure 7, is a platinum-palladium activated, porous nickel sinter with a supporting nickel screen. The noble metal loading is 20 mg/cm^2. This electrode is used in the PC8A, PC8B, PC9, and PC10 powerplants. The sinter is a 70-75 percent porous, 0.030 inches (0.762MM) thick structure with uniform pore size serving as a support for the catalyst. The catalyst provides a reaction site for the oxidation of hydrogen. The open pores in the electrode structure provide a path for the transport of hydrogen gas to these reaction sites. The pores filled with electrolyte permit the transport of hydroxyl ions to the liquid-gas interface. The nickel structure and support screen provide a low resistance path for electron flow to the cell housing.

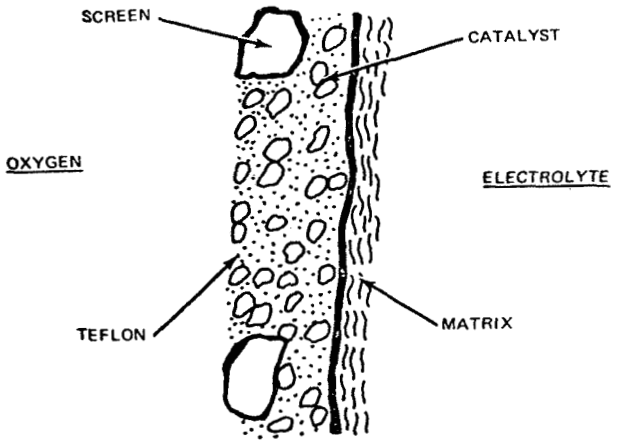

Figure 6 Oxygen Electrode Schematic

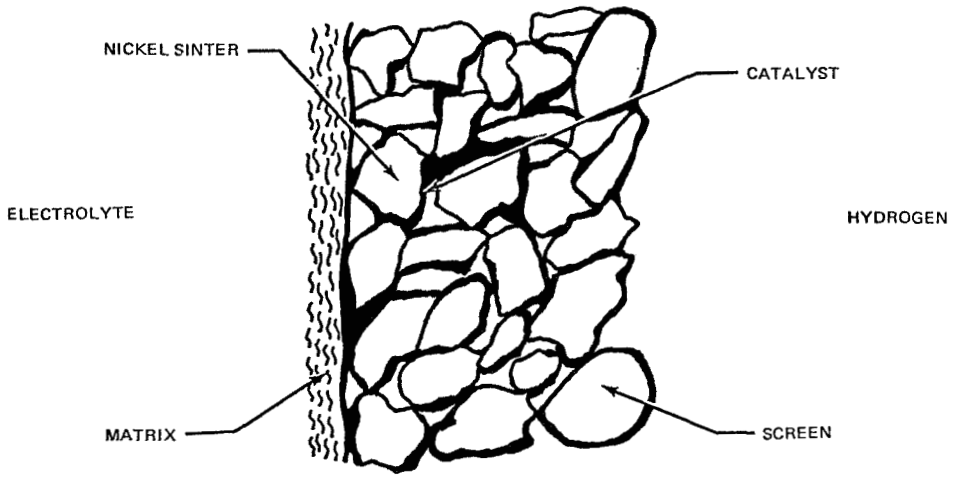

Figure 7 Hydrogen Electrode Schematic

The gas-electrolyte interface location in the hydrogen electrode is established by the fill conditions and is affected by the cell operating conditions. As noted earlier the hydrogen electrode structure is used as an accumulator, or reservoir, to accommodate changes in electrolyte volume imposed by load changes. For example, low load conditions result in a reduction in average cell temperature and a corresponding increase in water in the electrolyte; the increased electrolyte volume is contained in the hydrogen electrode structure. Within limits this electrolyte volume change causes slight variation in the cell voltage.

Instrumentation

Instrumentation is provided on each cell for determining:

- Inlet and exit hydrogen gas stream temperature
- Oxygen gas inlet temperature
- Hydrogen and oxygen electrode temperatures
- Cell voltage

Gas stream temperatures are measured by immersion type Chromel-Alumel thermocouples placed directly in the manifold ports.

Cell voltage is taken off pins soldered directly to the cell coolant plates. The coolant plates are silver plated and are designed with a multiple pin/bar arrangement. This results in high electrode to coolant plate contact area with negligible voltage losses.

Electrode temperatures are calculated from measured coolant plate temperature. Coolant plate temperature is measured at 2 locations on each coolant plate, Figures 4 and 5. At the current density levels in the program, coolant plate temperature provides a satisfactory basis for estimating electrode temperature.

Figure 8 shows the measured temperature difference between the oxygen electrode surface and oxygen coolant plate of the PC8B matrix cell as a function of current density. At current densities less than 200 amps per sq. ft. (215.2 MA/CM^2), the electrode temperature is within ½°C of the coolant plate, so that with the aid of a correlating curve such as that of Figure 8, electrode temperature can be precisely determined.

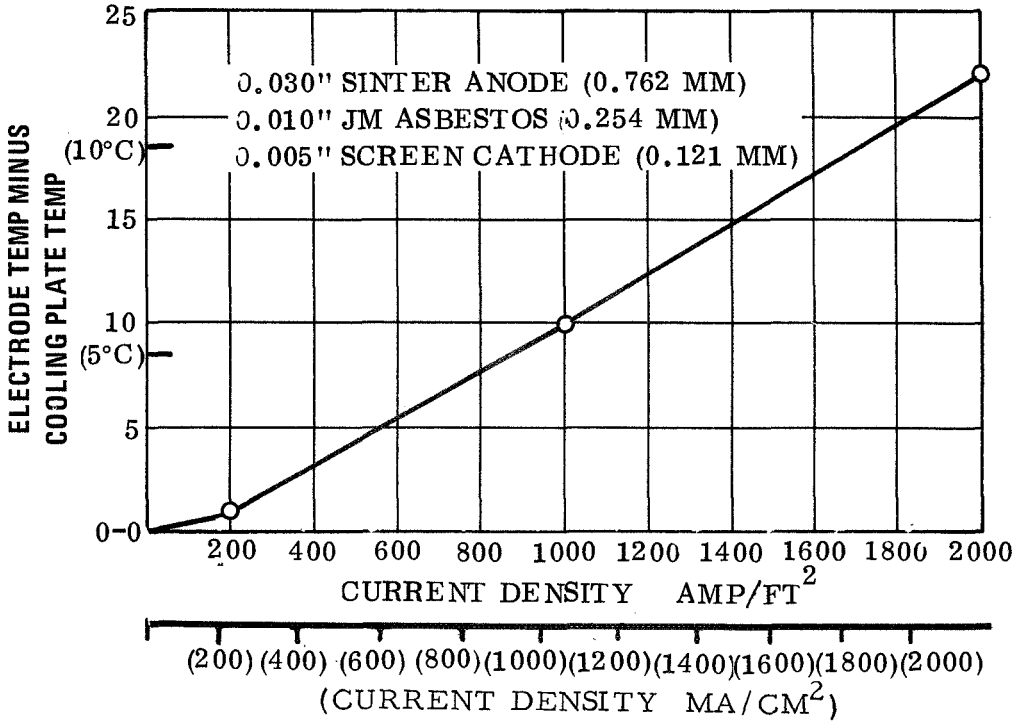

Figure 8 Correlation Between Oxygen Electrode Surface Temperature And Oxygen Coolant Plate Temperature

The location of the maximum oxygen electrode temperature was determined using a special rig instrumented with thermocouples in six locations adjacent to each coolant plate. Tests were run at various current densities, coolant flow rates, and hydrogen flow rates. The maximum temperature occurred in the last 25% of the "W" flow coolant path. This leg of the coolant flow path is near the oxygen inlet. A thermocouple was placed near the end of the coolant flow path in each cell tested to record the maximum oxygen electrode temperature.

B. FACTORS AFFECTING CELL PERFORMANCE AND ENDURANCE

The purpose of this program was to obtain data on the effect of several factors on the electrochemical performance and life of matrix-type alkaline fuel cells. The factors investigated include:

- Maximum oxygen electrode temperature at average load
- Carbon dioxide level in oxygen
- Matrix thickness
- Average current density
- Matrix material

These factors are discussed individually in the following paragraphs. Two levels of each factor were tested. The "low" values were selected based on past experience which indicated they have the best chance of producing a cell with one year life capability. The "high" values offer potential advantages of greater performance stability (matrix material), higher voltage (maximum oxygen electrode temperature), lower stack weight (current density), lower cost (carbon dioxide level in oxygen), and more rugged construction (matrix thickness).

Factor Levels

The levels assigned to the factors evaluated are given below:

		Low Level	High Level
a.	Maximum Oxygen Electrode Temperature at Average Load	176°F (80°C)	212°F (100°C)
b.	Carbon Dioxide Level in Oxygen	Less than ½ parts per million	4 parts per million
c.	Matrix Thickness	0.010 inch (0.254MM)	0.030 inch (0.762MM)
d.	Average Current Density	75 amps per square foot (80.7 MA/CM^2)	200 amps per square foot (215.2 MA/CM^2)
e.	Matrix Material	Asbestos	PKT

Maximum Oxygen Electrode Temperature

Increased cell operating temperatures produce direct cell performance improvements as indicated in Figure 9. In addition to the performance improvement, elevated operating temperatures allow higher heat rejection temperatures which reduce the required radiator area and permit operation in higher temperature environments. The disadvantage of higher cell operating temperature is that cell degradation may be accelerated.

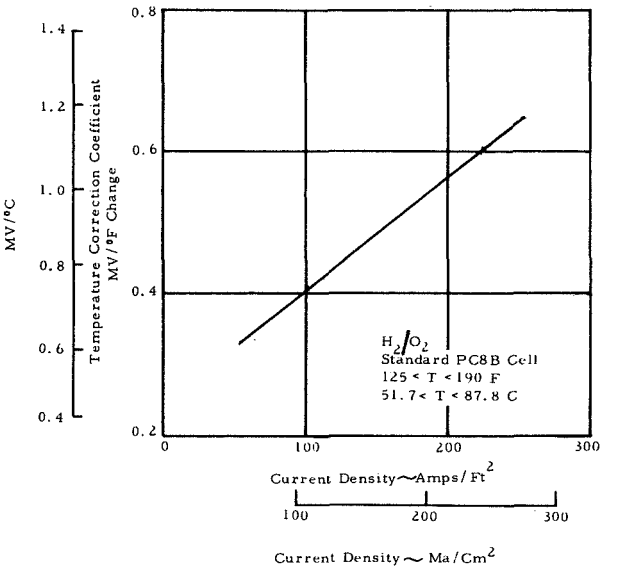

Figure 9 Typical Effect of Temperature on Cell Performance

CO_2 Level in Reactants

The CO_2 in the reactants entering the cell is immediately converted into carbonate ions, removing hydroxyl ions from the electrolyte in the process. As hydroxyl ions are depleted, concentration polarization increases, the ability of the cell to conduct is reduced, and the performance goes down.

In addition to the concentration polarization loss, electrolyte volume is reduced because of the increased water vapor pressure of the electrolyte as carbonation occurs. The volume reduction as a function of the degree of carbonation is shown in Figure 10. Typical performance change with volume is shown in Figure 11. These figures explain why it is commonly observed that peak performance "shifts" to higher reactant dewpoint or more dilute operation, or that some cell performance may be recovered by wetting the cell.

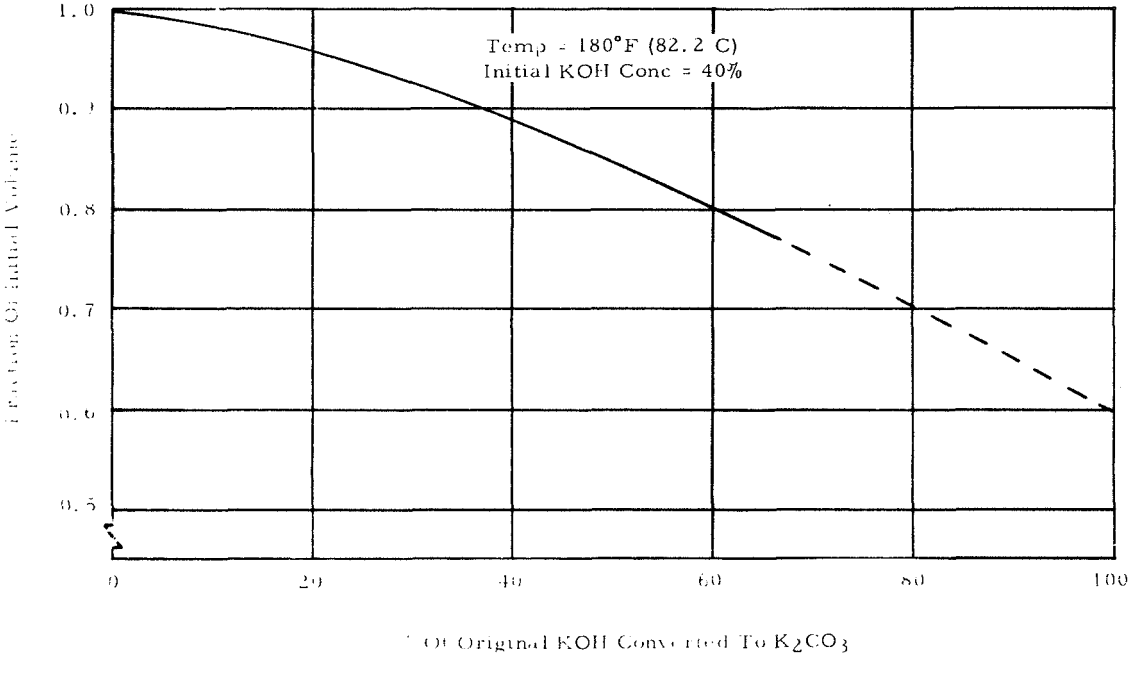

Figure 10 Volume Loss of Compact Fuel Cells Due to K_2CO_3 Formation

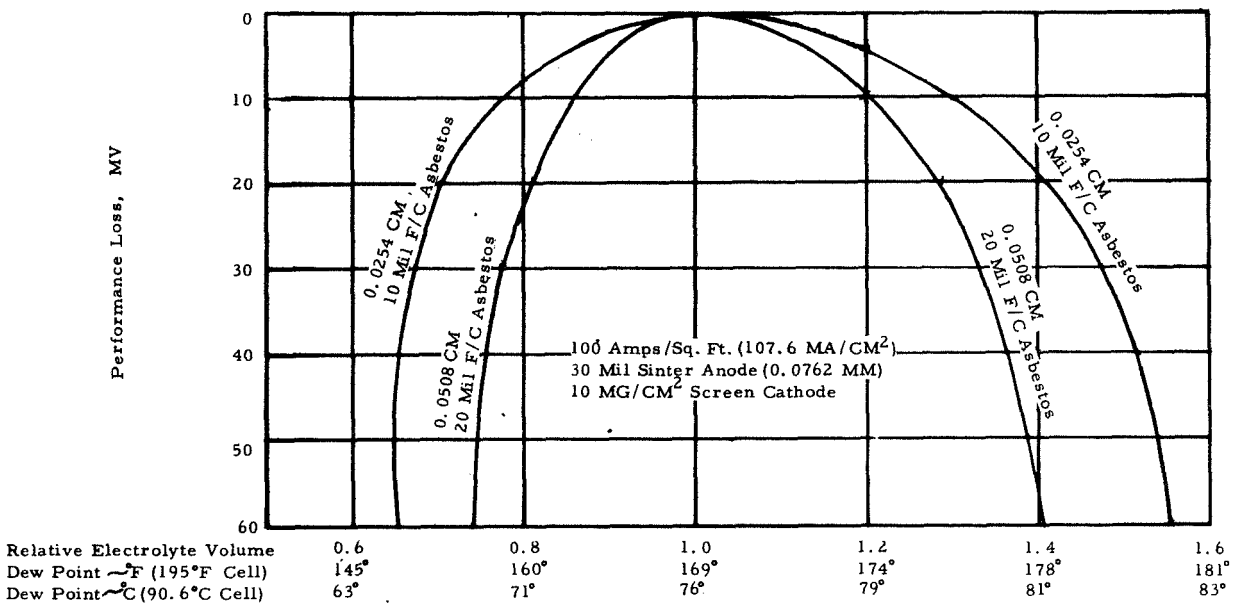

Figure 11 Performance Change Due to Electrolyte Volume Change

Matrix Thickness

The matrix thickness affects fuel cell initial performance, tolerance of performance to electrolyte changes, and cell bubble pressure. Cell performance is affected because of the dependency of cell internal resistance on matrix thickness. As the matrix thickness or the current level varies, the voltage loss varies proportionally. An increase in matrix thickness also results in less tolerance to a given change in electrolyte concentration because of the greater volume change of electrolyte which must be accommodated within the porous electrode. A typical electrolyte volume calculation appears on page 64. The effect of volume change on the performance of a trapped electrolyte cell with 10 mil (0.0254CM) and 20 mil (0.0508CM) asbestos matrices is shown in Figure 11. For these two reasons, a thin matrix is desirable.

Counteracting these effects, for a given level of CO_2 in the reactants, the larger quantity of KOH in the thicker cell takes a longer time to reach the same percentage conversion to carbonate than the smaller amount in the thinner cell. Also, the bubble pressure increases with thickness as shown in Figure 12. Thus, a thicker matrix will improve the capability of the cell to withstand off-design fluctuations in reactant gas pressure. However the use of a coupled reactant regulator eliminates the need for the cell to withstand more than a very few psi differential pressure. On the basis of the above criteria, 10 mil (0.0254CM) and 30 mil (0.0762CM) matrix thicknesses were selected as values for endurance testing.

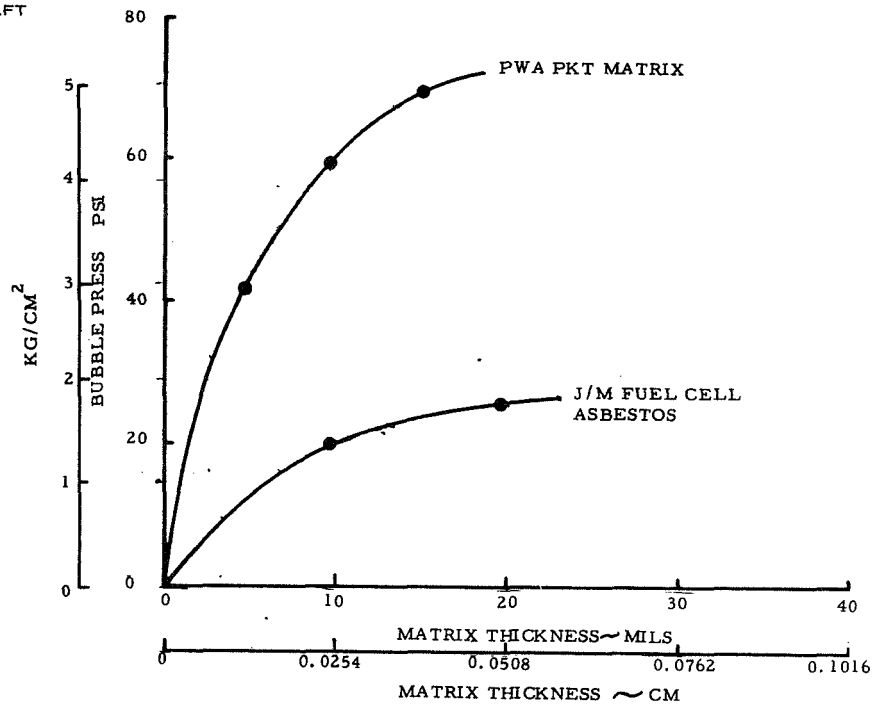

Figure 12 Effect of Matrix Thickness on Bubble Pressure

Average Current Density

The effect of current density on fuel cell voltage is well known from the typical performance curves, and can be explained by a combination of activation, ohmic, and diffusional polarizations. In addition average current density must be considered a significant factor in fuel cell endurance. The electrolyte carbonation due to contaminants in the reactants is proportional to the reactant consumption per unit cell area and is therefore dependent on current density. Also, the voltage loss due to a given amount of electrolyte carbonation is proportional to the current density.

The two levels evaluated in this investigation were selected based on system considerations. From the preliminary system study results 75 and 200 amp/ft^2 are suggested. A current density of 75 amps/ft^2 (80.7 MA/CM^2) was selected as a reasonable approximation to the average power point for a 5 KW (max) powerplant. A 200 amps/ft^2 (215.2 MA/CM^2) current density was selected as a reasonable approximation to the maximum load point (5 KW).

Matrix Material

Matrix materials must possess a variety of almost contradictory properties – high bubble pressure, low electrolytic resistance and chemical-mechanical stability. Changes in any of these properties affect performance and decay. The two matrix materials chosen for this investigation are (1) Johns Manville "Fuel Cell Grade" chrysotile asbestos, and (2) a blend of pigmentary potassium titanate (PKT) with 15 weight per cent asbestos binder.

Fuel cell grade asbestos was chosen because of the successful use of this material by numerous investigators.

Pratt & Whitney Aircraft has developed a pigmentary potassium titanate matrix with 15 weight percent asbestos binder material to facilitate fabrication. This matrix material has more chemical stability than fuel cell grade asbestos at higher electrolyte temperatures. Improvements in fabrication techniques have resulted in better uniformity and higher bubble pressure than asbestos. This matrix material has been used successfully in cell tests over 5000 hours at 160°F (71°C).

C. TEST SEQUENCE

The experimental program consisted of ten (10) tests. The tests were conducted in the sequence corresponding to the test number indicated in Table I. Test number 18 was moved up to tenth position in the planned sequence as shown. Cells were tested until the refurbishment criteria were met or until stopped by direction from the NASA Project Manager.

The letters in the table below refer to the particular "high" factors to be substituted for "low" factors as defined on page 11, Factor Levels. For example, Test 8 is designated "de" and, therefore, will operate with a PKT matrix at 200 amps/ft^2 (215.2 MA/CM^2).

TABLE I

TEST SEQUENCE

1.	cd	6.	be
2.	ad	7.	abcd
3.	ae	8.	de
4.	bc	9.	abce
5.	acde	18.	ac

IV. TEST APPARATUS

A. TEST STAND DESCRIPTION

Twelve single cell test positions are provided for cell testing. Each test position is designed to provide simple and reliable control of the fuel cell environments. The test stands are functionally very similar to the PC8B power system. Product water is removed from each cell by circulating hydrogen through the cell at a fixed flow rate and with an inlet dewpoint temperature selected to provide the desired electrolyte concentration. The selected dewpoint temperature is held constant throughout the test. Heat is removed from each cell by circulating liquid coolant through passages in the cell. Coolant flow rate is selected to achieve desired electrolyte concentration distribution. The coolant inlet temperature is controlled to maintain maximum oxygen electrode temperature at average load as specified. The maximum cell temperature and concentration distribution are permitted to change as the load varies in accordance with the specified load profile. The coolant flow rate is increased to maintain maximum oxygen electrode temperature at average load as the cell performance degrades with time.

A schematic of this test stand is shown in Figure 13. The hydrogen is supplied to the test facility with a purity of at least 99.95 percent. This gas is further purified using a heated palladium tube separator. The purified hydrogen is humidified at each test position with close dewpoint control. In order to simulate powerplant product water removal conditions, hydrogen utilization is kept low (recycle ratio is high). Ultra-pure hydrogen is required with this system. The hydrogen is not recirculated as it would be in a powerplant and the cell is exposed to much greater quantities of gas. Thus, even low levels of impurities can lead to high electrolyte contamination. The unconsumed hydrogen leaving the cell carries with it the water produced by the fuel cell reaction. Hydrogen flow and inlet saturator temperature remain constant throughout the tests.

The oxygen is supplied to the test facility with a purity of at least 99.99 percent. It is passed through a large scrubber to remove CO_2 but not the 6-10 ppm of hydrocarbons. The CO_2 level in the oxygen leaving this scrubber is monitored by a LIRA gas analyzer. Should the CO_2 level at any time exceed ½ ppm, the oxygen flow can be switched so that it flows through a second large CO_2 scrubber. Purified oxygen is ducted to all 12 test positions and fed without further treatment to the fuel cells. For tests which require the high CO_2 level in the oxygen supply, a special mixing valve furnished by NASA is used to introduce 4 ppm of CO_2 into the oxygen stream. This contaminated oxygen is ducted to the test positions by a separate supply system. The CO_2 level is monitored using the LIRA gas analyzer and the mixing valve is adjusted to provide a CO_2 level as close as practical to 4 ppm. Since all the oxygen flow is consumed at the cell, accumulated inerts must be removed periodically. This is accommplished by opening the downstream purge valve for two minutes every eight hours.

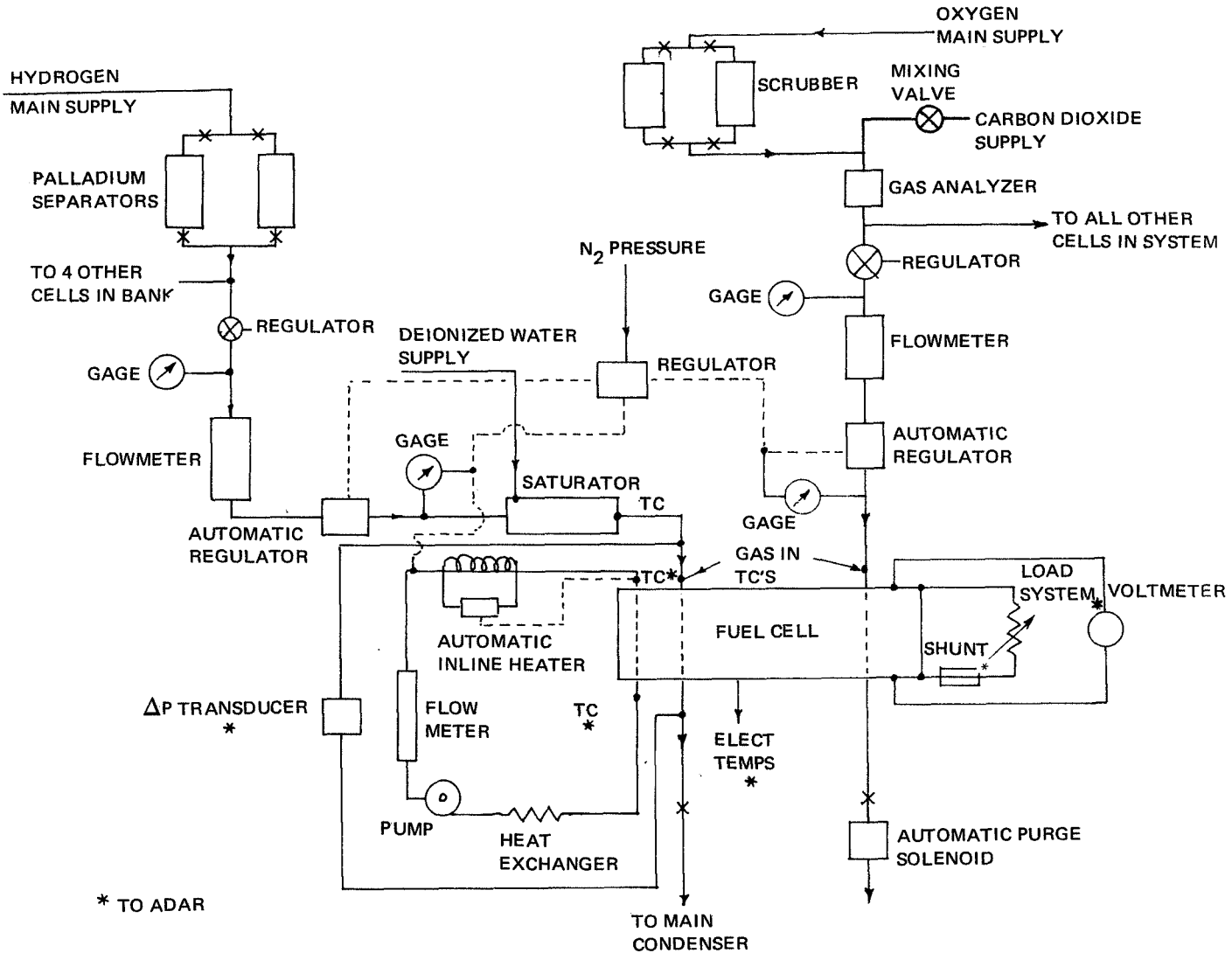

Figure 13 Test Stand Schematic

Reactant gas pressure is controlled by means of automatic regulators which are biased to the coolant pressure. This system ensures close pressure control while guarding against coolant overpressures. By referencing both the hydrogen and oxygen regulators to the coolant pressure the pressure differential across the cell is kept low. During startup and shutdown the cell is pressurized and depressurized by gradually changing the coolant pressure. The reactant regulators follow the coolant pressure maintaining a low pressure differential across the cell. Reactant flow is controlled with valves downstream of the fuel cell. Water removed from the cell on the hydrogen side is carried to a main condenser and trap which serves one bank of stands. The coolant pressure is regulated with nitrogen gas pressure while the temperature is controlled by means of an inline heater connected to an antomatic controller. A bypass system enables the coolant flow through the cell to be regulated while maintaining a constant flow through the pump. Coolant flow is initially set to insure that the maximum oxygen

electrode temperature on average load is within 3°C of the specified value. The coolant used is General Electric SF81-50, a silicone liquid with a specific heat of (0.36 CAL/GM – °C).

The load system consists of a transistorized load box controlled by a voltage biasing regulator.

Front and rear photographs of a bank of five test stands are shown in Figures 14 and 15. Each stand contains an oven mounted on a cart which also houses the coolant loop (Figure 16). The cart is plumbed rigidly to the test stand. The cell is mounted upright in the oven (Figure 17) with four reactant, two coolant, two voltage, and twenty thermocouple connections.

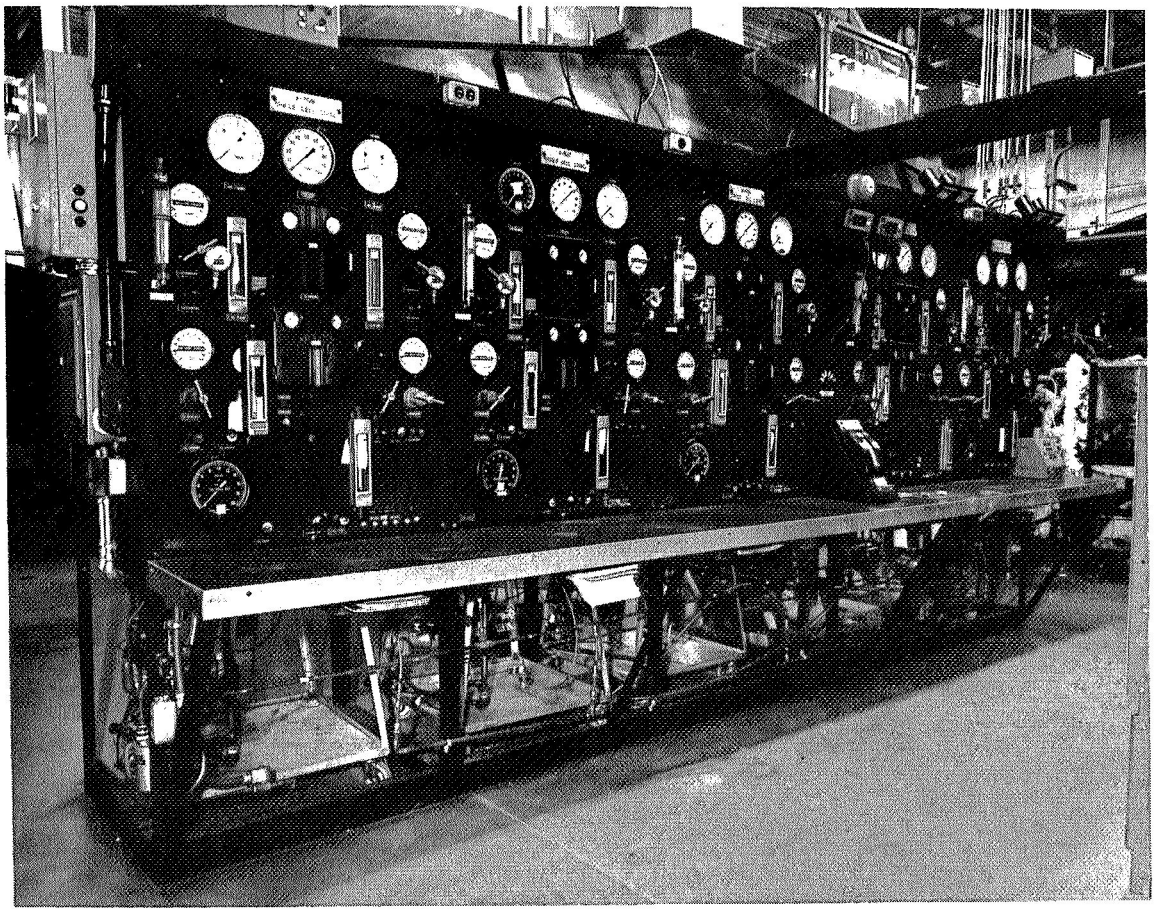

Figure 14 Front View of Bank of Five Test Stands, W677

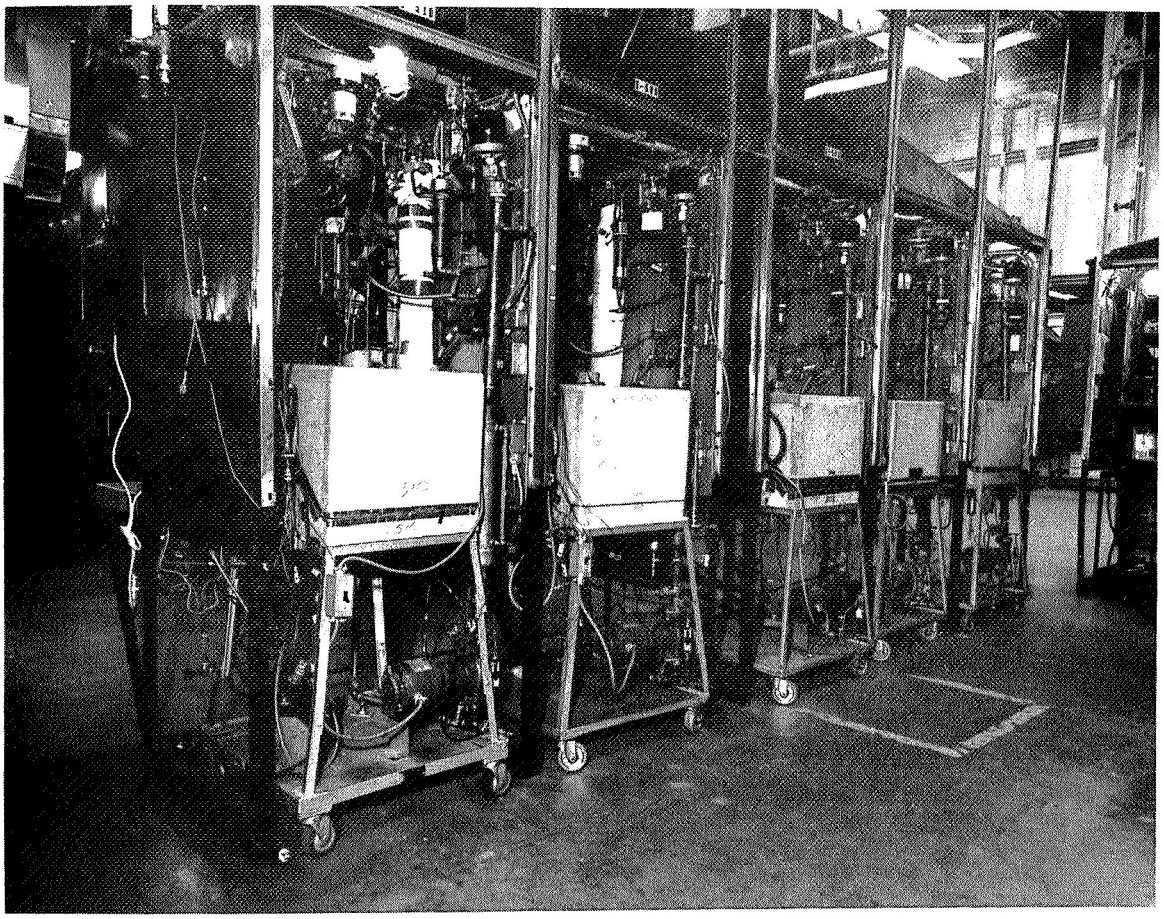

Figure 15 Rear View of Bank of Five Test Stands, W673

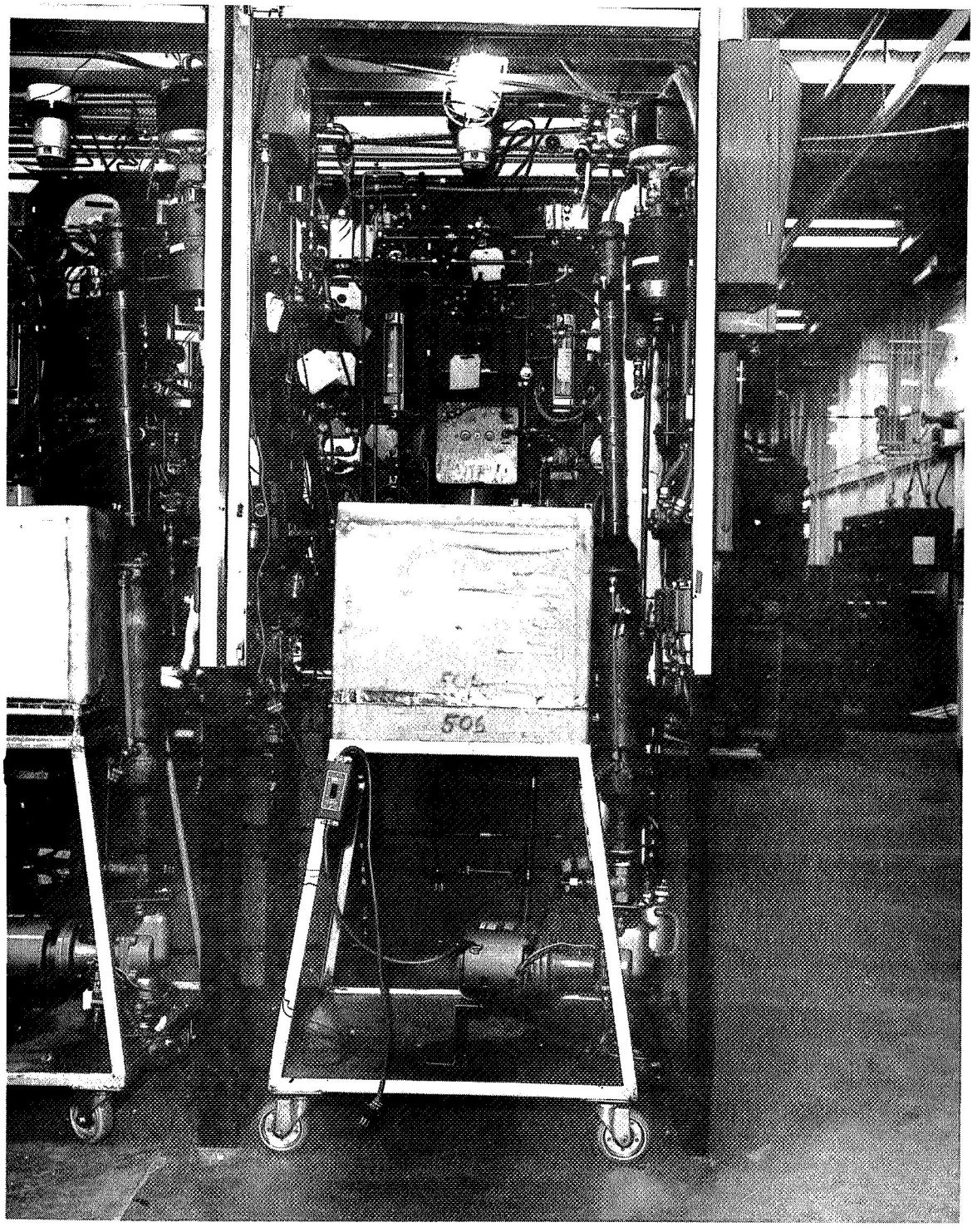

Figure 16 Cart Mounted Oven in Test Stand

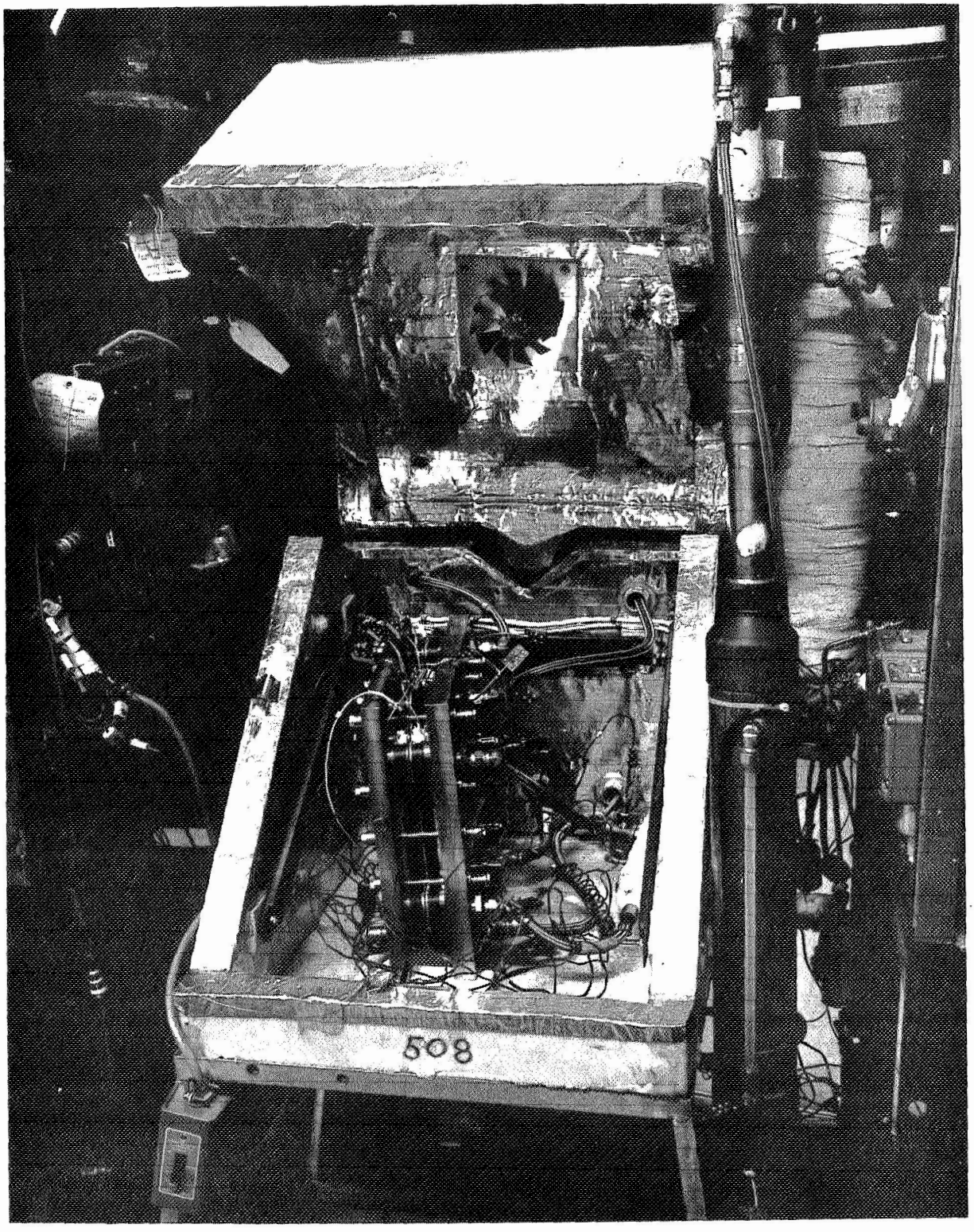

Figure 17 Cell Mounted in Oven, W753

In order to simulate actual cell stack operation, this single cell is sandwiched between layers of insulation and additional support plates as illustrated in Figure 18.

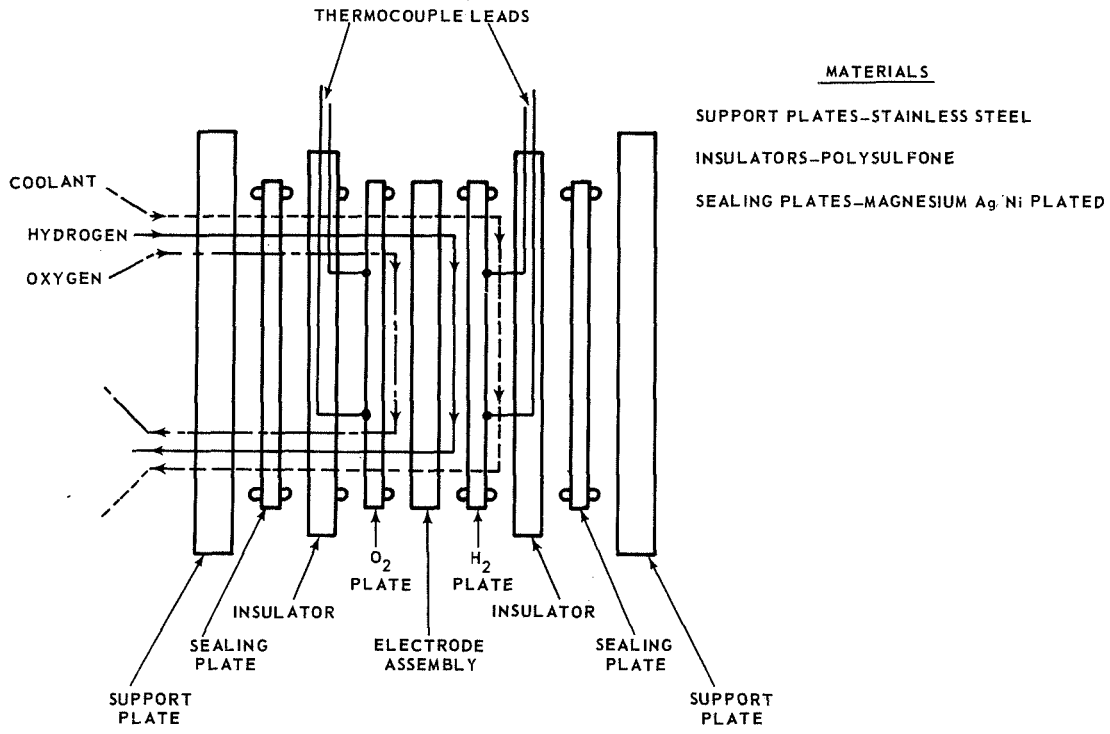

Figure 18 Typical Single Cell Rig Schematic

The polysulfone insulation helps maintain the temperature distribution within the single cell. The support plates seal the pressurized coolant and reactants and provide a uniform compressive load on the cell. A close-up photograph of this cell rig assembly is shown in Figure 19.

Each stand is similar to a powerplant in that each contains its own independent control and readout devices. Each cell environment is controlled and monitored separately from the control and alarm console (Figure 20). The load sequencing unit and the load bias controls are also mounted on the console. The control console is programmed for automatic shutdown to minimize the risk of damage to a cell in the event of a stand or cell malfunction. A lockout system is installed in the control console to prevent unnecessary stand shutdowns due to building line voltage fluctuations. This lock out consists of a time delay mechanism which when actuated by a small loss in line voltage will not allow shutdown for a period of ten seconds.

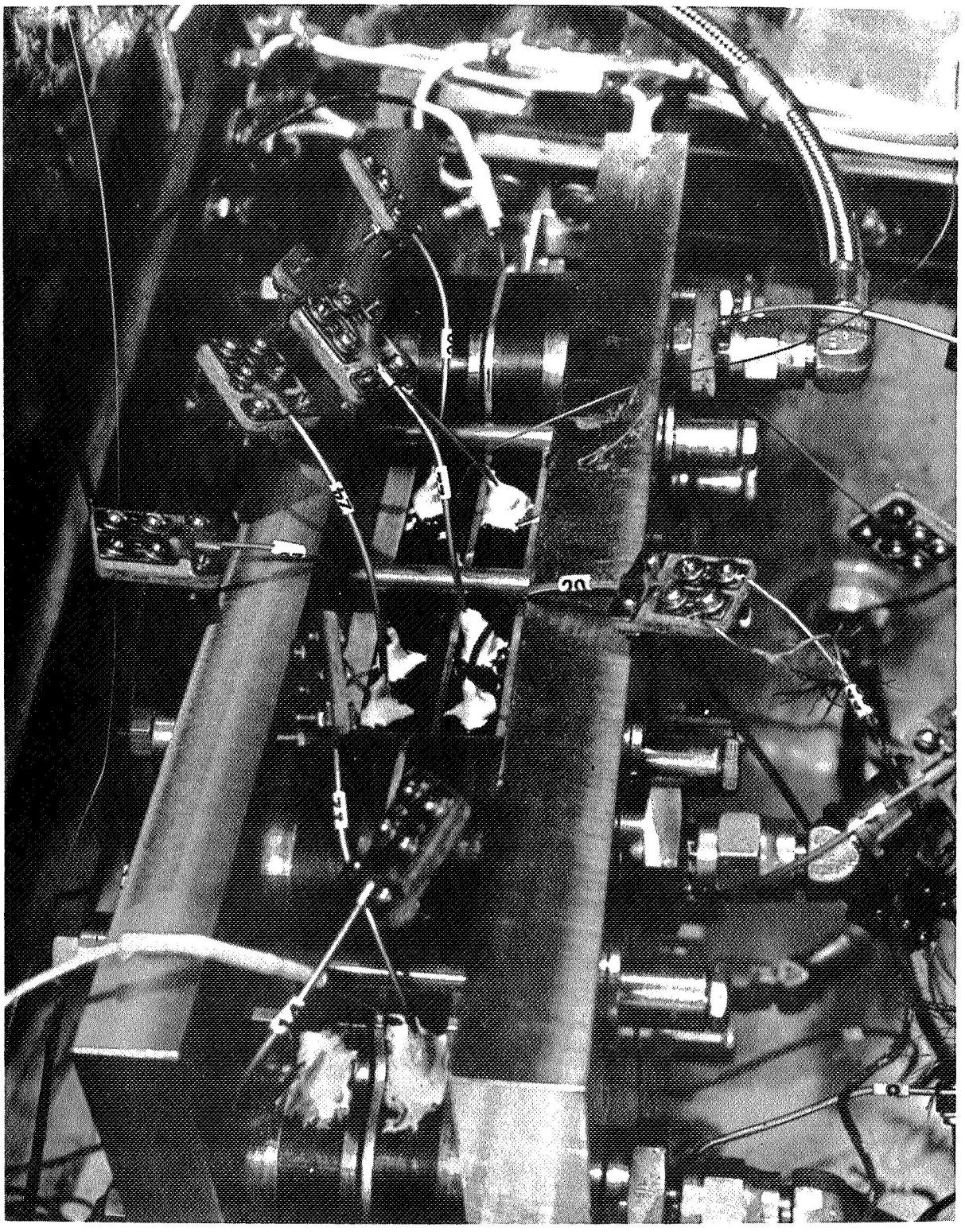

Figure 19 Closeup of Cell, W755

Figure 20 Automatic Control and Alarm Console, W678

Data acquisition is handled by the ADAR. A photograph of the central computer and remote teleprinters used in this system is shown in Figure 21. The system is composed of a computer subsystem and an acquisition subsystem. The Hewlett-Packard computer subsystem consists of: a 2116B computer with a 16K work core; a 1770A high-speed disc with 364K word capacity; three 275B heavy duty teleprinters; a 2737A high-speed paper tape photoreader; and a 2753A hgih-speed paper tape pumch. The acquisition subsystem consists of: a 2402A integrating digital voltmeter; a 2911B scanner control; a 8159 expander; and five 2911A crossbar scanners (200 channels each). The acquisition subsystem can monitor any test parameter that can be converted to an electrical voltage, frequency, or resistance.

The accuracy of the ADAR system is within one-half of one percent of full scale for all parameters. The system is internally calibrated by the computer once an hour and is externally calibrated every six months to certified standards traceable to the National Bureau of Standards.

Figure 21 Automatic Data Acquisition and Recording System, W-752

B. REACTANT PURIFICATION SYSTEMS

The reactant supply conditioning system consists of an oxygen gas analyzer, a hydrogen detector, three purifier units with controls and the oxygen scrubbers (Figure 22). The LIRA is capable of reading 0-5 ppm of carbon dioxide in oxygen and can continuously monitor the oxygen supply downstream of the scrubbers. The scrubbers are plumbed so that one bank may be recharged while the other is in operation.

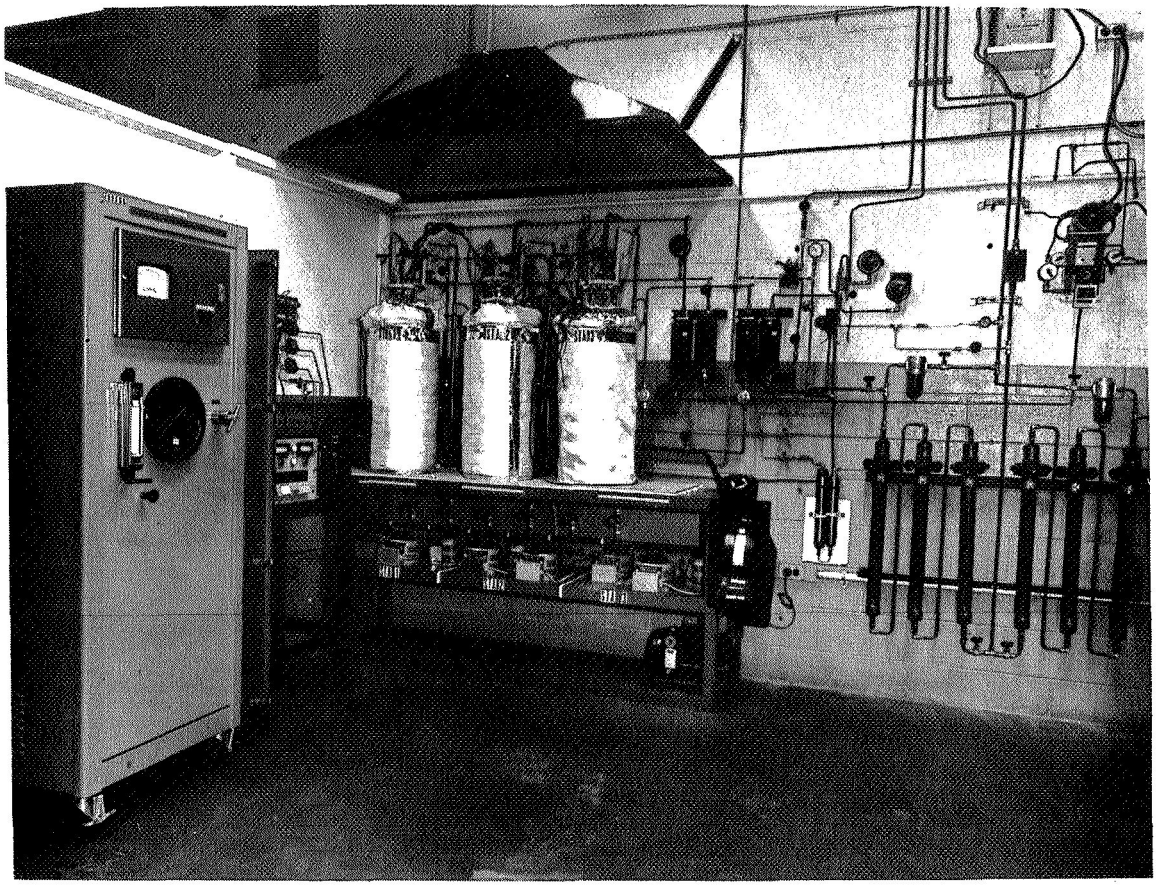

Figure 22 Reactant Supply Conditioning System, W672

Tests were run to establish the efficiency of the oxygen scrubber system. Measurements were made of the carbon dioxide level in the oxygen on both sides of the scrubbers. The carbon dioxide level upstream of the scrubbers was found to be 0.3 ppm. Downstream of the scrubbers the carbon dioxide level was not detectable. Gas was also sampled at a test stand. Again, the carbon dioxide level was not detectable. The sensitivity level of the LIRA measuring device is 0.1 ppm.

Laboratory analysis of samples taken from the oxygen supply to the test stands indicates six to ten parts per million of hydrocarbons. These hydrocarbons were about 90 percent methane.

For tests which require the high CO_2 level in the oxygen supply, a special mixing valve furnished by NASA is used to introduce 4 ppm of CO_2 into the oxygen stream. This mixture is ducted to the test positions by a separate supply system. The CO_2 level is monitored with the LIRA. The mixing valve installation is described in Appendix B.

The hydrogen purifier system consists of three units (Figure 23). Each unit is capable of providing sufficient ultra pure gas to run one bank of stands. In the event of a failure, the system is designed to automatically bypass the purifiers so that stand pressure would not be lost. Each unit includes three palladium silver separators inside an insulated container with the heating and monitoring elements needed to maintain the unit at the required operating temperature. A hydrogen detector constantly monitors the atmosphere inside each of the containers and is equipped to automatically shut down the purifier unit before a hazardous accumulation of hydrogen occurs. The atmosphere is monitored at the top of the container where hydrogen leakage will accumulate. Samples taken from the hydrogen supply to the test stands contained no detectable hydrocarbons.

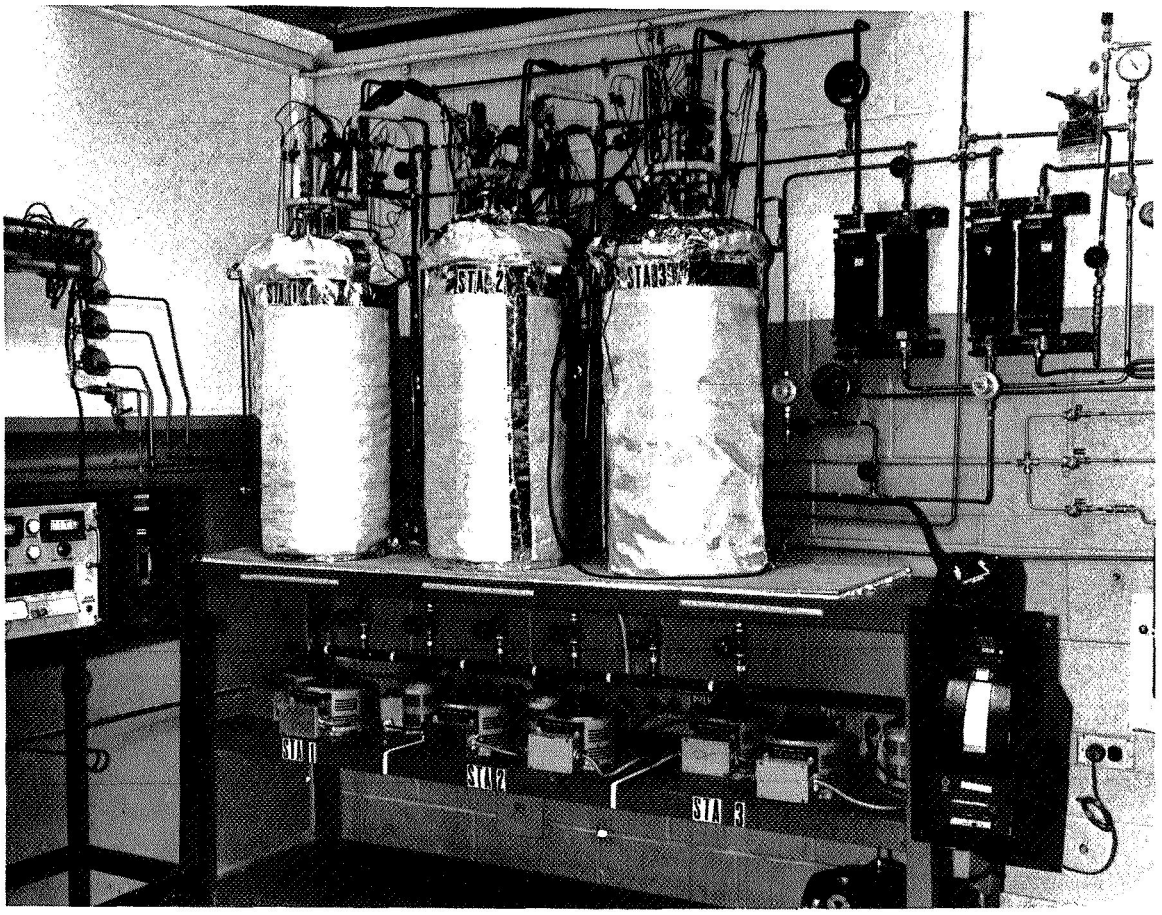

Figure 23 Hydrogen Purifier System

V. TEST PROCEDURES

A. Test Procedure Summary

Each cell test begins by filling the cell with electrolyte and assembling it in a set of test hardware including cooling plates, insulating plates, and end plates. This assembly is mounted in the test stand. The cell is pressurized with reactants and heated to operating temperature with the coolant and oven heaters. The hydrogen saturator is warmed up and hydrogen flow is set to stabilize the electrolyte concentration. Load is applied to the cell and a volume tolerance test is run by varying the hydrogen dewpoint. The cell is then run on the simulated shuttle load profile until its performance decays 0.050 volts. As the cell decays and its efficiency decreases, the coolant flow is increased in order to maintain stable temperature and concentration.

The cell is removed from the stand and refurbished by flushing it with fresh electrolyte. During this procedure the cell remains in its test hardware. The cell is then placed on test again. Another volume tolerance test is performed and the cell is run until the refurbishment criteria is met again. The cell is refurbished a second time, returned to test, and subjected to a third volume tolerance test. The cell is then tested for matrix integrity by subjecting it to a 5 psi (0.3515 Kg/cm^2) pressure differential and is removed from its test hardware for final inspection and analysis.

B. Load Profile

Each cell is alternately operated for six days using the following load profile and then stored for one day.

Relative Load	Load Duration - hours
0.8	6
1.25	1
1.1	6
1.0	121
1.25	1
1.1	6
1.0	1
0.8	2

The cell current density is equal to the average current density specified for the test multiplied by the relative load.

Upon completion of this load profile, the cell is shutdown with a dry nitrogen atmosphere in its reactant passages. At the end of the storage period, the cell is started up and testing continued.

C. Cell Activation and Fill

The electrolyte used in cell activation is prepared by mixing a predetermined amount of demineralized water and a certified solution of KOH typically containing:

KOH	45.8%
Pottasium Carbonate	0.01
Chloride	0.0005
Nitrogen Compounds	0.0005
Phosphate	0.0003
Sulfate	0.001
Ammonium Hydroxide ppt.	0.0007
Heavy Metals	0.001
Iron	0.0004
Sodium	0.004

A sample of the resulting mixture is then titrated to determine KOH and carbonate composition. Different concentrations of electrolyte are prepared by varying the amounts of demineralized water and 45 percent KOH solution utilized. Polyethylene bottles are used for electrolyte storage. The electrolyte is always handled in a nitrogen atmosphere to prevent contamination.

Prior to activation, the unitized electrode assembly is inspected, weighed, and assembled. The matrix pretreatment consists of flowing KOH electrolyte through the reactant gas passages of the cooling plates at a prescribed rate to permit KOH to be absorbed by the unitized electrode assembly. This procedure is in no way detrimental to the integrity of either the electrode structure or the matrix material. After a several hour soaking period, the excess KOH is drained from the gas passages by rotating the activation test fixture. A gas crossover check is made to ensure that the cell has suitably absorbed the electrolyte.

Upon completion of the activation procedure, the activation test fixture is placed in a nitrogen atmosphere (Figure 24) and the unitized assembly is unstacked. The electrode assembly is cleaned of excess KOH, weighed, and inspected. Weighing is required to ensure that the correct amount of KOH is retained by the electrode assembly. This correct amount of KOH is dependent on the particular cell configuration being activated. Final assembly of the cell begins at this point, still in a nitrogen atmosphere.

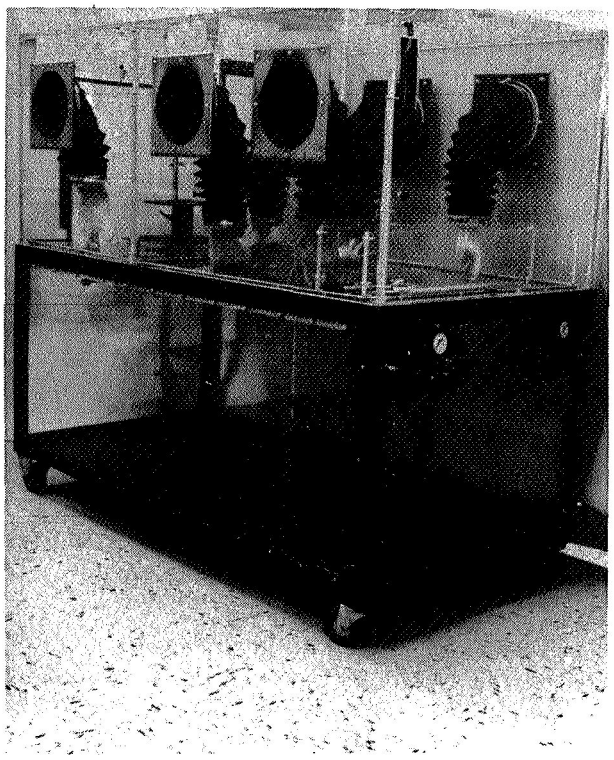

Figure 24 Nitrogen Tent for Handling Cells After Filling

The volume tolerance test is performed on all cells after the initial assembly and after each of the two refurbishments. The cells are subjected to the acceptance test as outlined below.

The volume tolerance tests consist of constructing a curve showing the cell performance as a function of electrolyte volume by varying the hydrogen dewpoint. This curve is constructed from at least five (5) data points. A cell is considered of acceptable quality if the electrolyte concentration of the cell can be adjusted to within two (2) percentage points of 32 percent and the electrolyte volume ratio remains within the range of 1.1 to 1.3. The optimum electrolyte volume (electrolyte volume ratio = 1.0) is estimated from the data points collected during the volume tolerance testing of the cell.

Cells which do not meet these acceptance criteria have their electrolyte volume adjusted by adding a predetermined quantity of electrolyte using the electrolyte fill tube.

D. Cell Refurbishment

Cell refurbishment criteria are defined as follows:

1. The loss of 0.050 volt at the average current density – The mean voltage at this current density over the first 100 hours is used as the initial load voltage.

2. When direct combination of the reactant gases occurs – This is detected by an increase in coolant flow required over and above that needed to remove the heat generated within a slowly degrading, properly-functioning fuel cell.

There are two refurbishments of each cell. After the first refurbishment endurance testing continues. After the second refurbishment the cell is disassembled and inspected.

Each cell is refurbished by flowing KOH electrolyte through the reactant gas passages of the cooling plates to permit high purity KOH to displace the old electrolyte in the matrix. The excess KOH is drained from the gas passages by rotating the cell fixture. After refurbishment a volume tolerance test is performed and the cell's voltage at average load is tested. In addition, after the second refurbishment, the ability of the matrix to withstand overpressure up to 5 psi (0.3515 Kg/cm^2) is tested.

E. Cell Analysis

At the completion of each test the cell is carefully disassembled, examined, and analyzed as described below.

1. Measurement of polarization curves on specimens cut from each electrode after removal from cell and washing. Such post-test performance evaluations utilize a single cell design of 2-inch (5.08 cm) diameter active area with fresh electrolyte and matrix. The cell incorporates suitable reference electrode probes to determine separate polarizations of each electrode. Temperature control is maintained at 200° ± 5°F (93° ± 3°C) except where effects of temperature are of particular interest. Reactant gas pressures are normally 20 psia (1.406 Kg/cm^2) or less. In selected cases, polarization of the oxygen electrode are also determined by using air to elucidate changes in oxygen diffusional losses.

2. Measurement of electrolyte concentration at termination of the endurance test. The method used consists of titration of a suitable sample of electrolyte to determine hydroxyl ion concentration. This titration will also measure the carbonate ion content. The electrolyte sample is obtained by washing the cell with distilled water.

3. Examination of all cell components for corrosion or other forms of deterioration.

4. Analysis of carbonate build up in cell. The method used for analysis of carbonate in the cell is a titration incorporated with that for hydroxyl ion described above under measurement of electrolyte concentration. Accurate measurement of carbonate ion content in the cell depends upon careful collection of the sample and prompt protection of the sample from additional carbonation due to exposure to air. Sample protection is accomplished by sealing samples in plastic bags containing inert gas and by solution of electrolyte and carbonates by injection of a known volume of water into the package. A fraction of this solution can then be titrated.

F. Data Acquisition

The ADAR System measures the following parameters for each cell once every hour.

Parameters	Accuracy
Cell Voltage	±5 mv
Cell Current	±3 amps
Pressure Drop Across Hydrogen Cavity	±0.2 psia (±.01406 Kg/cm^2)
Maximum Electrode Temperatures	±5°F (±2.78°C)
Minimum Electrode Temperatures	±5°F (±2.78°C)
Hydrogen Inlet Temperature	±5°F (±2.78°C)
Oxygen Inlet Temperature	±5°F (±2.78°C)
Hydrogen Saturator Temperature	±5°F (±2.78°C)
Coolant Inlet Temperature	±5°F (±2.78°C)
Coolant Exit Temperature	±5°F (±2.78°C)

The system is tailored to minimize experimental error and reduce the amount of manual data handling for cost effectiveness. It consists of a programmed digital computer receiving input signals from a common scanner which surveys the instrumentation output signals in sequence. This input is then transcribed into engineering units, converted to corrected voltage, temperature, pressure, etc. in accordance with the programmed instructions and displayed in a predetermined format in typed output at the test stand. This occurs in a matter of minutes, making it a "real time system." The experimental error or variation from test to test attributable to instrumentation is minimized because of the common computer and scanner. Also, rapid calibration scans are made to detect instrumentation problems. The system continuously monitors all test stands for the duration of each test, generating a complete test log.

The total load hours, the date, and the time of day is automatically recorded with each set of data on standard teleprinter paper. This paper record was forwarded with each Monthly Technical Progress Narrative. A sample printout is shown in Figure 25. The rig number identifies each cell. For example, rig 37605-1 is cell test number four. The printout symbols used are defined below.

Parameter	Printout Symbol
Cell Voltages	VOLTS
Cell Current	AMPS
Pressure Drop Across H_2 Cavity	H_2 DP
Maximum H_2 Electrode Temperature	H_2 ELEC 2
Maximum O_2 Electrode Temperature	O_2 ELEC 2
Minimum H_2 Electrode Temperature	H_2 ELEC 1
Minimum O_2 Electrode Temperature	O_2 ELEC 1
H_2 Inlet Temperature	H_2 IN
O_2 Inlet Temperature	O_2 IN
H_2 Saturator Temperature	H_2 SAT
Coolant Inlet Temperature	COOL IN
Coolant Outlet Temperature	COOL EX

```
   RIG 37603-1   ST X-510   TIME 22 0  DATE  7/31/70  R HRS 2287
AMPS  102.7 A  H2 ELEC1 146. F  02 ELEC1 146. F  COOL IN 144. F
VOLTS  .829 V  H2 ELEC2 169. F  02 ELEC2 169. F  COOL EX 174. F
H2 SAT 134. F  H2 IN    137. F  02 IN    152. F  H2 D P  .232 PSI

   RIG 37625-1   ST X-526   TIME 22 0  DATE  7/31/70  R HRS 2610
AMPS   38.7 A  H2 ELEC1 155. F  02 ELEC1 156. F  COOL IN 154. F
VOLTS  .965 V  H2 ELEC2 164. F  02 ELEC2 165. F  COOL EX 165. F
H2 SAT 133. F  H2 IN    148. F  02 IN    161. F  H2 D P  .167 PSI

   RIG 37607-2   ST X-527   TIME 22 0  DATE  7/31/70  R HRS  277
AMPS   37.9 A  H2 ELEC1 152. F  02 ELEC1 151. F  COOL IN 155. F
VOLTS  .933 V  H2 ELEC2 164. F  02 ELEC2 164. F  COOL EX 165. F
H2 SAT 124. F  H2 IN    143. F  02 IN      . F  H2 D P  .382 PSI

   RIG 37669-1   ST X-528   TIME 22 0  DATE  7/31/70  R HRS 1363
AMPS  101.1 A  H2 ELEC1 187. F  02 ELEC1 187. F  COOL IN 192. F
VOLTS  .885 V  H2 ELEC2 206. F  02 ELEC2 207. F  COOL EX 212. F
H2 SAT 155. F  H2 IN    176. F  02 IN    188. F  H2 D P -.129 PSI
```

Figure 25 Sample ADAR Printout

Figure 26 shows the basic system component arrangement in block diagram form. The heart of the ADAR system is a Hewlett-Packard Model 2114A digital computer which receives input data in the form of digital signals from the Hewlett-Packard Model 2402 Digital Voltmeter. The computer controls the data-taking process, reduces the data, and prints out the results in accordance with programmed instructions.

A Hewlett-Packard Model 2752 teleprinter is used to give program instructions to the computer and also to print out the test "log". The test instrumentation is scanned, or surveyed, by a Hewlett-Packard Model 2911 Guarded Crossbar Scanner. This unit receives analog input signals from the instrumentation and transfers them sequentially to an Integrating Digital Voltmeter, which is a Hewlett-Packard Model 2402 with a long term accuracy of 0.01% of reading. The Integrating Digital Voltmeter converts the signals from analog to computer-compatible digital form and transfers them to the computer.

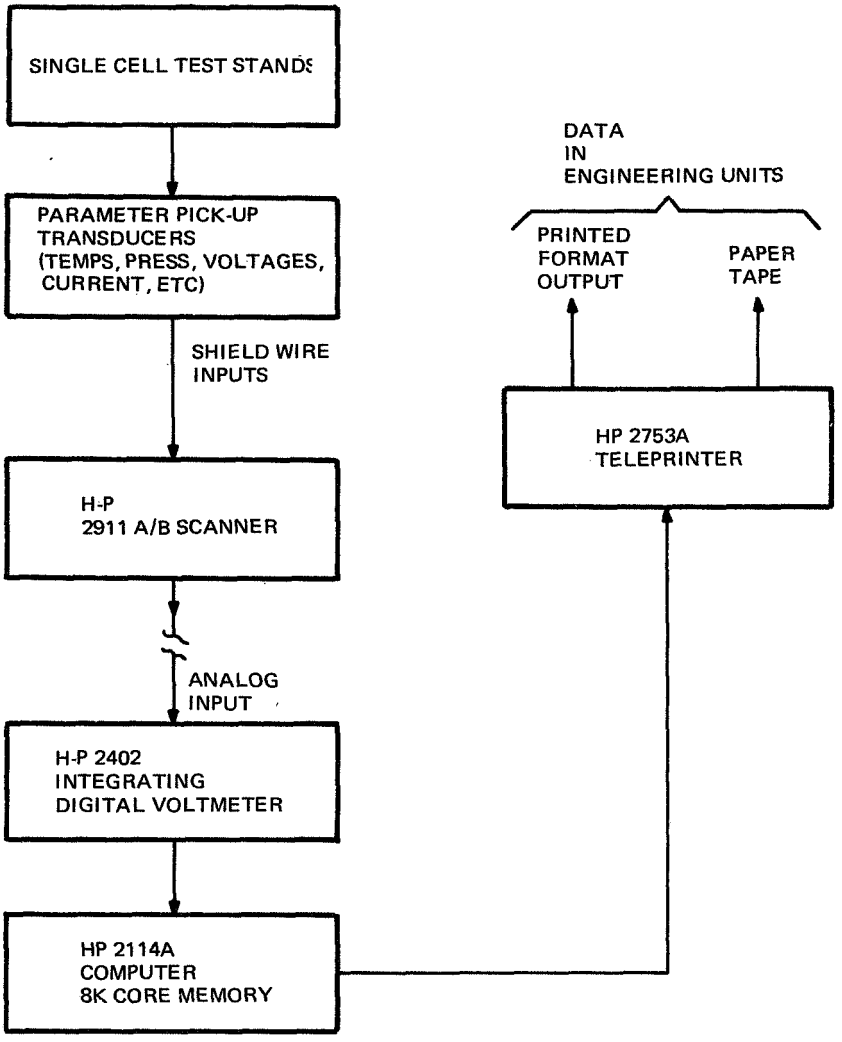

Figure 26 Block Diagram of Automatic Data Acquisition and Recording System

The test instrumentation or parameter pickup and conditioning items consist of thermocouples and reference ovens to record cell, fluid, and environmental temperatures; test stand positioned total and differential pressure transducers; individual cell voltage leads and cell current shunts. These items feed their signals to this Model 2911 Guarded Crossbar Scanner.

The cell voltage is taken off pins attached to the coolant plates adjacent to the electrodes. The current is read out as a voltage drop across a calibrated shunt and transformed to current on the ADAR printout sheet. The hydrogen pressure drop across the cell is read out from a transducer located across the cell hydrogen inlet and exit lines. The electrode temperatures are taken from thermocouples imbedded in the polysulfone insulator plates. The temperatures are measured at the surface of the magnesium coolant plates and have been shown to closely approximate actual electrode temperatures. Cell gas and coolant temperatures are taken from inside the manifolds adjacent to the inlet and exit ports. The hydrogen saturator gas temperature is measured in the saturator exit line to the cell.

VI. TEST RESULTS

A. Cell Test Histories

Cell Test Number 1

Cell test number one in the test sequence accumulated a total of 2468 load hours and 17 cycles (Figure 27 and Figure 28). Initial cell voltage was 0.855v at 200 ASF (215.2 MA/CM^2). This rose to 0.865v at 600 hours and decayed until the low voltage refurbishment criteria was reached at 1246 hours. After refurbishment the cell voltage was equivalent to the initial voltage at 0.855v. At 1534 hours, a loss of line voltage to the facility caused an automatic stand shutdown. This resulted in some loss of cell electrolyte. Electrolyte was added to the cell through the electrolyte fill tube on two occasions and the test was continued. At 1680 hours 5 cc of 30 weight % KOH was injected into the cell. At 1810 hours 3 cc of 30% KOH was injected. The cell was refurbished again at 2399 hours. Performance after stabilization was 0.821v. The cell was subjected to 5 psi (0.3515 Kg/CM^2) overpressure prior to shutdown in order to test matrix integrity. No evidence of gas leakage through the matrix was observed. This cell was temperature sensitive throughout the latter stages of its life both on the initial run and after refurbishment. Small changes in cell temperature resulted in large differences in cell voltage. This was probably due to the combination of a thick matrix with a relatively thin anode which would result in large movements of the electrolyte interface with small concentration changes. Visual inspection of the cell after disassembly disclosed no significant deterioration or discoloration of the electrodes. Some frame discoloration was noted at the oxygen inlet ports.

The short load cycles which appear occasionally in the test data are the result of automatic shutdown and cool off occurring before the scheduled shutdown. When this happens, the cell is not restarted. Instead, the cell is stored on nitrogen for one day and the load cycle is terminated.

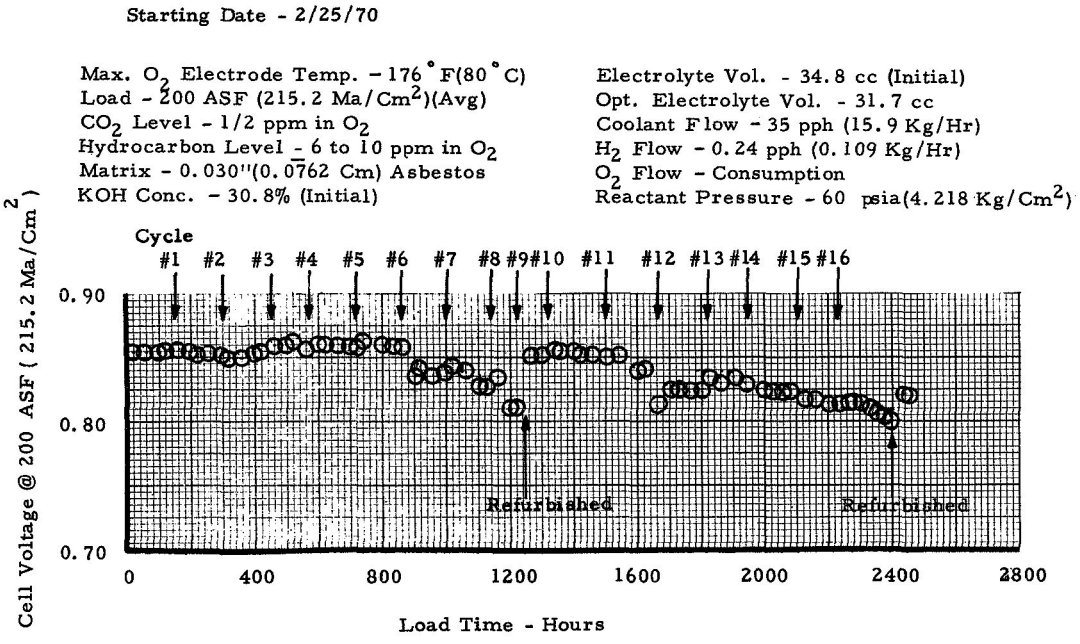

Figure 27 Cell Test No. 1 - Endurance History

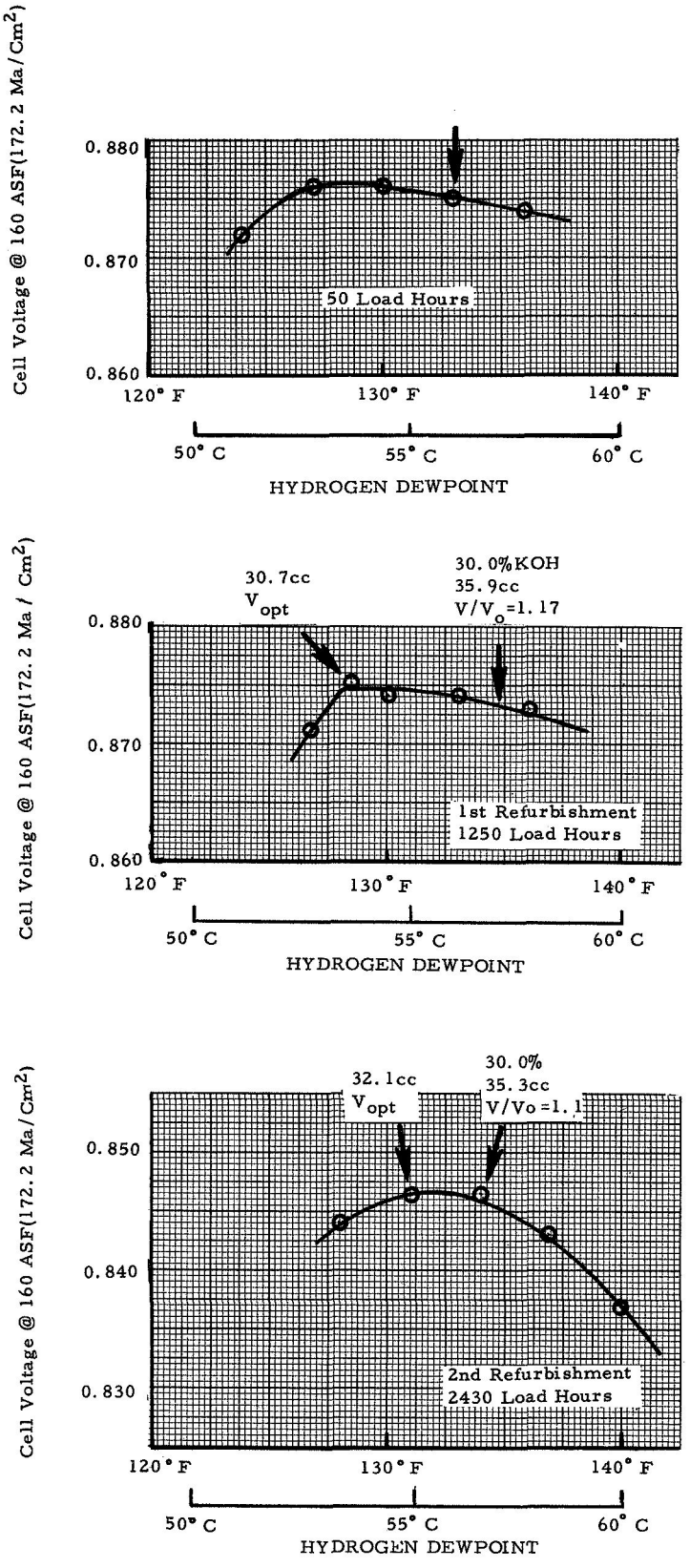

Figure 28 Cell No. 1 Volume Tolerance Tests

Cell Test Number 2

Cell test number 2 accumulated 1010 hours of load time and seven cycles prior to reaching the low voltage refurbishment level, (Figure 29 and Figure 30). The initial performance of the cell was 0.906v at 200 ASF (215.2 MA/CM^2). The cell voltage rose throughout the first 200 hours to 0.927v. At approximately 500 hours the voltage began to decay and this continued until it was shutdown at 1010 hours. The cell was then refilled with electrolyte and restarted. Cell voltage after restart was 0.862v at 200 ASF (215.2 MA/CM^2) which was below the refurbishment level. The cell was again shutdown and refilled. No improvement in the cell voltage was seen and the test was terminated. No evidence of gas crossover was noted prior to shutdown. Inspection of the cell showed loss of catalyst in a small area of the cathode and a crack at the interface of the hardframe and electrode assembly. The crack probably occurred during the disassembly of the cell and did not contribute to the low cell performance since there was no evidence of gas crossover.

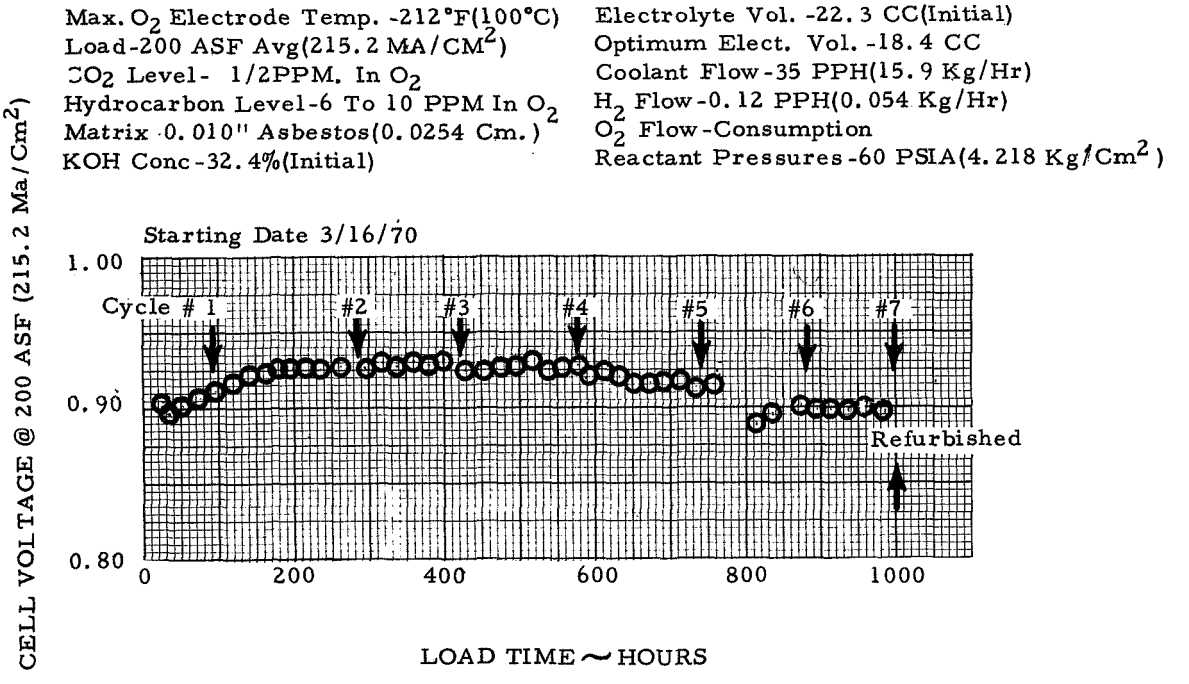

Figure 29 Cell Test No. 2 - Endurance History

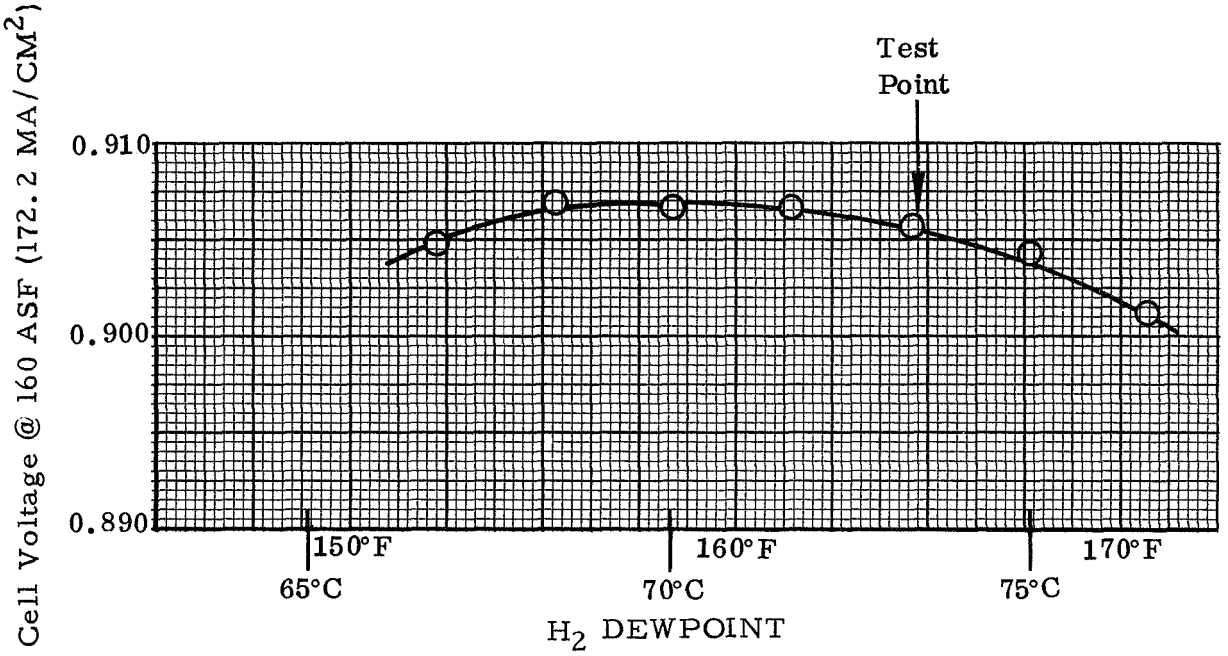

Figure 30 Cell No. 2 - Volume Tolerance Test

Cell Test Number 3

Cell test number three completed 1820 hours and eleven cycles. Initial cell voltage was 0.935v at 75 ASF (80.7 MA/CM^2), (Figure 31 and Figure 32). The voltage decayed steadily until 1354 hours when it was shutdown for refurbishment. Before taking the cell off test a dew-point excursion was run which revealed that the electrolyte volume was less than the optimum. After restart the initial cell voltage was 0.918v at 75 ASF (80.7 MA/CM^2). Rapid voltage decay led to shutdown at 1791 hours. The voltage was again restored to 0.920v after the second refurbishment. Prior to shutdown the matrix was checked for gas crossover; none was found. Disassembly of the cell showed some discoloration of the frame near the oxygen inlet and exit ports. No deterioration of the electrodes was observed.

CELL TEST #3 - ENDURANCE HISTORY

Max. O_2 Elect. Temp. - 212° F (100° C)
Load - 75 ASF (Avg) (80.7 Ma/Cm^2)
CO_2 Level - 1/2 ppm in O_2
Hydrocarbon Level - 6 to 10 ppm in O_2
Matrix - .010" (0.0254 Cm) Pkt
KOH Conc. - 34.5% (Initial)

Opt. Elect. Vol. - 15.3 cc
Electrolyte Vol. - 19.9 cc (Initial)
Coolant Flow - 30 pph (13.6 Kg/Hr)
H_2 Flow - 0.11 pph (0.050 Kg/Hr)
O_2 Flow - Consumption
Reactant Pressure - 60 psia (4.218 Kg/Cm^2)

Starting Date - 8/3/70

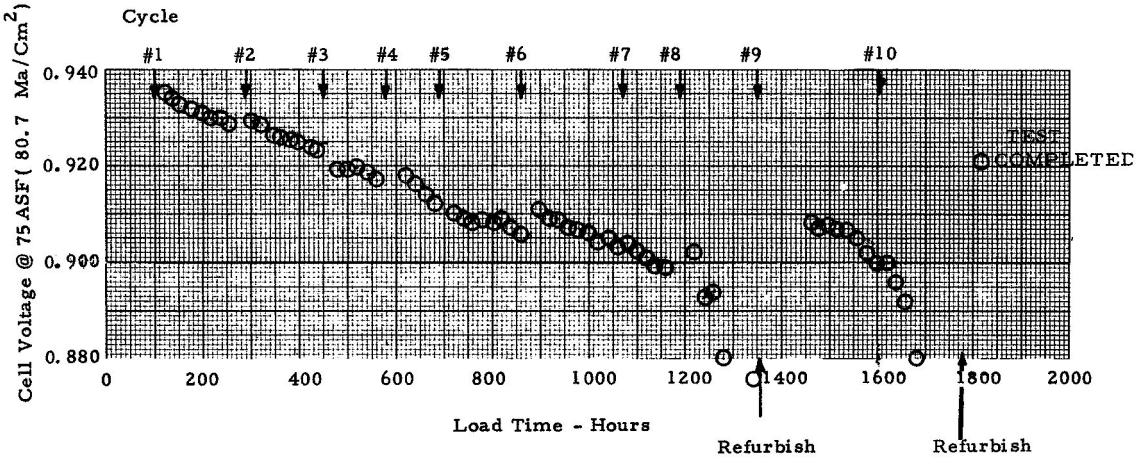

Figure 31 Cell Test No. 3 - Endurance History

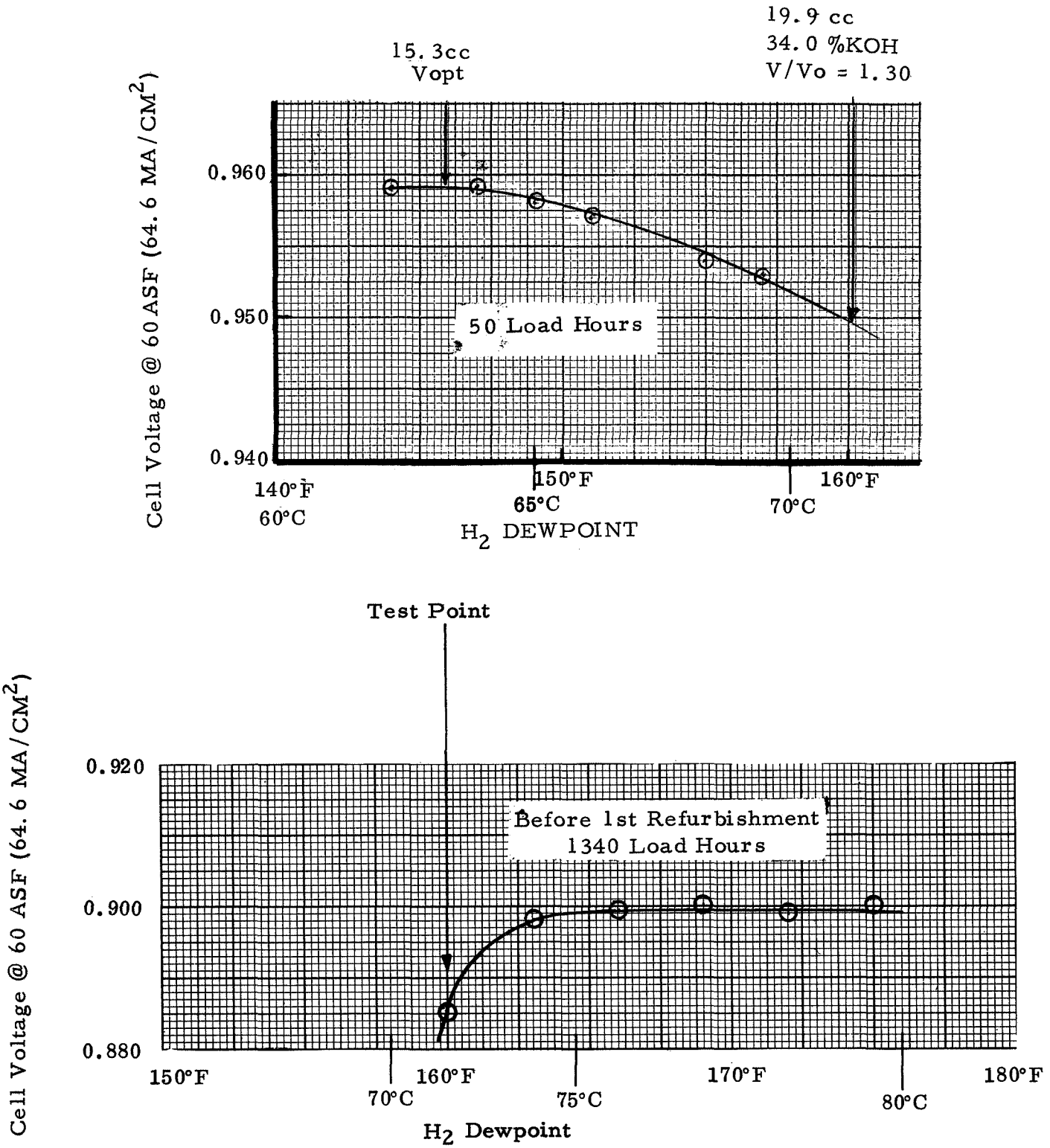

Figure 32 Cell No. 3 - Volume Tolerance Tests

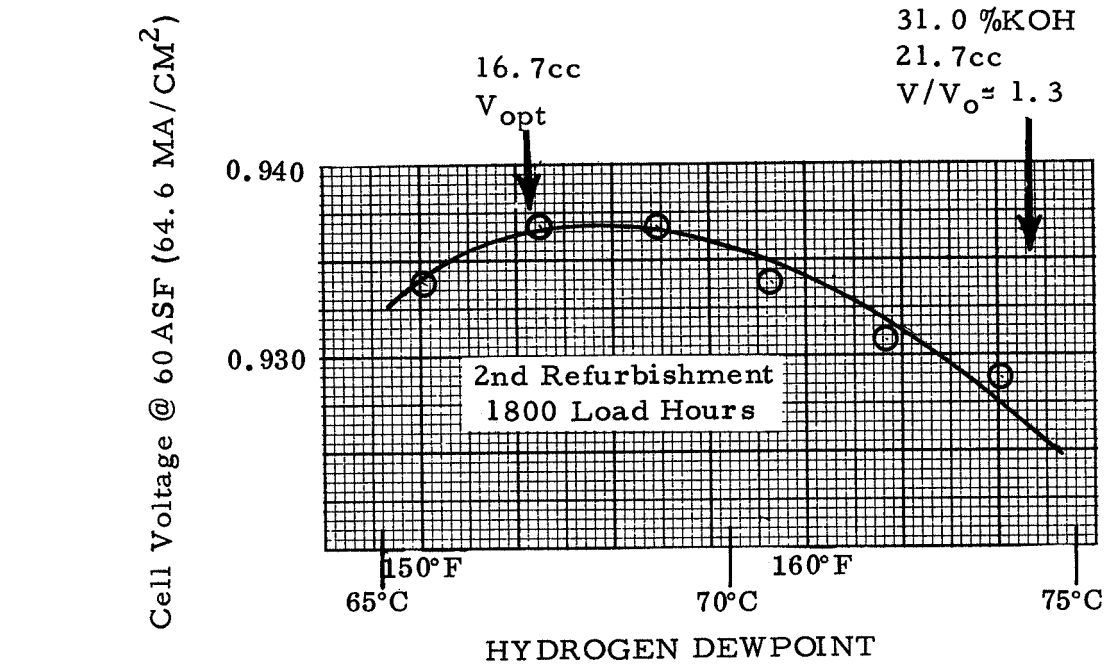

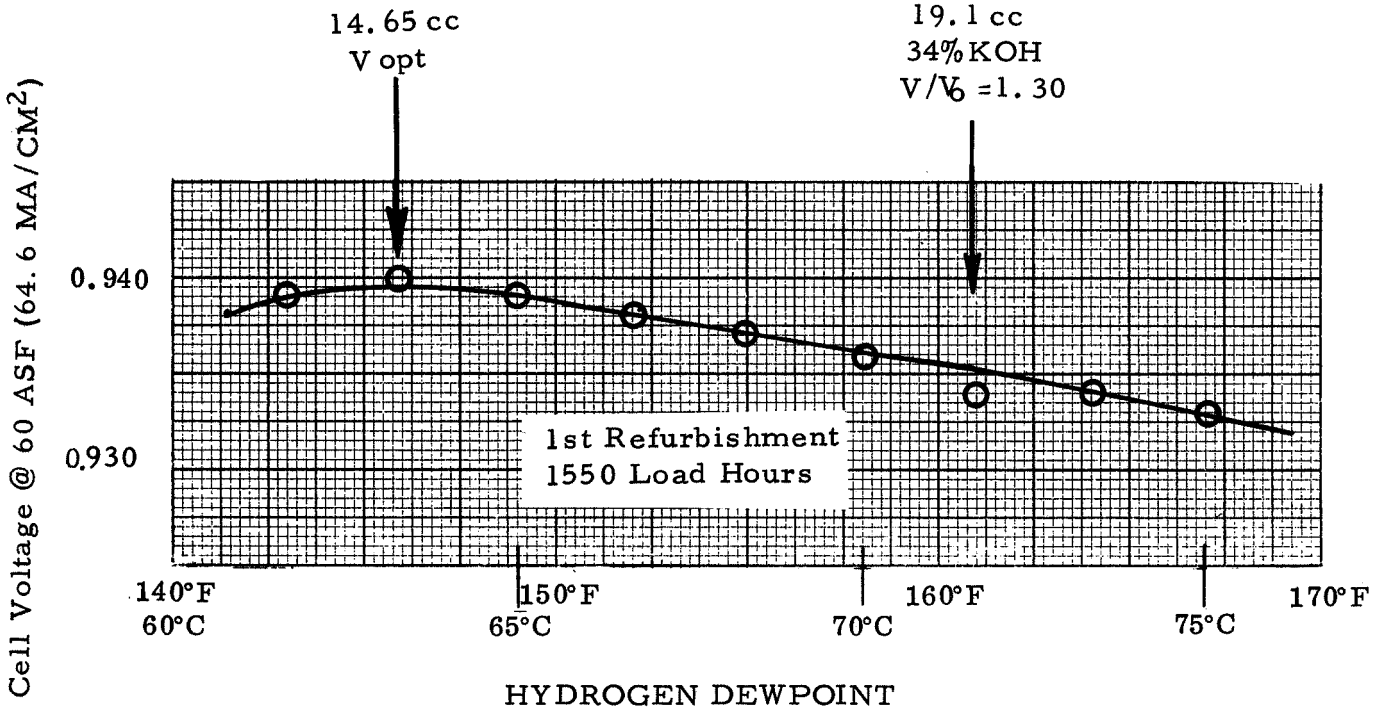

Figure 32 Cell No. 3 - Volume Tolerance Tests (Continued)

Cell Test Number 4

Cell test number four accumulated 5000 hours and 36 cycles prior to its first refurbishment. (Figure 33 and Figure 34). The cell was refurbished to allow measurement of the electrolyte carbonation level prior to the end of the test program even though the refurbishment criteria had not been met. The initial cell voltage was 0.920v at 75 ASF (80.7 MA/CM^2) which remained constant for the first 950 hours. Over the next 400 hours the cell voltage increased to 0.960v and remained at this level until 3900 hours when it began to decay slowly until the 0.940v level was reached at 4760 hours. When the cell was started for the 34th cycle, the cell voltage was 0.895v. No external reason could be found for this drop in performance. The voltage rose of 0.901v by the time the cell was shutdown for refurbishment at 5000 hours prior to the end of the contract. After restart the initial stablized performance was 0.920v.

This cell test was continued into 1971 and at 5800 hours the voltage increased to 0.945v after a startup. The total load time accumulated as of this writing is 6400 hours.

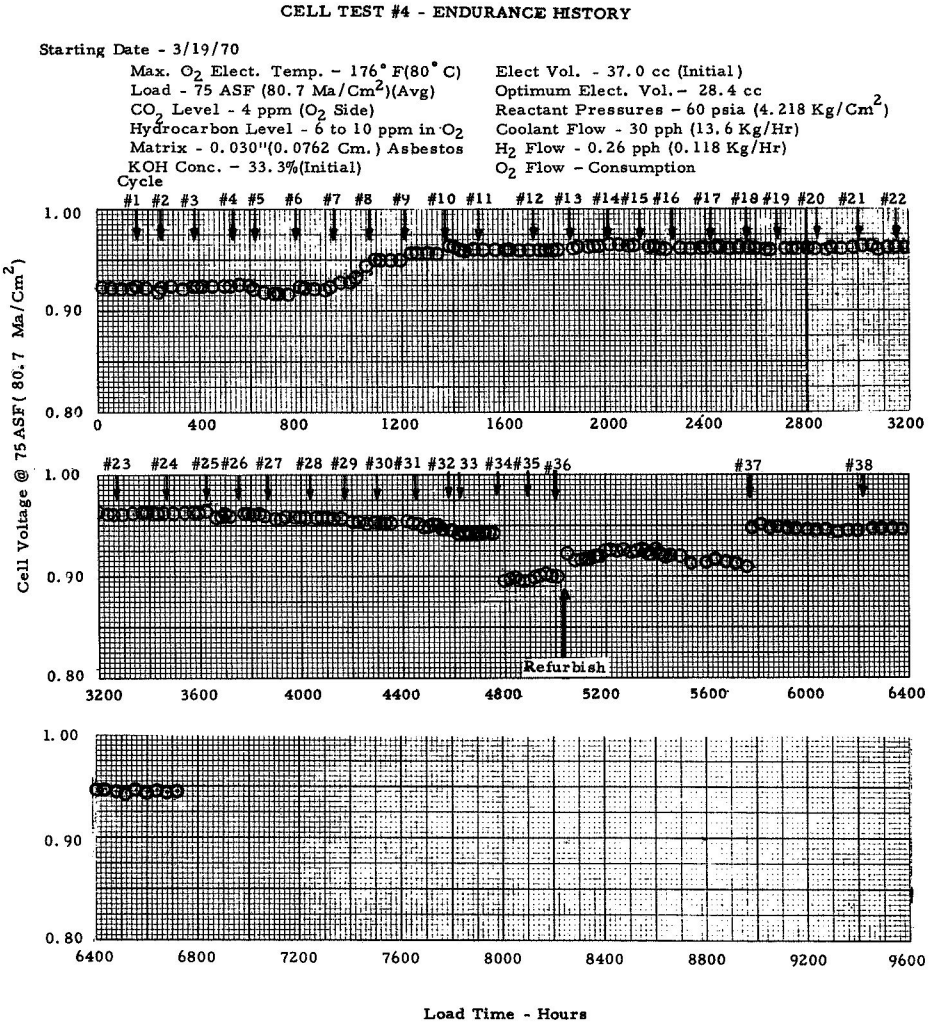

Figure 33 Cell Test No. 4 - Endurance History

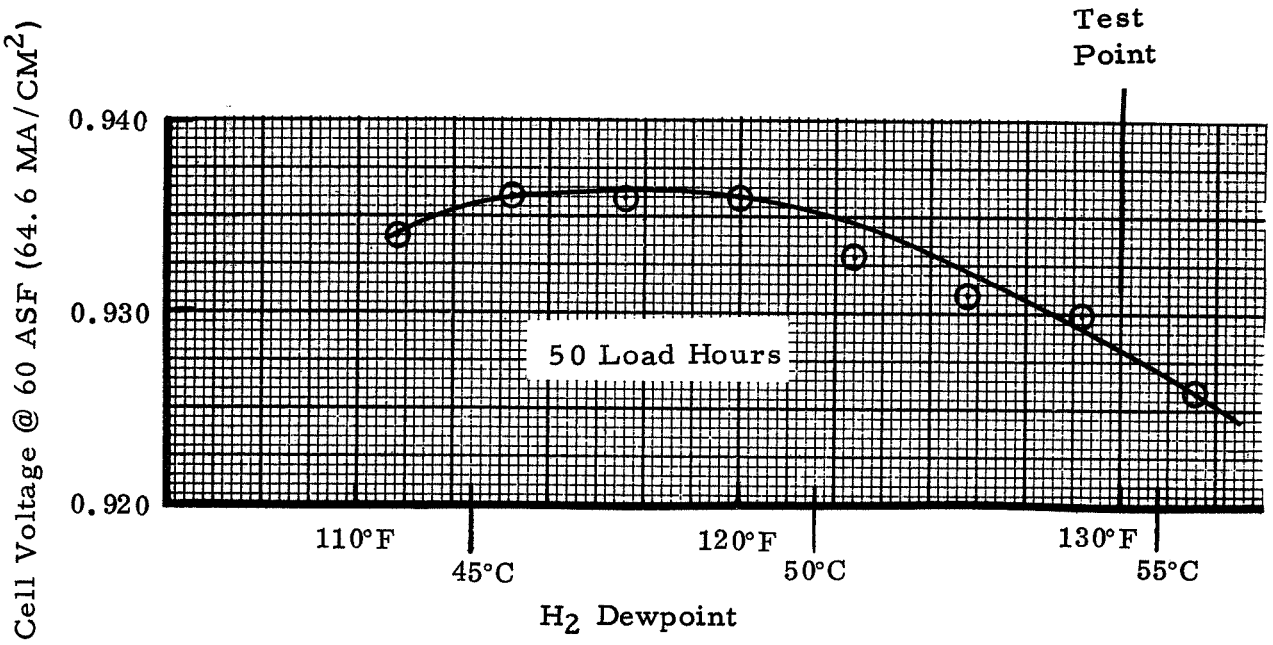

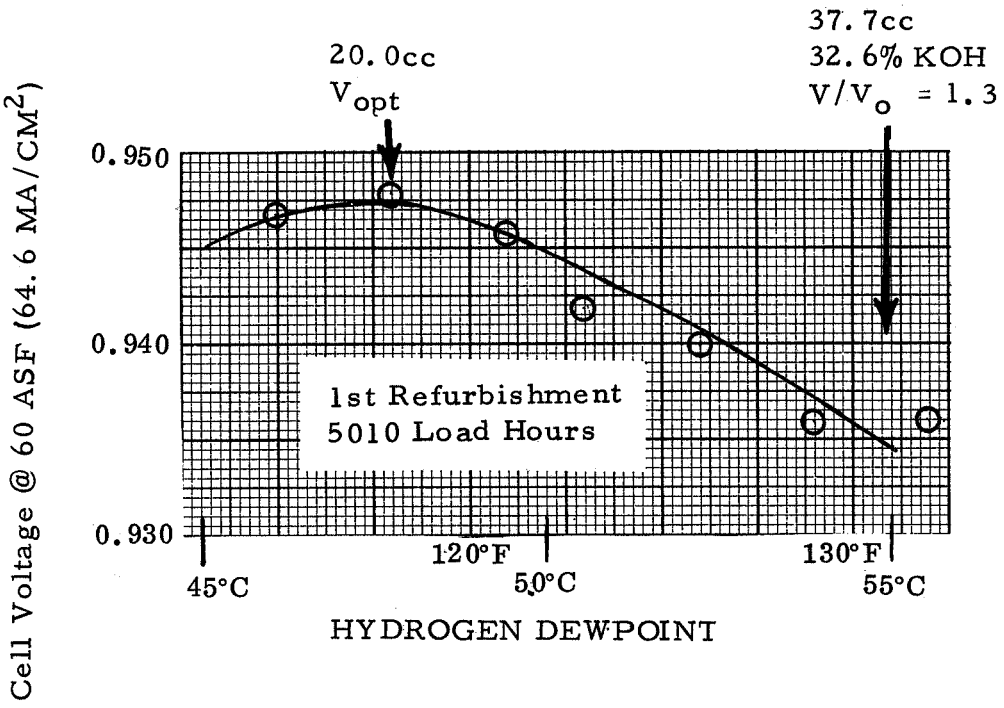

Figure 34 Cell No. 4 - Volume Tolerance Tests

Cell Test Number 5

Cell test number five completed 1425 hours and nine cycles (Figures 35, 36, and 37). Initial cell voltage was 0.890v at 200 ASF (215.2 MA/CM^2). The voltage decayed steadily in a manner similar to other PKT matrix cells in the program. The first refurbishment was done at 645 hours due to low cell voltage. The cell voltage recovered initially after refurbishment to 0.876v at 200 ASF (215.2 MA/CM^2), but began immediately to decay and continued until its second refurbishment at 1320 hours. The cell voltage after refurbishment was 0.872v. No evidence of gas crossover was noted prior to shutdown. This cell showed temperature sensitivity similar to the other thick matrix cells in the latter stages of its life. Inspection of the cell showed carbonate deposits around the foil at the oxygen inlet.

Starting Date - 3/30/70

Max O_2 Electrode Temp. - 212° F (100° C)
Load - 200 ASF (215.2 Ma/Cm^2)(Avg)
CO_2 Level - 1/2 ppm in O_2
Hydrocarbon Level - 6 to 10 ppm in O_2
Matrix - 0.030" (0.0762 Cm) Pkt.
KOH Conc. - 32% (Initial)
Electrolyte Vol. - 46.2 cc (Initial)
Optimum Elect Vol. - 39.1 cc
Coolant Flow - 35 pph (15.9 Kg/Hr)
H_2 Flow - 0.12 pph (0.054 Kg/Hr)
O_2 Flow - Consumption
Reactant Pressure - 60 psia (4.218 Kg/Cm^2)

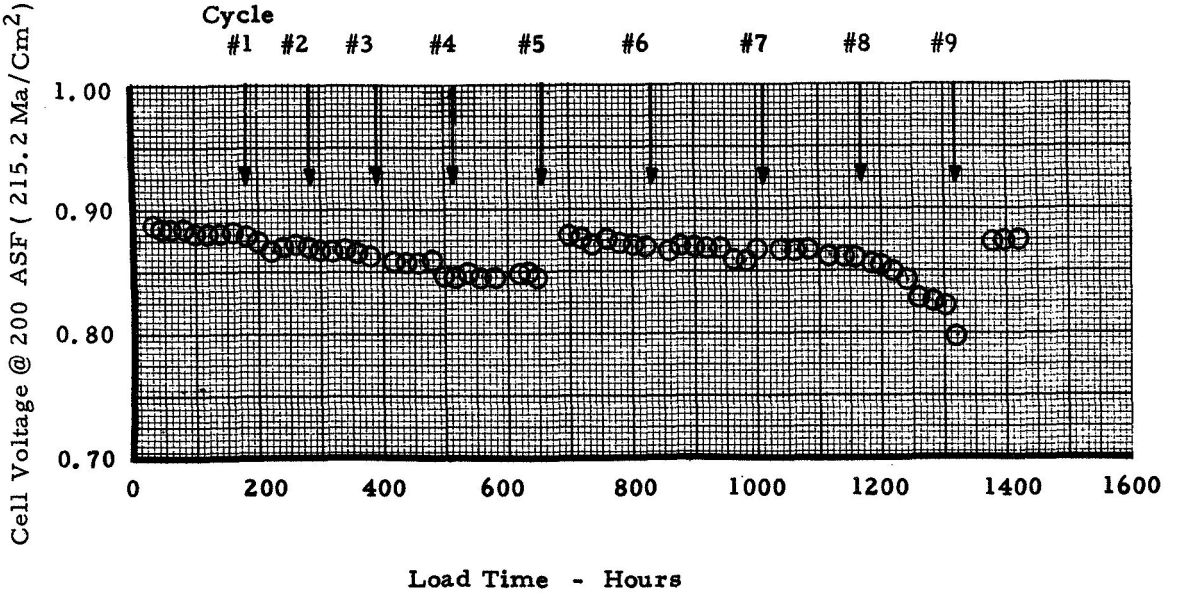

Figure 35 Cell Test No. 5 - Endurance History

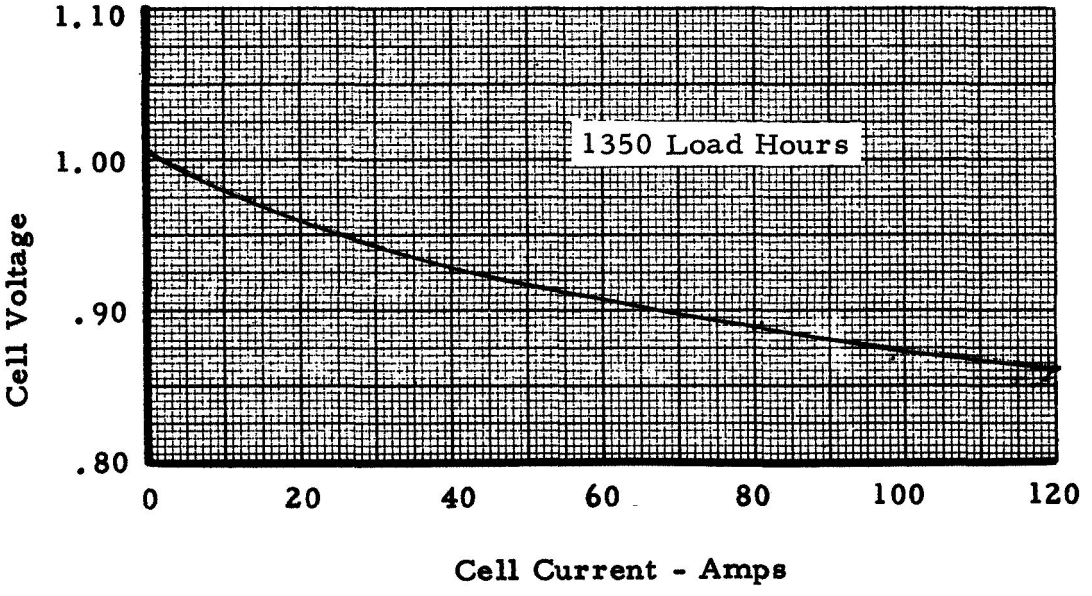

Figure 36 Cell No. 5 - Performance After Second Refurbishment

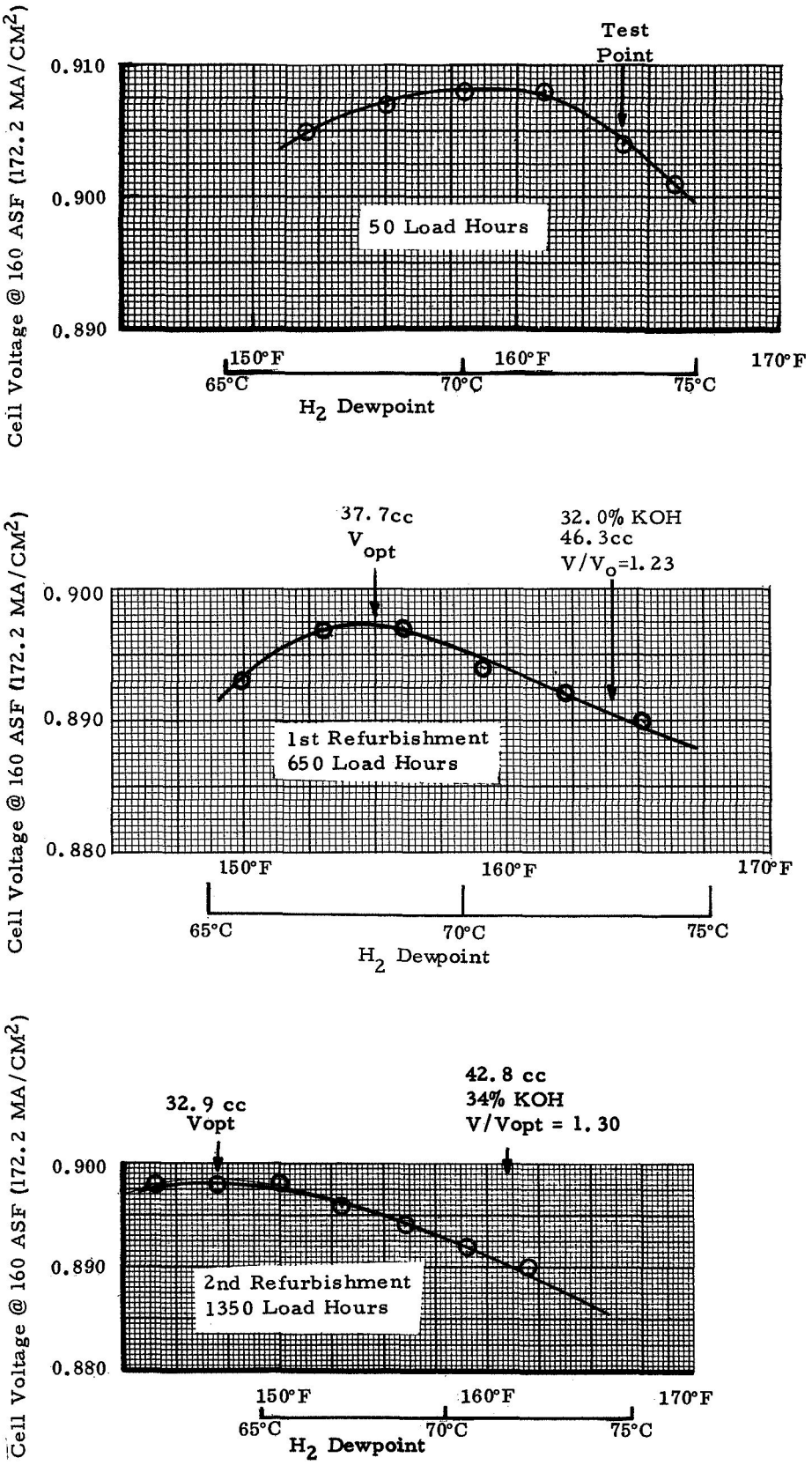

Figure 37 Cell No. 5 - Volume Tolerance Tests

Cell Test Number 6

Cell test number six was terminated at 529 hours due to gas crossover, (Figure 38 and Figure 39). The initial cell voltage was 0.903v at 75 ASF (80.7 MA/CM^2). This level had decreased to 0.888v when the crossover occurred. The cell was refurbished with no success and was then disassembled for inspection. Inspection of the cell revealed that the crossover had taken place in the vicinity of the electrolyte fill tube installation at the inner edge of the frame. It is believed that the fill tube installation may have been the cause of failure. One other attempt was made to run this cell test. In this attempt the cell accumulated 370 hours before gas mixing occurred. Investigation showed the failure to again be the result of the fill tube installation. Severe discoloration of the cathode was noted at the oxygen inlet and at the site of the crossover.

Max. O_2 Electrode Temp. -176°F(80°C)
Load-75 ASF (80.7 Ma/Cm^2)(Avg)
CO_2 Level-4 ppm in O_2
Hydrocarbon Level-6 to 10 ppm in O_2
Matrix- .010" (0.0254 Cm) Pkt
KOH Conc. -34%(Initial)

Electrolyte Vol. -22.6 cc (Initial)
Opt. Elect. Vol. -17.0cc
Coolant Flow-30 pph (13.6 Kg/Hr)
H_2 Flow-0.26 pph (0.118 Kg/Hr)
O_2 Flow-Consumption
Reactant Pressure-60 psia (4.218 Kg/Hr)

Starting Date - 7/15/70

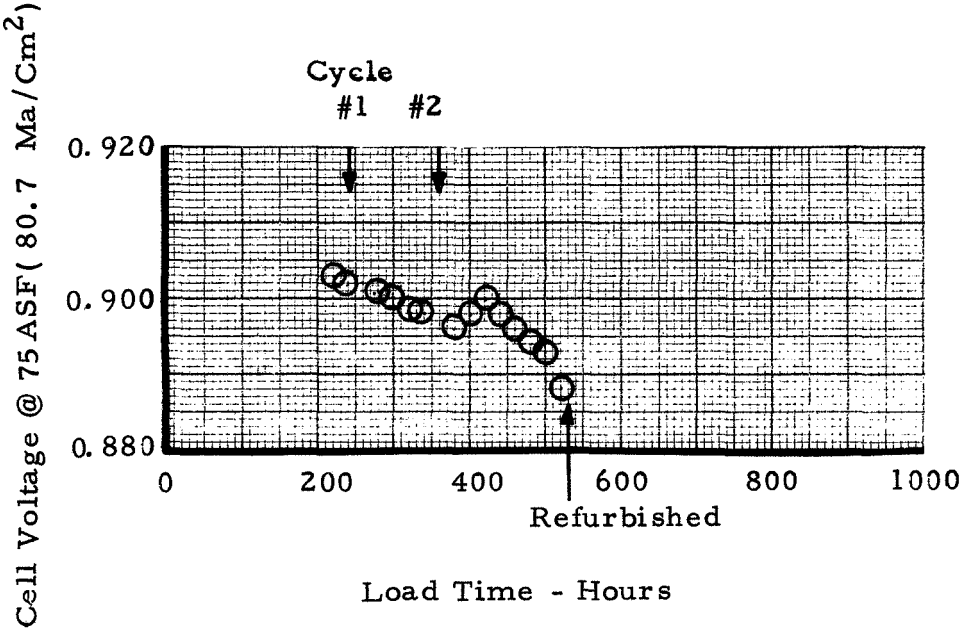

Figure 38 Cell Test No. 6 - Endurance History

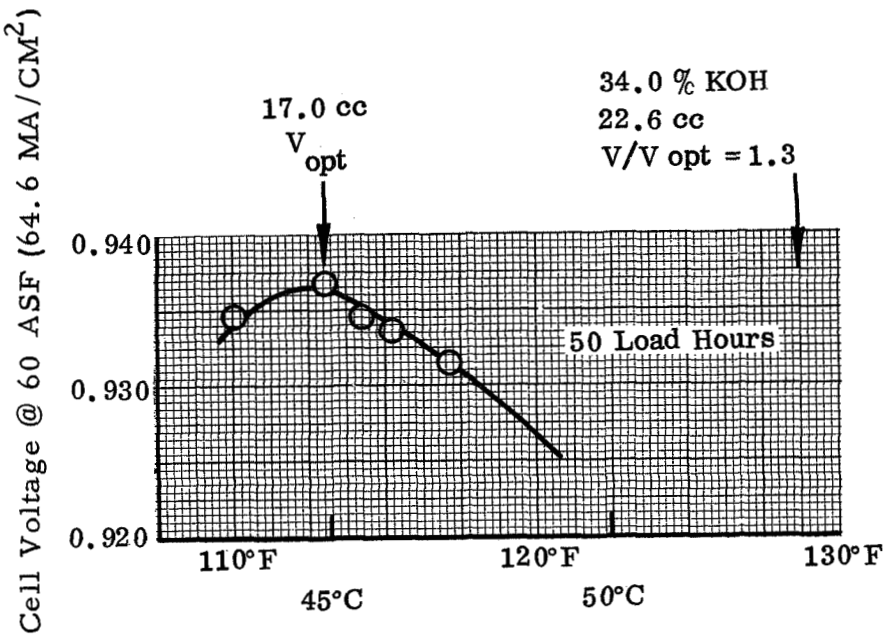

Figure 39 Cell No. 6 - Volume Tolerance Tests

Cell Test Number 7

Cell test number seven completed 2344 hours and 15 cycles, (Figure 40 and Figure 41). The cell voltage which initially was 0.870v at 200 ASF (215.2 MA/CM^2) rose throughout the first 300 hours to a level of 0.895v. This level was maintained for the next 350 hours. At 650 hours the cell began to decay and continued until the low voltage refurbishment criteria was reached at 1173 hours. The cell voltage recovered to 0.890v after refill. A steady voltage decay thereafter led to its second refurbishment at 2292 hours. This cell exhibited extreme temperature sensitivity throughout much of the test; probably due to the thick matrix as in the other temperature sensitive cells. This resulted in control problems and several automatic shutdowns. Prior to shutdown a dewpoint excursion was run which showed the electrolyte volume to be less than the optimum. Increasing the dewpoint 10°F (5.6°C) resulted in a 60 millivolt gain. After refurbishment the cell voltage recovered to 0.858v. No gas crossover was found upon subjecting the matrix to 5 psig (1.38 Kg/CM^2) overpressures

Teardown of the cell showed carbonate deposits around the oxygen inlet foil and some frame delamination near the oxygen inlet ports on the anode side. A slight discoloration of the cathode near the oxygen exit ports was also seen.

Starting Date - 4/29/70

Max. O_2 Elect. Temp. -212°F (100°C)
Load-200 ASF (215.2 Ma/Cm)(Avg)
CO_2 Level-4 ppm in O_2
Hydrocarbon Level-6 to 10 ppm in O_2
Matrix-0.030" (0.0762 Cm) Asbestos
KOH Conc. -30.0%(Initial)
Electrolyte Vol. -40.8 cc (Initial)

Opt. Elect. Vol. -35.4cc
Coolant Flow-35 pph (15.9 Kg/Hr)
H_2 Flow-0.12 pph(0.054 Kg/Hr)
O_2 Flow - Consumption
Reactant Pressure-60 psia (4.218 Kg/Hr)

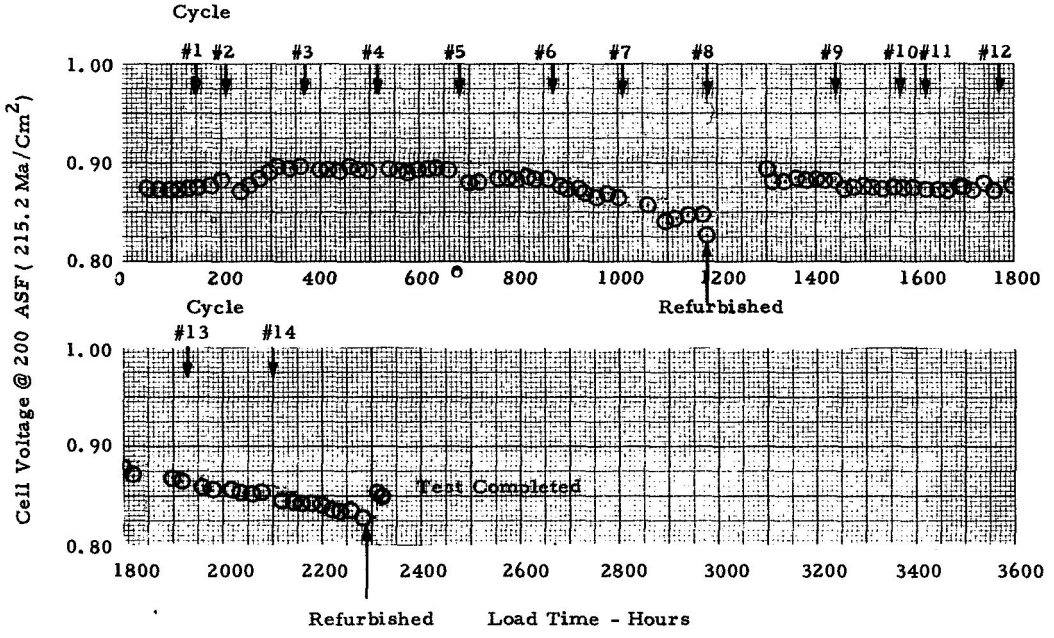

Figure 40 Cell Test No. 7 - Endurance History

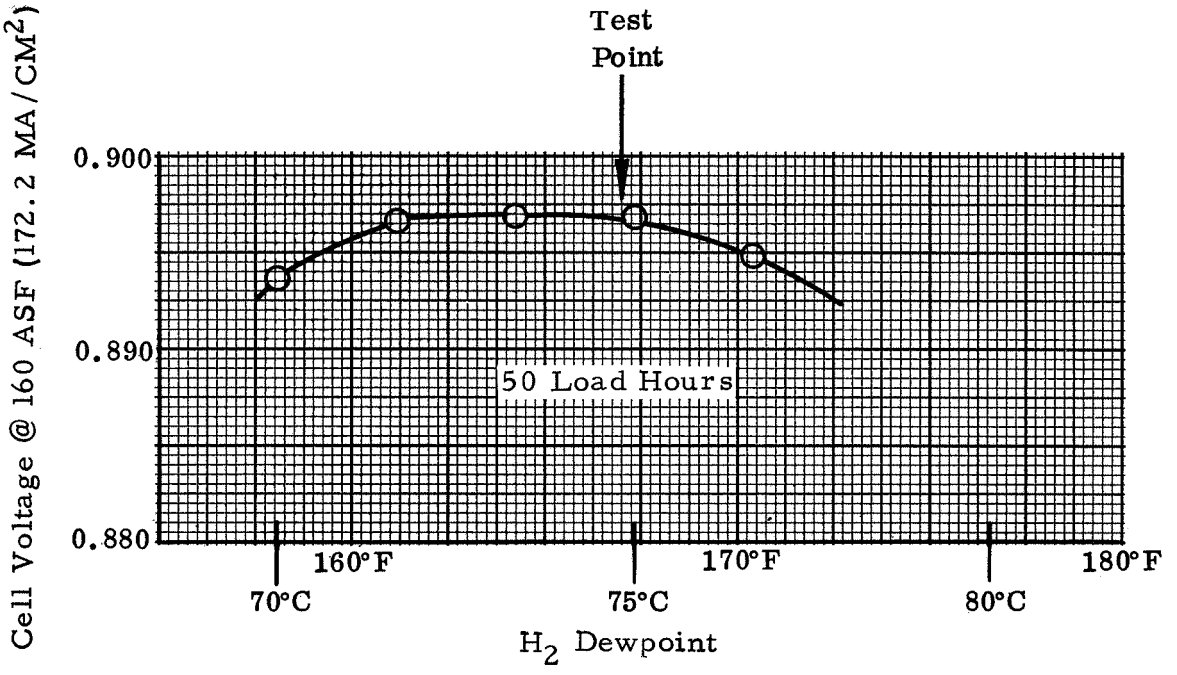

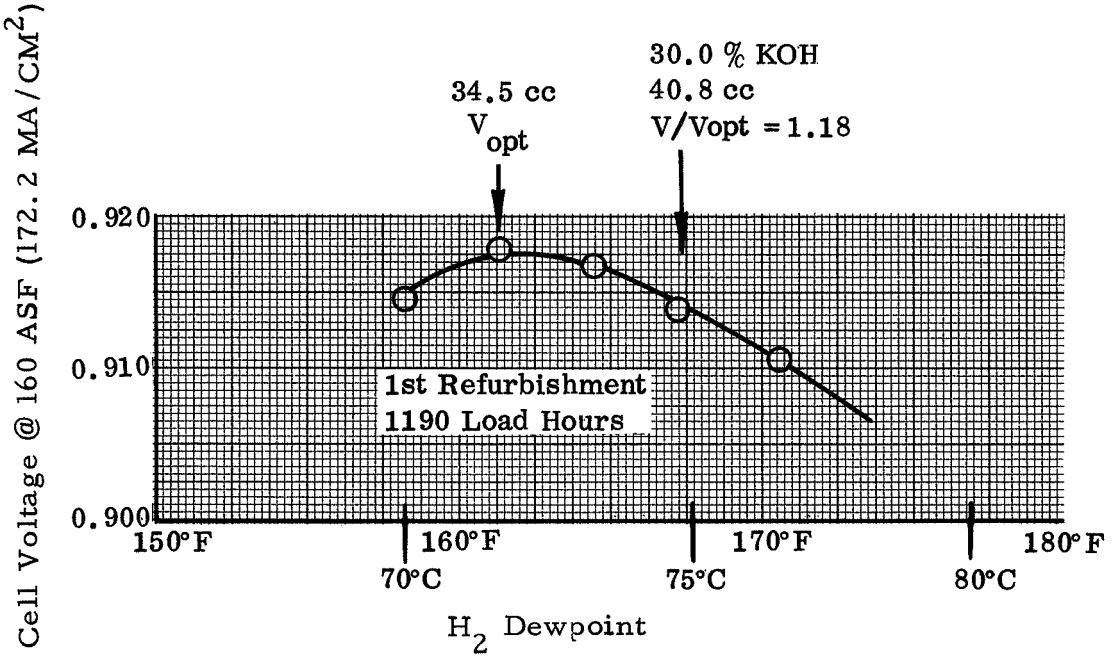

Figure 41 Cell No. 7 - Volume Tolerance Test

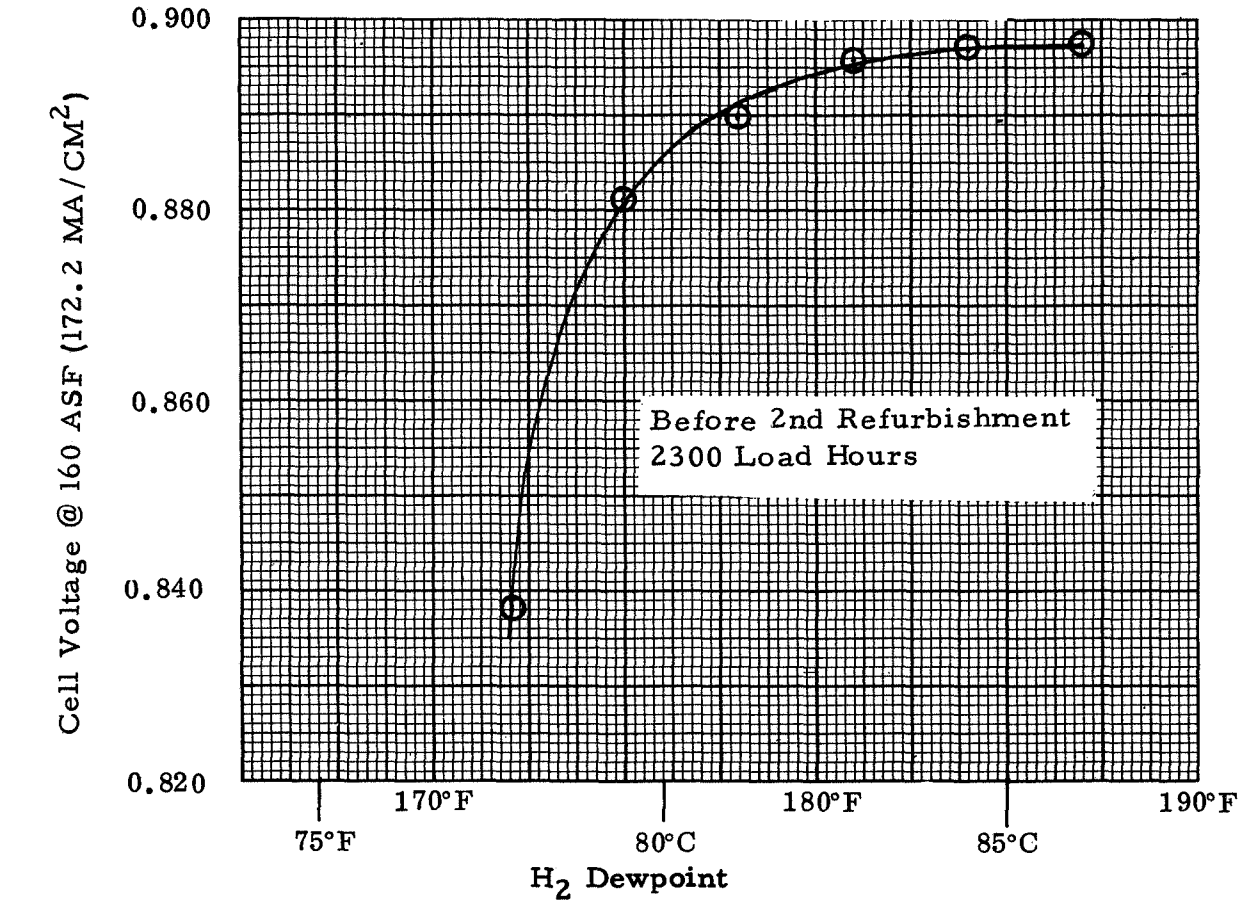

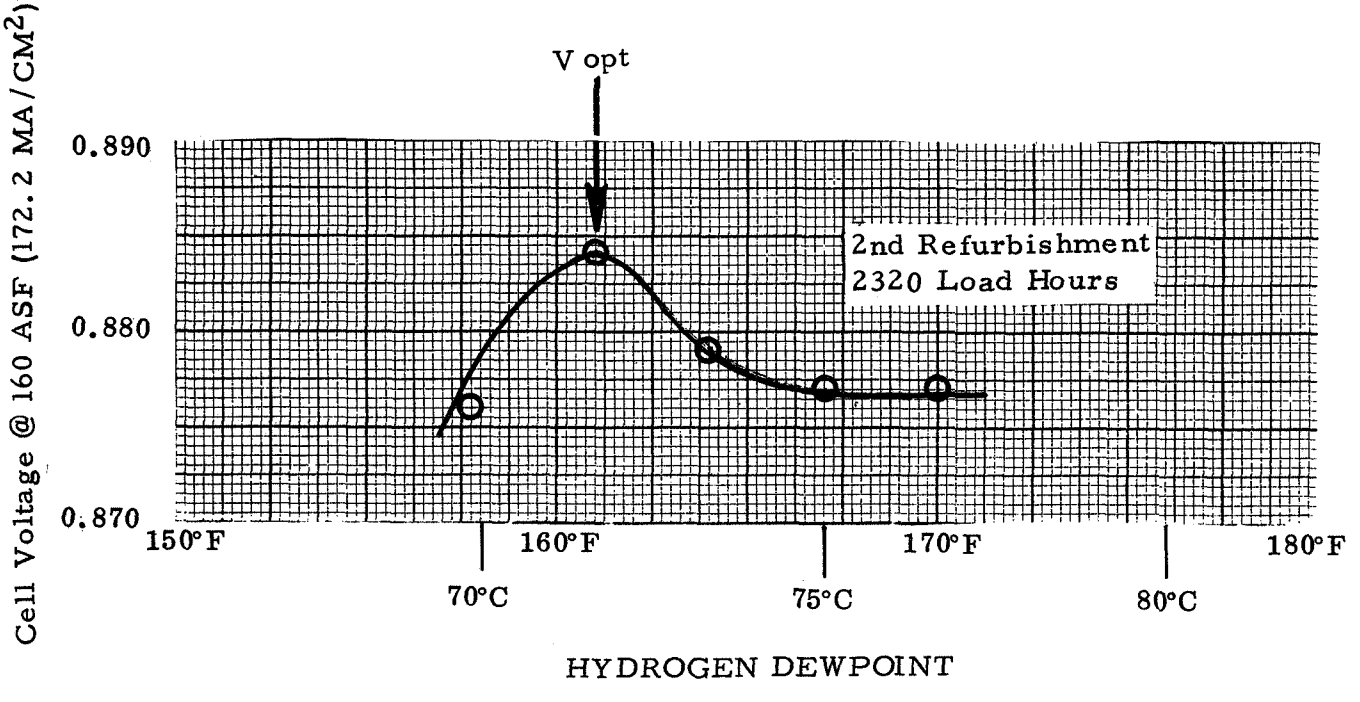

Figure 41 Cell No. 7 - Volume Tolerance Tests (Continued)

Cell Test Number 8

Cell test number eight accumulated a total of 1360 hours and 9 cycles, (Figure 42 and Figure 43). This cell exhibited a similar decay characteristic to the other PKT matrix cells dropping from an initial cell voltage of 0.920v at 200 ASF (215.2 MA/CM^2) to 0.840v in 800 hours. After refurbishment the voltage recovered to 0.895v but again decayed to 0.840v at 1315 hours when the cell was again refurbished. Recovery was to 0.868v. Subjecting the cell matrix to 5 psig (1.38 Kg/CM^2) overpressure prior to shutdown disclosed no evidence of gas cross-over. Disassembly of the cell disclosed traces of carbonate deposits around the oxygen inlet foil. Some discoloration of the cathode at the oxygen exit port was observed.

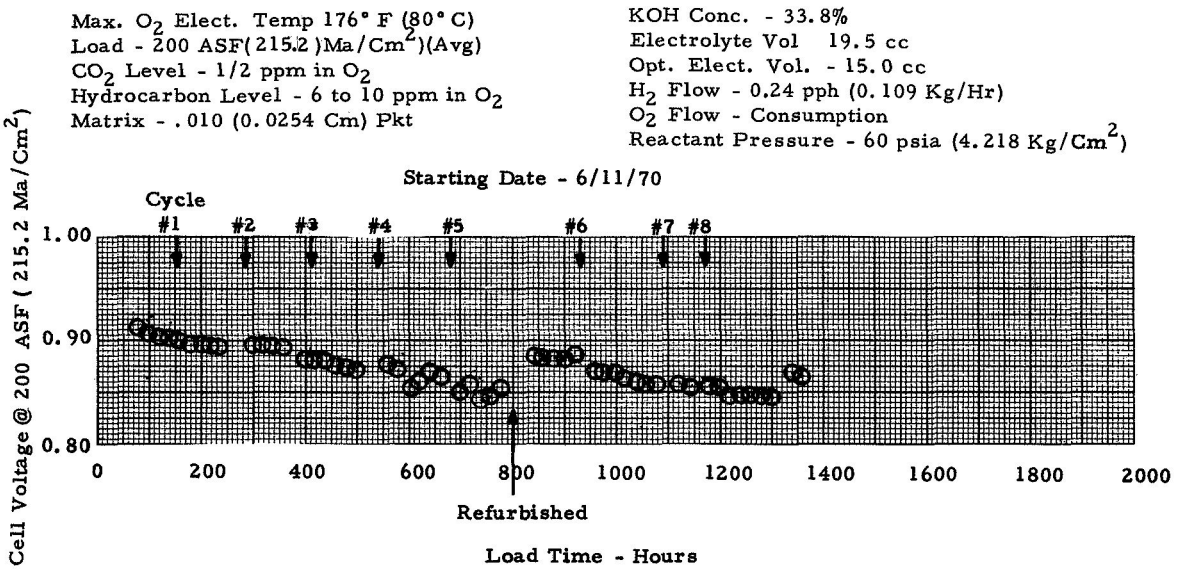

Figure 42 Cell Test No. 8 - Endurance History

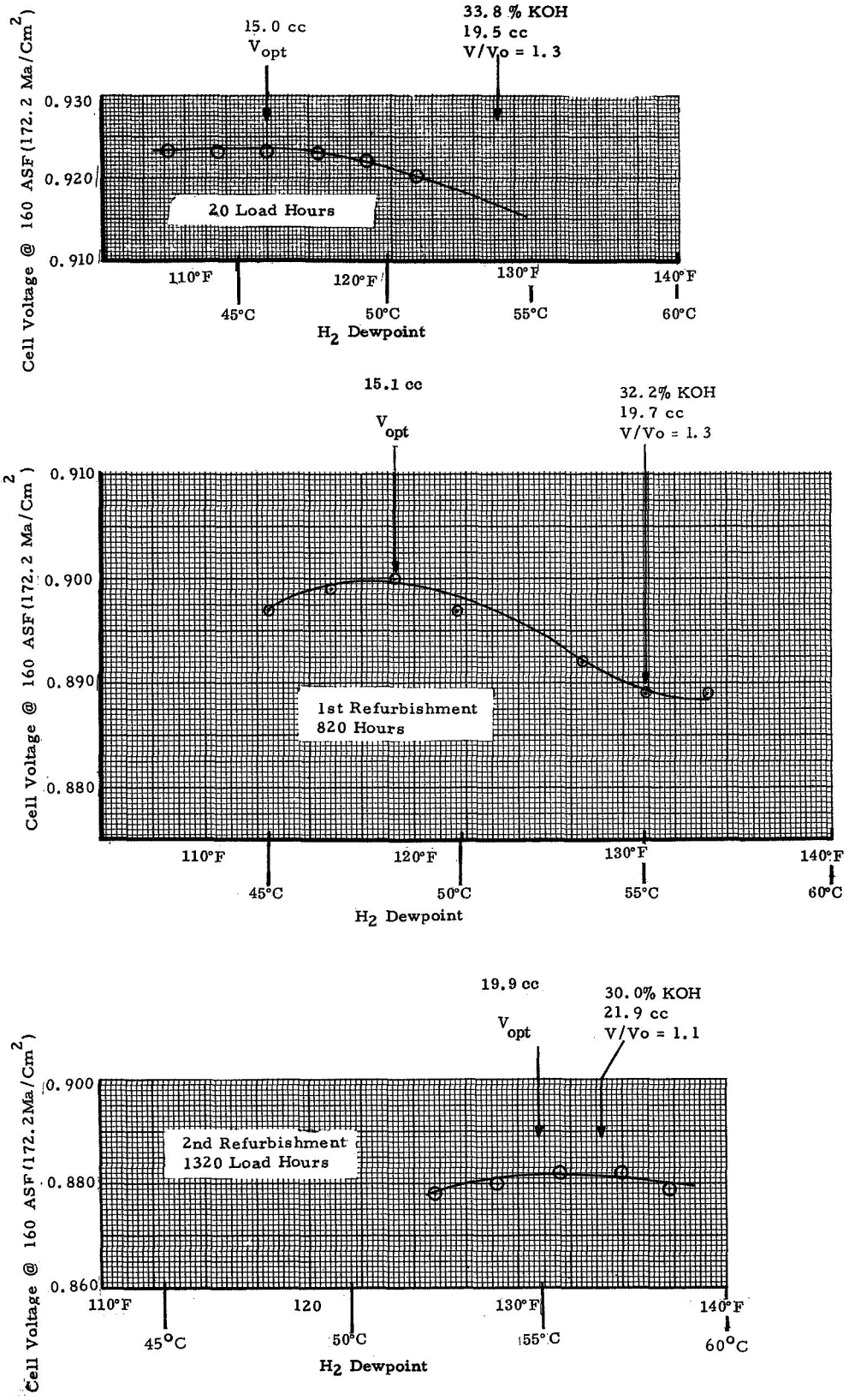

Figure 43 Cell No. 8 Volume Tolerance Test

Cell Test Number 9

Cell test number nine completed 168 load hours before gas crossover terminated the test. The initial volume tolerance characteristic is shown in Figure 44. Initial cell voltage was 0.944v at 75 ASF (80.7 MA/CM^2). This had decreased to 0.937v by the time failure occurred. Inspection of the cell at teardown disclosed no apparent reason for the crossover, although drying of the PKT matrix may have been the cause.

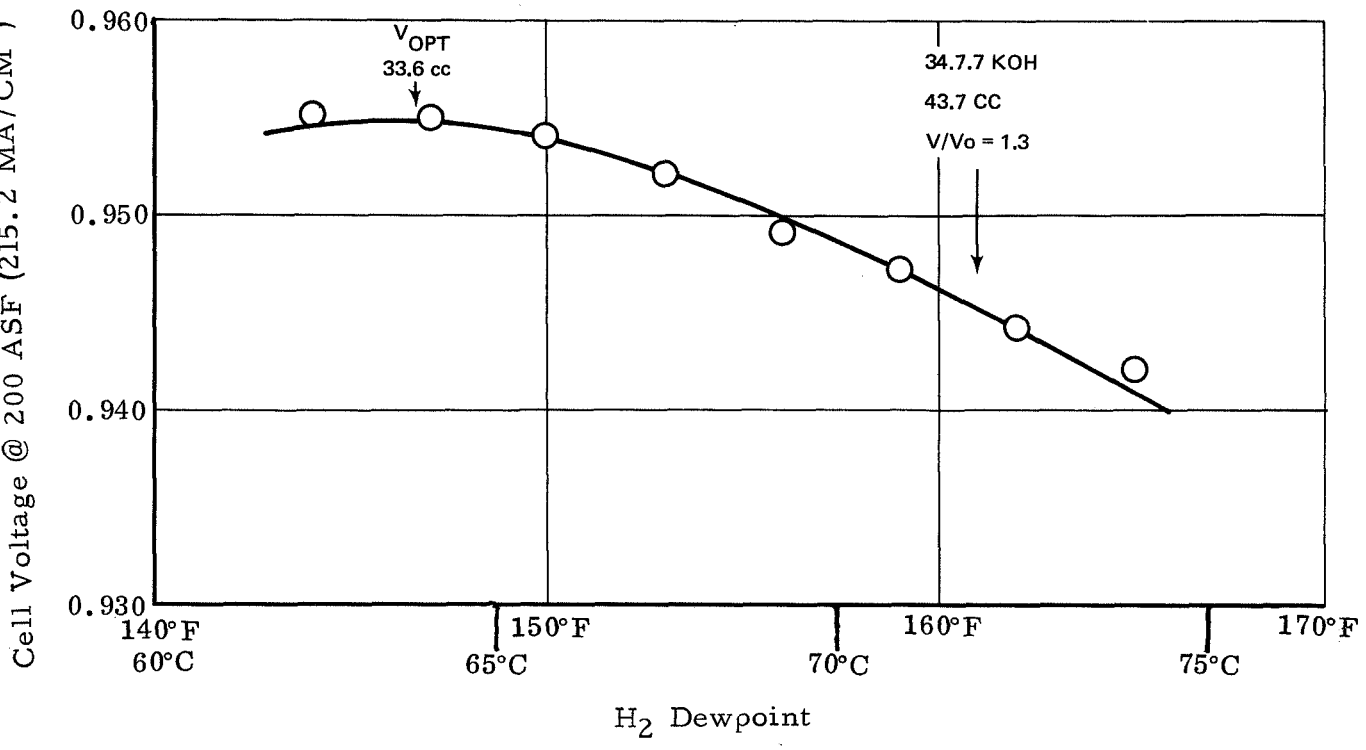

Figure 44 Cell No. 9 Volume Tolerance Test

Cell Test Number 18

Cell test number eighteen was voluntarily terminated at the end of the contract period. The cell had accumulated 410 load hours and voltage had risen from 0.926v at 75 ASF (80.7 ma/cm^2) to 0.963v in the first 260 hours. (Figure 45 and Figure 46). No evidence of crossover was found prior to shutdown. No evidence of frame or electrode deterioration was noted at teardown.

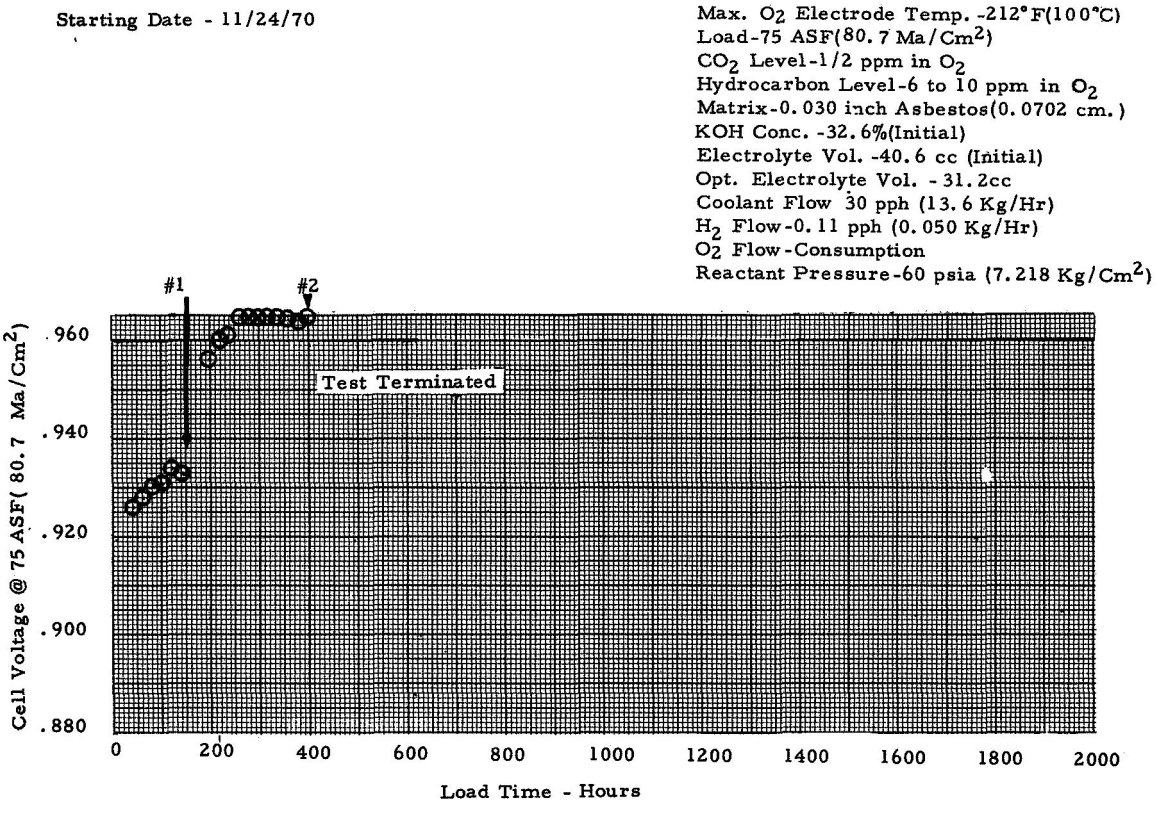

Figure 45 Cell Test No. 18 - Endurance History

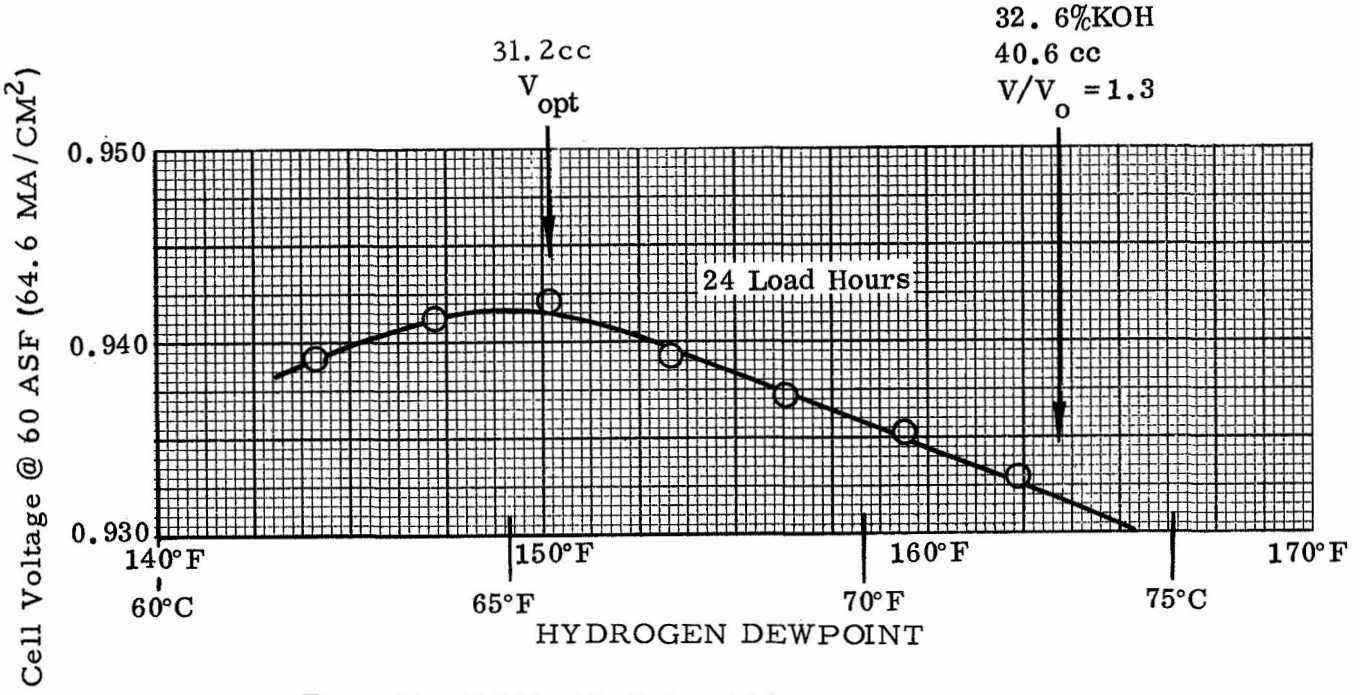

Figure 46 Cell No. 18 - Volume Tolerance Test

High Power Density Cell Test Number 1

High power density cell number one has accumulated 6100 load hours to date with no refurbishment, (Figure 47 and Figure 48). The initial performance of the cell was 0.945v at 75 ASF (80.7 ma/cm^2). The voltage varied between 0.940 and 0.945 until 1200 hours. At this time the voltage began a gradual rise which continued until 0.973v was reached at 2350 hours. The voltage remained in this region until 4300 hours when it began to decrease gradually to the present level of 0.958v at 6100 hours. Hydrogen dewpoint excursions have been run periodically which indicate no loss of electrolyte volume tolerance.

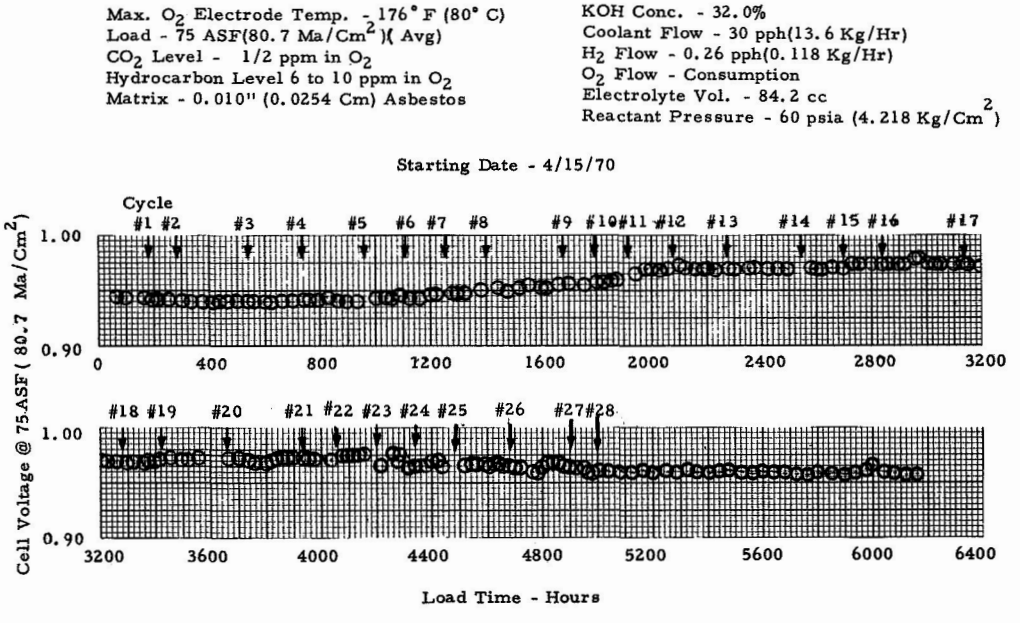

Figure 47 High Power Density Cell Test No. 1 - Endurance History

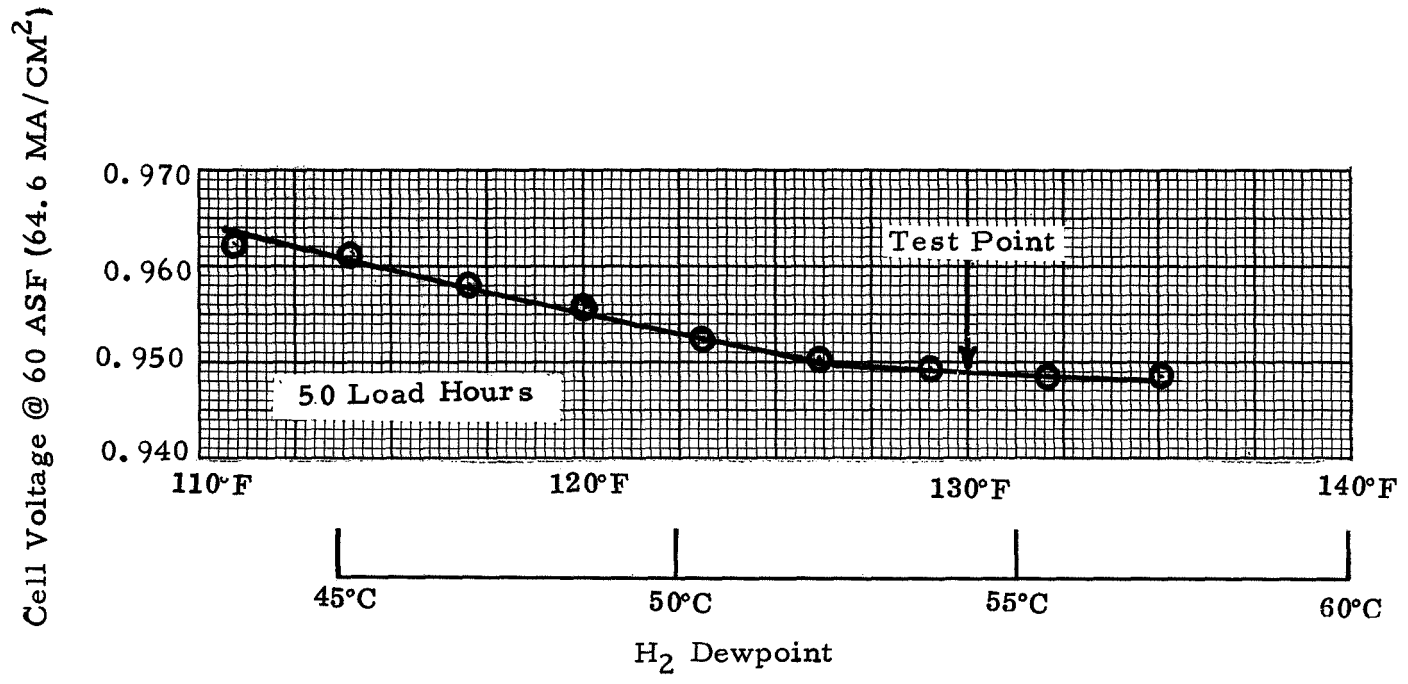

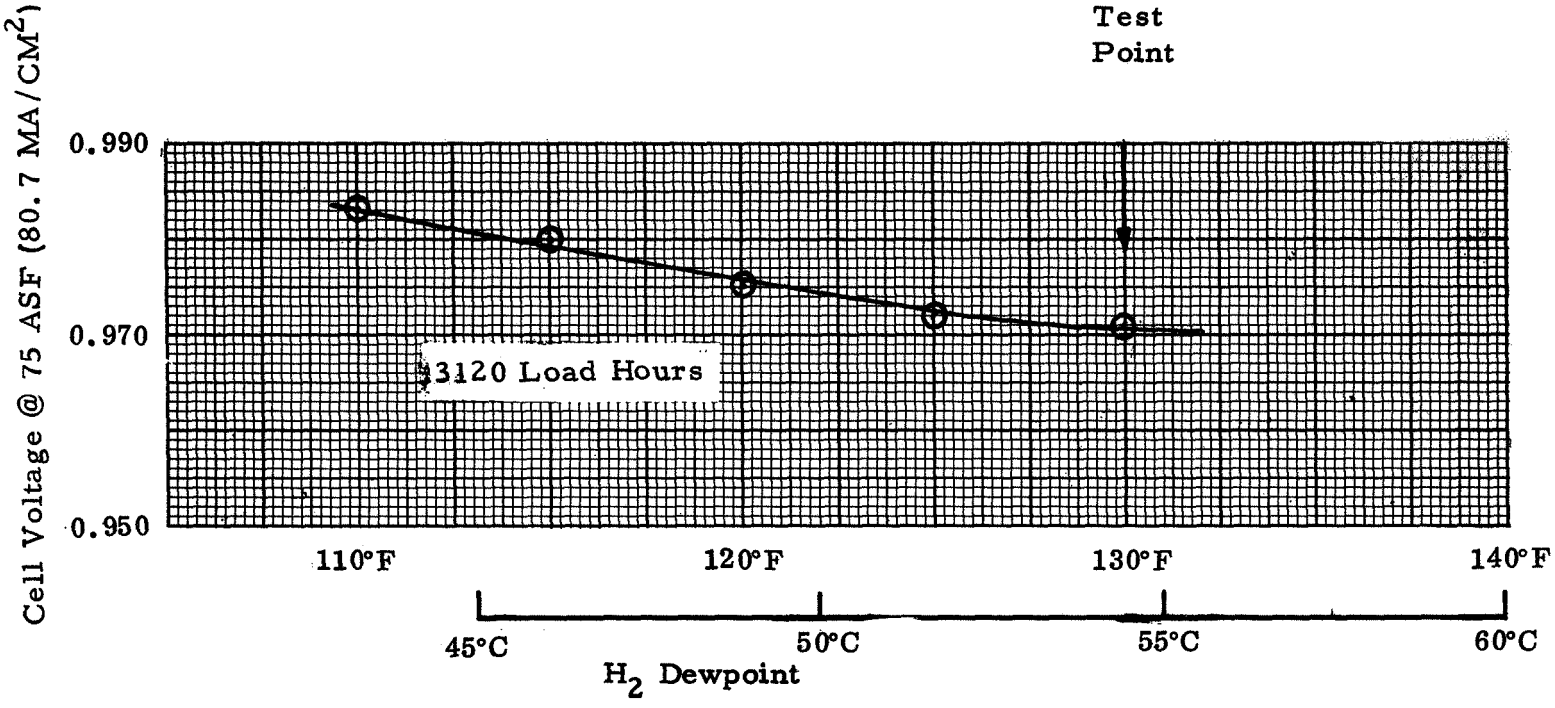

Figure 48 High Power Density Cell No. 1 - Volume Tolerance Tests

High Density Cell Test Number 2

High power density cell test number two completed 3587 hours before a malfunction in the stand hydrogen vent system resulted in cell flooding and termination of the test, (Figure 49 and Figure 50). The cell voltage which initially was 0.904v at 200 ASF (215.2 ma/cm^2) remained steady until 2400 hours. Following a restart, the cell voltage was down 0.010v, however. The voltage continued to increase over the next 560 hours until the cell voltage reached 0.937v. After this the voltage decreased to 0.921v at the end of the test. Hydrogen dewpoint excursions had revealed no loss of electrolyte volume tolerance up to 3000 hours.

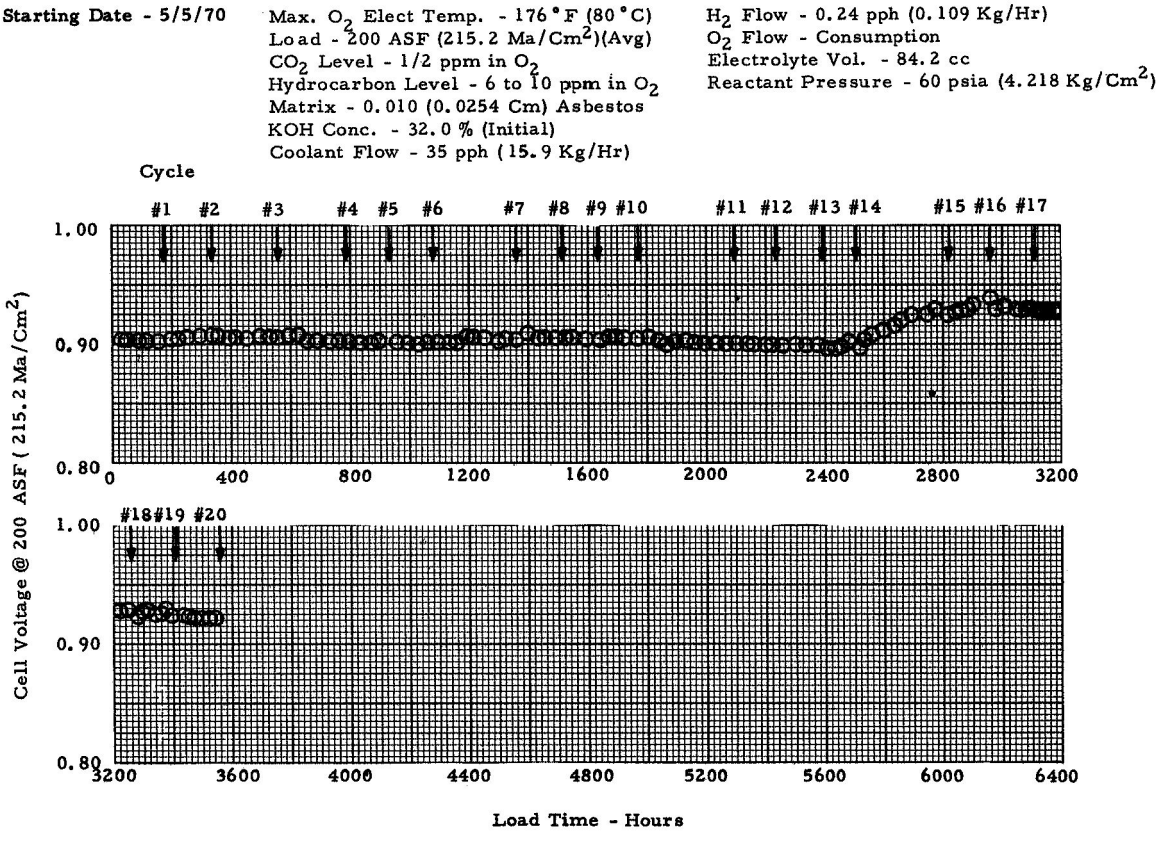

Figure 49 High Power Density Cell Test No. 2 - Endurance History

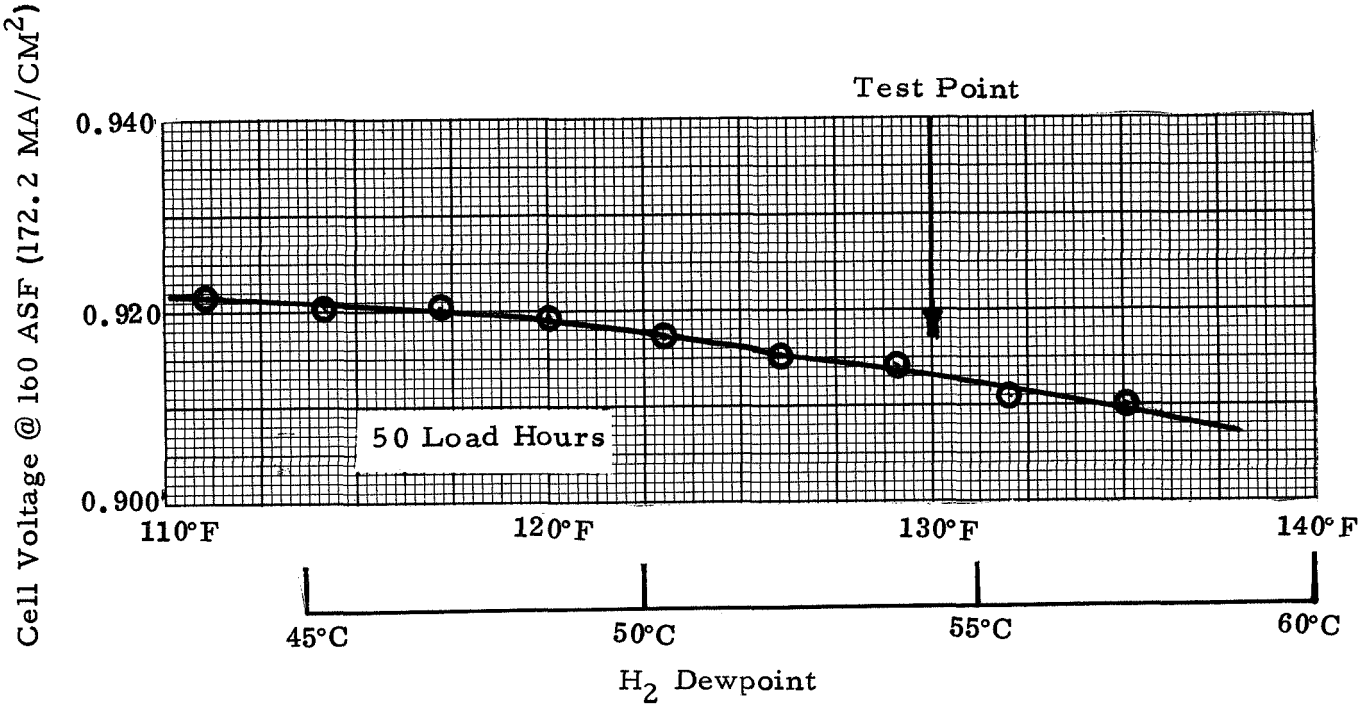

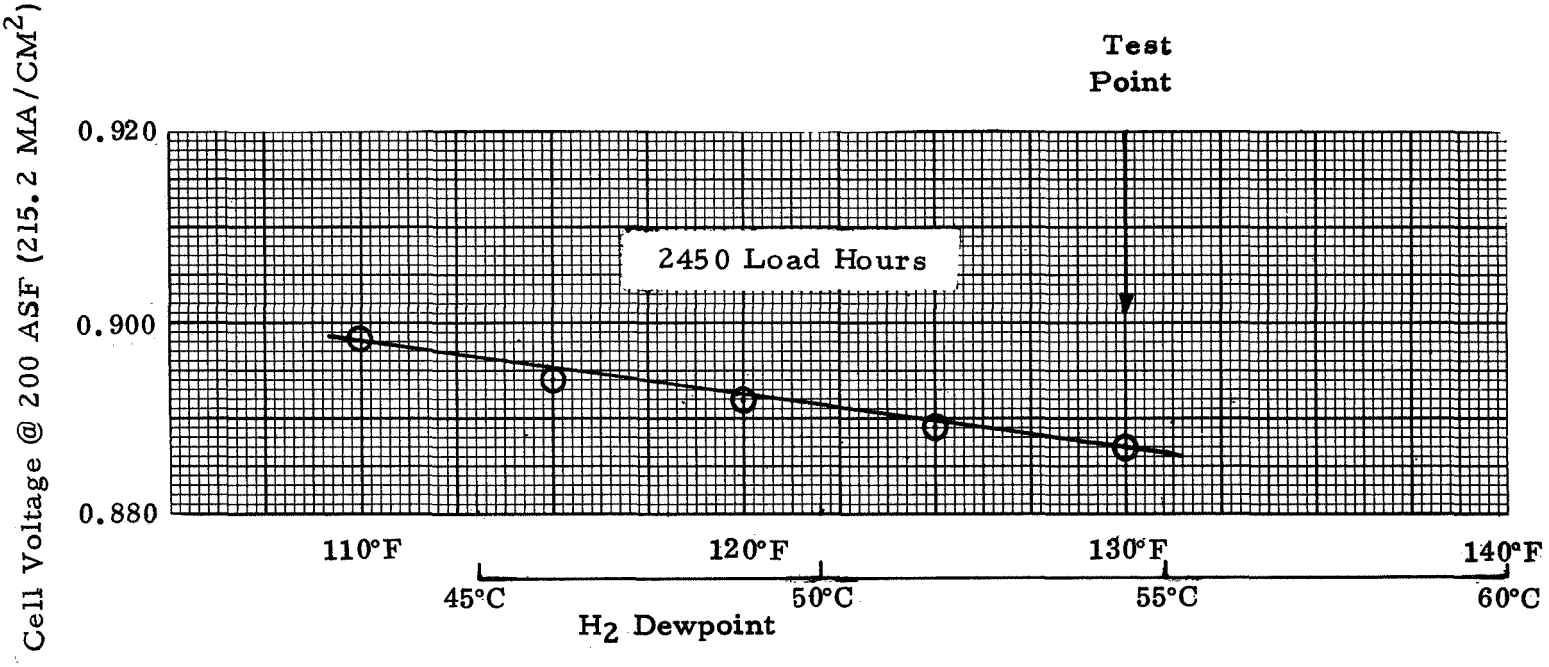

Figure 50 High Power Density Cell No. 2 - Volume Tolerance Tests

B. Cell Test Data Summary

This section summarizes the data obtained from all cell tests run under the contract. Information is included on cell physical configuration and test conditions as well as data on life, electrolyte fill and analysis, and electrode analysis.

The cells tested are identified in Table 2 by their sequence number. This table shows the combination of factor levels for each test. Additional details of the physical configuration of each cell are shown in Table 3. The actual uncompressed thickness of the matrix used is shown as matrix thickness and the amount of matrix compression when clamped in the test hardware is shown as matrix pinch. Porosimeter tests were performed on each sinter anode and the results are shown under hydrogen electrode porosity. The measured thickness of the hydrogen and oxygen electrodes and the actual catalyst loading for each are listed.

Cell operating conditions are summarized in Table 4. The coolant inlet and exit temperatures were measured by thermocouples in the coolant plates. The hydrogen dewpoint temperature is the temperature of the saturated hydrogen stream entering the cell. The hydrogen flow is the mass flow of dry hydrogen passing into the cell. This hydrogen is humidified in the saturator before entering the cell. The carbon dioxide level is the parts per million by volume of CO_2 in the oxygen supply. This level is monitored continuously by the LIRA gas analysis device.

The life data obtained is summarized in Table 5. The load time shown excludes the one day each week that the cell is shutdown and stored on dry nitrogen. The number of weekly load cycles is also shown. Cell No. 4 is continuing on test and has accumulated over 6400 hours to date.

Electrolyte fill data for the cells is shown in Table 6. The fill weight was determined by weighing a new unitized cell before and after filling with electrolyte. The difference between these two weights is the weight of electrolyte in the cell. At the first and second refurbishments the cell was not removed from the test hardware, and consequently it was not possible to measure the fill weight. The initial fill weight can be used for the fill weight at the refurbishments when necessary. The initial fill concentration is selected to allow cell operation with concentration between 30 and 34 percent and electrolyte volume between 1.1 and 1.3 times the optimum volume. In certain cases the fill concentration for the first and second refurbishments was different than for the initial fill as a result of experience with the first fill. The fill weight for all the cells with 0.010 inch (0.0254 cm) thick matrices was between 43 and 48 grams. The fill weight for all the 0.030 inch (0.0762 cm) thick matrix cells was between 59 and 74 grams.

It was never necessary to use the electrolyte fill tube to adjust the electrolyte volume in a cell after filling. In the test of cell No. 1 electrolyte was lost during operation due to an automatic stand shutdown. The lost electrolyte was successfully replaced using the electrolyte fill tube.

Post-Test Analysis

The carbonate and hydroxyl ion concentrations of the electrolyte and the polarization of the hydrogen and oxygen electrodes were measured after disassembly of the cell. All components were visually examined for corrosion and other forms of deterioration when the cell was disassembled. The results of this visual examination are included in Section VI.A. Additional data obtained includes hydroxyl and carbonate ion concentrations before each refurbishment and the air-oxygen voltage gain after disassembly of the cell.

The electrolyte analysis data is summarized in Table 7. The data was obtained just prior to each refurbishment and after disassembly of the cell upon completion of the test. In the column "number of refurbishments" a "0" indicates the data was obtained during the first endurance run. A "1" indicates the data was obtained during the second endurance run. A "2" indicates the data was obtained after the second refurbishment when the cell was disassembled. The optimum electrolyte volume is calculated from the fill weight, concentration, cell temperature and hydrogen stream dewpoint temperature. The optimum volume is the volume which results in the highest cell voltage immediately after the cell is filled. A typical calculation of optimum volume is shown below:

Average Cell Temperature – 195°F (90.6°C)
Optimum H_2 Dewpoint – 170°F (76.7°C)

From properties of KOH:

Concentration – 32%
Specific Gravity – 1.27 gm/cc

From cell fill data:

Fill concentration – 15%
Fill Weight – 40 gm
Weight of KOH in Cell – .15 x 40 = 6 gm

Weight of Electrolyte at Optimum Dewpoint:

$$\text{Weight} = \frac{6 \text{ gm KOH}}{.32} = 18.7 \text{ gm}$$

Volume of Electrolyte at Optimum Dewpoint:

$$\text{Optimum Volume} = \frac{18.7}{1.27} = 147\text{cc}$$

The electrolyte is flushed from the cell with distilled water. The volume of flush water used is also shown in Table 7. The electrolyte flush prior to the first and second refurbishment is accomplished by filling the reactant passages in the cell test rig with water. The water and electrolyte are allowed to equilibrate for six hours and then the water is drained from the test rig and analyzed. The final electrolyte flush after the second refurbishment is accomplished after the cell is removed from the test hardware by immersing the cell in a container of water and allowing the water and electrolyte to equilibrate for six hours. The hydroxyl and carbonate ion concentration, are determined using a double end point titration. The table shows the measured concentrations in grams of KOH or K_2CO_3 per cubic centimeter of flush water solution. If it is desired to determine the total grams of KOH or K_2CO_3 in the cell, the volume of electrolyte in the cell prior to flushing must be estimated. Eighty percent of the optimum electrolyte volume can be used for those cells on which the refurbishment criteria was met because their voltage decay is usually due to low electrolyte volume. The volume in the cell is added to the flush water volume and the sum is multiplied by the KOH or K_2CO_3 concentration to obtain the total grams of each constituent in the cell.

Total silicon content can be obtained in the same way using the silicon concentration data in the last column of Table 7

Both electrodes were analyzed at the termination of each cell test. The potential of the sinter anode was measured and the screen cathode was analyzed for oxygen potential and air potential. The results of these tests are summarized in Table 8.

The potential of each electrode is measured on two inch diameter specimens assembled into a single cell using a new 0.010 inch (0.0254 cm) asbestos matrix. This cell incorporates a hydrogen reference electrode probe to determine separate polarizations of each electrode. The cell is tested at 15 psia (1.05 Kg/cm^2) and 160°F (71.1°C) with a 140°F (60°C) oxygen dewpoint. Three current densities were run: 100, 200, and 300 AMPS/FT^2 (107.6, 215.2, 322.8 ma/cm^2). The cathode potential is measured relative to the reference electrode. The potential difference between the anode and the reference electrode is the anode potential. The cell voltage is the cathode potential minus the anode potential. This voltage is lower than the voltage of the full size test cell because of the lower pressure used in the electrode tests and because the electrolyte volume is not adjusted to the optimum value. Cathode potential was also measured on scrubbed air as well as oxygen. The difference between the air and oxygen potentials is shown in Table 8 also, and is a measure of oxygen diffusional losses in the cathode. A new cathode typically has an air-oxygen potential gain of 36 millivolts at 100 amps/ft^2, (107.6 ma/cm^2), 57 millivolts at 200 amps/ft^2 (215.2 ma/cm^2) and 83 millimillivolts at 300 amps/ft^2 (322.8 ma/cm^2).

TABLE 2

CELL TEST SEQUENCE AND FACTOR LEVELS

Test Number	Max. O_2 Elec. Temp.		CO_2 in O_2	Matrix Thickness		Current Density ASF	Current Density ma/cm^2	Matrix Material
1	176°F	(80°C)	< ½ PPM	0.03"	(0.0762 cm)	200	(215.2)	ASB
2	212°F	(100°C)	< ½ PPM	0.01"	(0.0254 cm)	200	(215.2)	ASB
3	212°F	(100°C)	< ½ PPM	0.01"	(0.0254 cm)	75	(80.7)	PKT
4	176°F	(80°C)	4 PPM	0.03"	(0.0762 cm)	75	(80.7)	ASB
5	212°F	(100°C)	< ½ PPM	0.03"	(0.0762 cm)	200	(215.2)	PKT
6	176°F	(80°C)	4 PPM	0.01"	(0.0254 cm)	75	(80.7)	PKT
7	212°F	(100°C)	4 PPM	0.03"	(0.0762 cm)	200	(215.2)	ASB
8	176°F	(80°C)	< ½ PPM	0.01"	(0.0254 cm)	200	(215.2)	PKT
9	212°F	(100°C)	4 PPM	0.03"	(0.0762 cm)	75	(80.7)	PKT
18	212°F	(100°C)	< ½ PPM	0.03"	(0.0762 cm)	75	(80.7)	ASB

TABLE 3

CELL CONFIGURATION DATA

Test No.	Matrix Type	Matrix Thickness (inches)	(cm)	Matrix Pinch (inches)	(cm)	H_2 Elect Porosity %	H_2 Elect Thickness (inches)	(cm)	H_2 Elect Catalyst Loading (mg/cm^2)	O_2 Elect Thickness (inches)	(cm)	O_2 Elect Catalyst Loading (mg/cm^2)
1	ASB	0.030	(0.0762)	0.005	(0.0127)	73	0.0305	(0.0775)	20	0.005	(0.0127)	10.8
2	ASB	0.0105	)0.0267)	0.0045	(0.0114)	73	0.0305	(0.0775)	20	0.0055	(0.0140)	10.4
3	PKT	0.010	(0.0254)	0.004	(0.0102)	73	0.0305	(0.0775)	20	0.0055	(0.0140)	10.0
4	ASB	0.0305	(0.0775)	0.0045	(0.0114)	74	0.0305	(0.0775)	20	0.005	(0.0127)	10.4
5	PKT	0.030	(0.0762	0.006	(0.0152)	73	0.030	(0.0762)	20	0.0055	(0.0140)	10.8
6	PKT	0.010	(0.0254)	0.0045	(0.0114)	73	0.0305	(0.0775)	20	0.0055	(0.0140)	9.7
7	ASB	0.030	(0.0762)	0.0045	(0.0114)	72	0.0305	(0.0775)	20	0.0055	(0.0140)	10.8
8	PKT	0.010	(0.0254)	0.0040	(0.0102)	74	0.0305	(0.0775)	20	0.005	(0.0127)	10.6
9	PKT	0.030	(0.0762)	0.0045	(0.0114)	73	0.0305	(0.0775)	20	0.0055	(0.0140)	10.3
18	ASB	0.030	(0.0762)	0.0045	(0.0114)	73	0.0305	(0.0775)	20	0.0055	(0.0140)	9.8

TABLE 4
CELL OPERATING CONDITIONS

Test #	Load (ASF)	Load (MA/CM^2)	Coolant Inlet Temp (°F)	Coolant Inlet Temp (°C)	Coolant Exit Temp (°F)	Coolant Exit Temp (°C)	Coolant Flow (PPH)	Coolant Flow (Kg/Hr)	H_2 Dewpoint Temp (°F)	H_2 Dewpoint Temp (°C)	H_2 Flow (PPH)	H_2 Flow (Kg/Hr)	Reactant Press (PSIA)	Reactant Press (Kg/CM^2)	Coolant Press (PSIA)	Coolant Press (Kg/CM^2)	CO_2 Level (PPM)
1	200	(215.2)	154	(67.8)	174	(78.9)	35	(15.9)	133	(56.1)	0.24	(0.109)	60	(4.218)	55	(3.867)	< 1/2
2	200	(215.2)	190	(87.8)	210	(98.9)	35	(15.9)	164	(73.3)	0.12	(0.054)	60	(4.218)	55	(3.867)	< 1/2
3	75	(80.7)	190	(87.8)	198	(92.2)	30	(13.6)	161	(71.7)	0.11	(0.050)	60	(4.218)	55	(3.867)	< 1/2
4	75	(80.7)	154	(67.8)	162	(72.2)	30	(13.6)	130	(54.4)	0.26	(0.118)	60	(4.218)	55	(3.867)	4
5	200	(215.2)	190	(87.8)	210	(98.9)	35	(15.9)	164	(73.3)	0.12	(0.054)	60	(4.218)	55	(3.867)	< 1/2
6	75	(80.7)	154	(67.8)	162	(72.2)	30	(13.6)	129	(57)	0.26	(0.118)	60	(4.218)	55	(3.867)	4
7	200	(215.2)	190	(87.8)	210	(98.9)	35	(15.9)	167	(75)	0.12	(0.054)	60	(4.218)	55	(3.867)	4
8	200	(215.2)	154	(67.8)	174	(78.9)	35	(15.9)	129	(57)	0.24	(0.109)	60	(4.218)	55	(3.867)	< 1/2
9	75	(80.7)	190	(87.8)	198	(92.2)	30	(13.6)			0.11	(0.050)	60	(4.218)	55	(3.867)	4
18	75	(80.7)	190	(87.8)	198	(92.2)	30	(13.6)	163	(72.8)	0.11	(0.050)	60	(4.218)	55	(3.867)	< 1/2

TABLE 5
CELL LIFE DATA

Test No.	Total Load Time	No. of Cycles	Time to 1st Refurb.	Time to 2nd Refurb.	Max. O_2 Elec. Temp.	CO_2 in O_2	Matrix Thickness	Current Density (ASF)	Current Density (NA/CM^2)
1	2468	17	1426	2399	176°F (80°C)	< ½ PPM	0.03" (0.0762CM)	200	(215.2)
2	1010	7	1010	---	212°F (100°C)	< ½ PPM	0.01" (0.0254CM)	200	(215.2)
3	1820	11	1354	1791	212°F (100°C)	< ½ PPM	0.01" (0.0254CM)	75	(80.7)
4	6400	38	5000		176°F (80°C)	< 4 PPM	0.03" (0.0762CM)	75	(80.7)
5	1425	9	645	1320	212°F (100°C)	< ½ PPM	0.03" (0.0762CM)	200	(215.2)
6.	529	3	---	---	176°F (80°C)	4 PPM	0.01" (0.0254CM)	75	(80.7)
7	2344	15	1173	2292	212°F (100°C)	4 PPM	0.03" (0.0762CM)	200	(215.2)
8	1360	9	800	1315	176°F (80°C)	< ½ PPM	0.01" (0.0254CM)	200	(215.2)
9	168	1	---	---	212°F (100°C)	4 PPM	0.03" (0.0762CM)	75	(80.7)
18	410	2		---	212°F (80°C)	< ½ PPM	0.03" (0.0762CM)	75	(80.7)

TABLE 6

ELECTROLYTE FILL DATA

Test Number	Fill Weight (grams)	Initial Fill Conc. (% KOH)	1st Refurb. Fill Conc. (% KOH)	2nd Refurb. Fill Conc. (% KOH)
1	59.4	22.8	22.8	22.5
2	43.8	20.8	20.8	20.8
3	47.9	18.0	20.7	17.6
4	65.1	24.3	24.3	--
5	72.7	26.0	26.0	26.0
6	47.6	20.8	--	--
7	64.1	23.5	23.5	23.5
8	46.0	19.8	19.0	19.0
9	73.5	26.1	25.5	--
18	64.4	26.0	--	--

TABLE 7

POST-TEST
ELECTROLYTE ANALYSIS DATA

Test Number	Number of Refurb.	Optimum Elect. Volume (cc)	Flush Water Volume (cc)	Flush KOH Conc. (gm/cc)	Flush K_2CO_3 Conc. (gm/cc)	Flush Si Conc. (mg/cc)	KOH Convert to K_2CO_3 (%)
1	0	–	–	– –	– –	–	–
	1	30.7	190	0.0552	0.00358		5.1
	2	30.7	200	0.0584	0.00145		2.0
2	0	18.4	158	0.0353	0.0130		23.0
	1	–	–	– –	– –	–	–
	2	–	–	– –	– –	–	–
3	0	15.3	200	0.0256	0.0090	–	22.2
	1	14.6	194	0.0248	0.00228	0.14	7.0
	2	16.7	189	0.0361	0.00158	–	3.5
4	0	30.4	186	0.0443	0.0312	0.15	36.5
	1	–	–	– –	– –	–	–
	2	–	–	– –	– –	–	–
5	0	39.6	–	– –	– –	–	–
	1	37.7	184	0.0625	0.00554	–	6.9
	2	32.9	200	0.0780	0.00255	–	2.6
6	0	17.0	200	0.0290	0.0077	0.20	17.9
	1	–	–	– –	– –	–	–
	2	–	–	– –	– –	–	–
7	0	35.4	186	0.0444	0.0173	–	24.0
	1	34.5	172	0.0478	0.0174	–	22.3
	2	34.5	180	0.0627	0.0024	–	3.1
8	0	15.0	185	0.0296	0.00621	–	14.7
	1	15.1	187	0.0367	0.00396	–	8.2
	2	19.9	–	– –	– –	–	–
9	0	33.6	–	– –	– –	–	–
	1	–	–	– –	– –	–	–
	2	–	–	– –	– –	–	–
18	0	31.2	179	0.0635	0.0068	–	8.2
	1	–	–	– –	– –	–	–
	2	–	–	– –	– –	–	–
PWA o/c	0	18.4	150	0.0370	0.0118	–	20.7

TABLE 8

ELECTRODE POLARIZATION DATA

Test Number	Anode Potential 100 ASF (107.6 ma/cm^2)	200 ASF (216.2 ma/cm^2)	mv 300 ASF (322.8 ma/cm^2)	Cathode Potential 100 ASF (107.6 ma/cm^2)	200 ASF (215.2 ma/cm^2)	mv 300 ASF (322.8 ma/cm^2)	Cathode Air - O_2 Gain 100 ASF (107.6 ma/cm^2)	200 ASF (215.2 ma/cm^2)	mv 300 ASF (322.8 ma/cm^2)
2	16	46	80	870	788	718	88	107	160
3	9	17	27	752	640	590	127	159	167
4	Cell Still On Test								
5	62	118	–	839	719	–	96	403	–
6	32	62	79	886	842	833	88	109	228
7	34	82	174	784	706	619	64	134	297
8	4	16	37	738	611	453	122	215	241
9	9	29	58	884	840	800	–	–	–
18	15	28	43	813	750	720	56	85	148

NOTE: Cell Voltage = Cathode Potential - Anode Potential

VII. DATA ANALYSIS

The objective of this program is to examine the effects of changing the following variables from a low to high level on time-to-refurbishment of the fuel cell:

Variable	Level Low	Level High
Maximum O_2 Electrode Temperature	176°F (80°C)	212°F (100°C)
CO_2 Level in Reactants	1/2 ppm	4 ppm in O_2
Matrix thickness	10 mils (0.254 MM)	30 mils (0.762 MM)
Current Density	75 asf (80.7 MA/CM^2)	200 asf (215.2 MA/CM^2)
Matrix Material	ASB	PKT

The refurbishment criterion is the loss of 0.05 volts from the average voltage exhibited for the first hundred (100) hours of operation.

A one-half (1/2) fractional factorial program was initially designed to study the effects of the above variables. However, only seven cell tests were completed. A formal Yates method of analysis cannot be completed on this data set. However, by implementing the technique of regression analysis, some insight can be gained concerning the trends exhibited by the data.

The regression equations presented explain the fuel cell operating life as "best" as possible given the limited sample. The data used in the analysis was normalized, -1 for the low level and +1 for the high level, in order to examine the main effects and interactions of the input variables on the operating life of the fuel cell. The regression analysis is then used to select the variables which seem to be most responsible for controlling the life capability of the cells. Care must be taken when investigating the cause-and-effect relationships because of the small sample tested which causes confounding of the variables and loss of balance between variables.

A two-phase analysis was performed to investigate the effect of the variable on the fuel cell's time to first refurbishment and time to second refurbishment. The data available for analysis is shown in Figure 51.

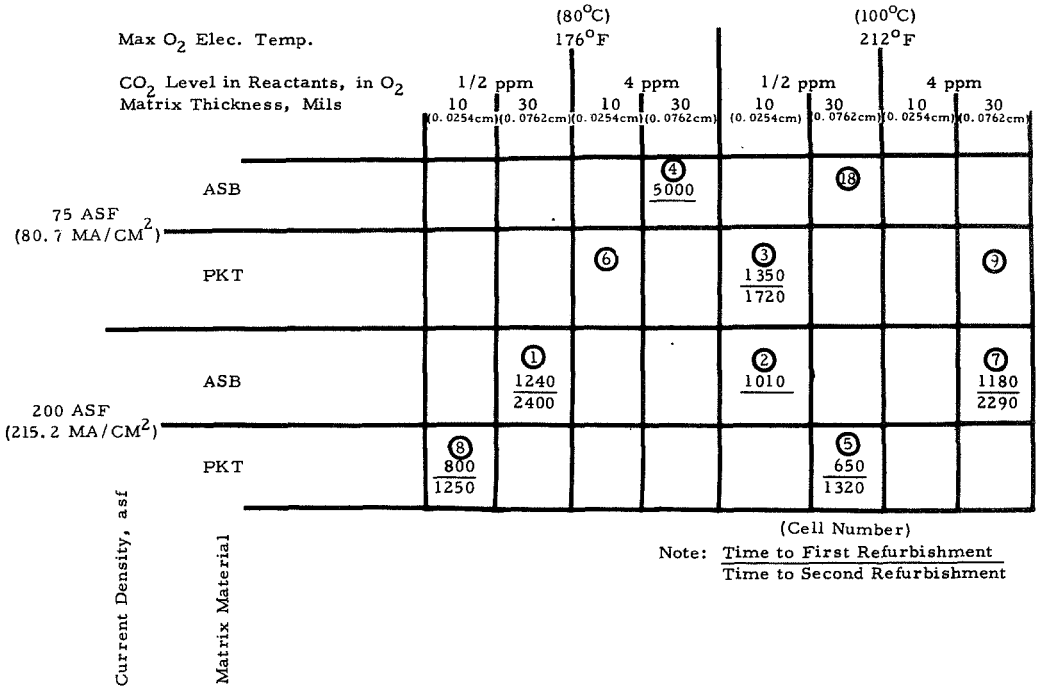

Figure 51 Cell Life Data

The correlation coefficients for the time to the first refurbishment for each of the variables and their two factor interactions are shown in Figure 52. All comparisons for significant correlation coefficients were based on a 95% confidence level. Current density has the highest coefficient. Although CO_2 level also has a high coefficient it is confounded with current density. The least-square regression equation for time to first refurbishment of the fuel cell is:

$$\text{Time to Refurbishment} = 2054.6 - 1120.4\,X_4 - 1070.8\,X_5 + 807.9\,(X_4X_5) \pm 115.1$$

with: X_4 = Current Density

X_5 = Matrix Material

-1 = Low Level

+1 = High Level, for each input variable

This equation signifies that two variables are of primary importance in explaining the number of hours to cell refurbishment. These are current density and matrix material, both of which should be at the low level (75 ASF and asbestos, respectively) to take advantage of the interaction effect and further promote long-life capability in fuel cells. Fuel cell average operating life decreased from 3175 to 976 Hours by increasing the current density from 75 to 200 ASF (80.7 to 215.2 MA/CM^2) (Figure 53). The average operating life decreased from 2107 to 933 hours by changing the matrix material from asbestos to PKT (Figure 54). An interaction between current density and matrix material has a significant effect on the fuel cell life. The last term in the equation, ± 115.1 hours, represents the standard error of the estimate. It is expected that 68% of the data will fall within this interval.

Five cell tests were completed through the second refurbishment. The least-square regression equation for the time to the second refurbishment is:

$$\text{Time to second refurbishment} = 2032.5 - 530.0\,X_5 - 217.5\,X_4 \pm 65.2$$

Again, current density and matrix material are shown to affect time to refurbishment with the low level for these variables and should be used in order to maximize the number of hours before cell failure. A decrease in the average operating life from 2345 to 1430 hours was exhibited as the matrix material was changed from asbestos to PKT (Figure 55.)

Variable	Correlation Coefficient
X_1	-0.46
X_2	0.67
X_3	0.34
X_4	-0.71
X_5	-0.41
X_1X_2	-0.33
X_1X_3	-0.45
X_1X_4	0.29
X_1X_5	0.37
X_2X_3	0.30
X_2X_4	-0.15
X_2X_5	-0.22
X_3X_4	-0.41
X_3X_5	-0.35
X_4X_5	0.34

Figure 52 Correlation Coefficients

Recommended Additional Tests

If NASA wishes to further optimize cell performance it is recommended that the planned block of 18 tests be completed. This will allow use of the Yates method of analysis from which a plan for a second experimental test series can be developed. The 18 tests are as follows:

Test Number	Factor Combination	Test Number	Factor Combination
1	c d	10	c e
2	a d	11	d e
3	a e	12	b c
4	b c	13	a b d e
5	a c d e	14	b d
6	b e	15	b c d e
7	a b c d	16	(Low)
8	d e	17	a b
9	a b c e	18	a c

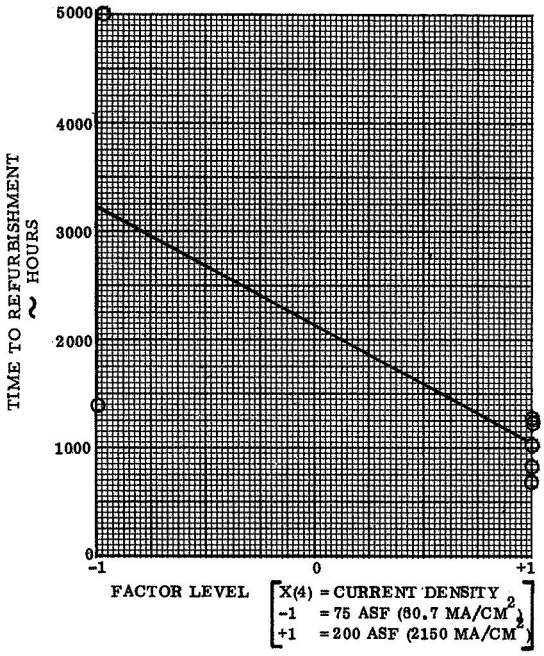

Figure 53 Effect of Current Density on Average Fuel Cell Time to First Refurbishment

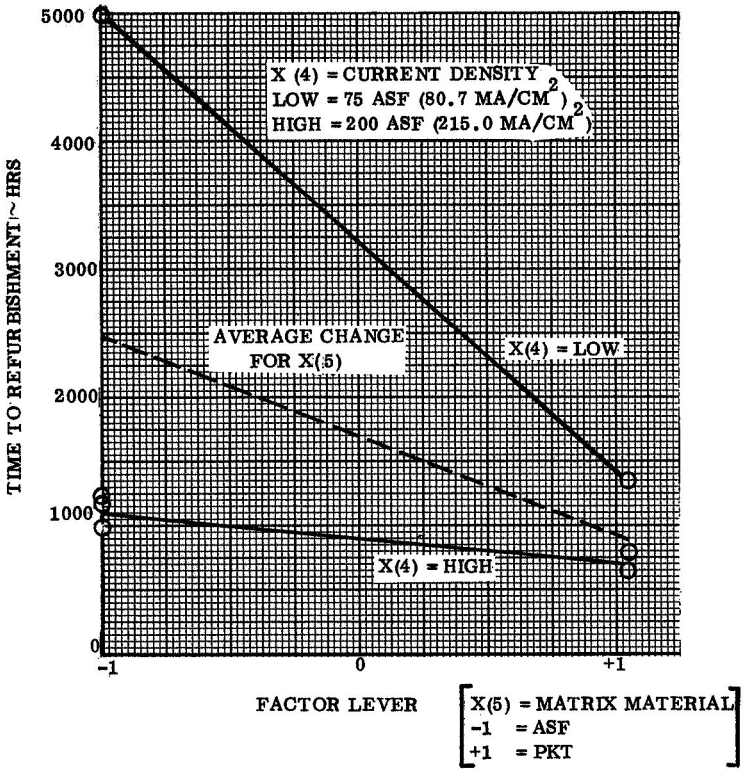

Figure 54 Effect of Matrix Material on Time to First Refurbishment

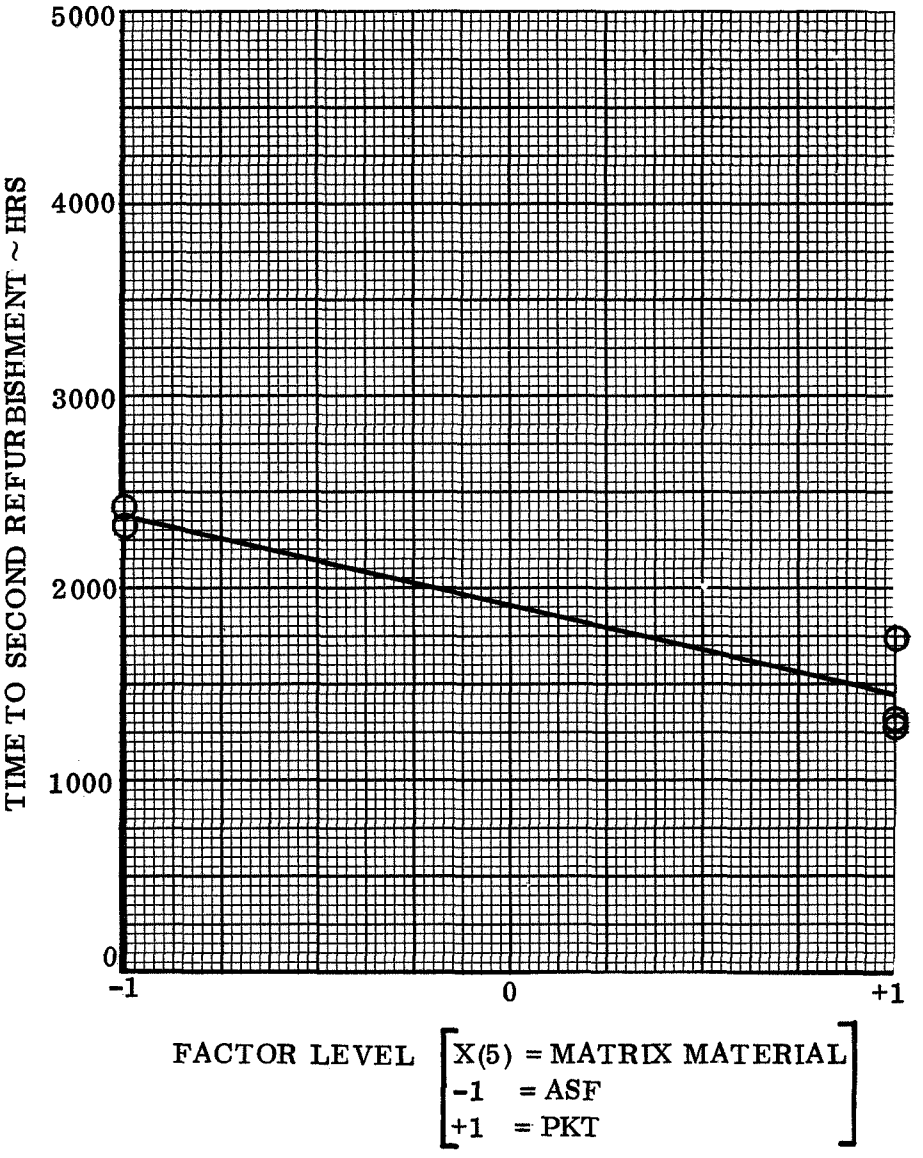

Figure 55 Effect of Matrix Material on Time to Second Refurbishment

VIII. DISCUSSION OF RESULTS

The primary cause of cell degradation was found to be reduction of electrolyte volume. This volume reduction results primarily from carbonation which increases the water vapor pressure over the electrolyte causing an increase in concentration. Electrolyte carbonation is due to contaminants in the reactant gases and corrosion of cell structural materials. Loss of electrolyte also contributes to volume reduction. It is believed that KOH is lost to voids in the cell frame and possibly to the PKT matrix material. All of the performance loss of cell number 7 was restored by simply wetting up the cell to increase electrolyte volume. The solids in this cell's electrolyte were 27% K_2CO_3 by weight.

The design of a cell can influence its tolerance to electrolyte volume change. Cell number 7 was especially sensitive to electrolyte volume changes due to its 30 mil (0.762 MM) thick matrix. The load changes in the simulated space shuttle load profile caused electrolyte volume changes which caused voltage fluctuation. Although the longest life cell, Number 4, used a 30 mil (0.762 MM) matrix, this volume sensitivity reduced the operating life of some 30 mil (0.762 MM) matrix cells. More complex fuel cell system controls may be required to maintain precise control of the operating environment for this cell configuration.

The high power density cell design is not affected by electrolyte volume change because it maintains a fixed electrolyte interface in the electrodes and thus is not subject to the decay associated with volume reduction. This is demonstrated by high power density cell test number 1 run in conjunction with this program. This cell has run for over 6000 hours without decay despite exposure to the same carbonation sources as the sinter-screen cells run under the contract. The same reactant supply with 6 to 10 ppm of hydrocarbons was used as was the conventional fiberglass-epoxy laminated frame.

An important factor investigated in this program is the effect of reactant contaminants on cell life. Four parts per million of carbon dioxide was added to the oxygen supply for certain tests. In addition, 6 to 10 ppm of hydrocarbons were present in the oxygen supply to all cells. Cell number four in this program ran 5000 hours without decay or refurbishment. This cell used oxygen with 6 to 10 ppm of hycrocarbons and 4 ppm of carbon dioxide and experienced 43 percent conversion of its electrolyte to potassium carbonate without adverse effect. In actual fuel cell system applications the reactant contamination should be below these levels because the carbon dioxide can be scrubbed to less than 1 ppm. In addition, spacecraft propulsion grade reactants supplied from cryogenic tanks will probably have less than 6 ppm hydrocarbon contamination.

Only a part of the total electrolyte carbonation observed can be explained by contamination in the cells tested indicating that there is an internal source of carbonation. Cell number four, for example, had 43 percent conversion to carbonate but only 15 percent can be accounted for by the reactant contaminants even if all the contaminants are converted to carbonate. P&WA sponsored corrosion tests have shown that the glass fiber and epoxy cell frame is the only cell component contributing to electrolyte carbonation. The quantity of carbonate formed was similar to that found in cell tests. The results of these tests are summarized in Figure 56. The amounts of material exposed were similar to that in an actual cell. The data shown includes the result of a corrosion test on Arylon, a polyaryl ether which shows promise as a carbonate-free cell frame material. Other cell structural materials candidates are listed in Figure 57.

Electrolyte carbonation data was obtained from many of the cell tests just prior to each refurbishment. The effect of operating temperature and time on carbonation due to frame corrosion is illustrated in Figure 58. This figure shows the millimoles of K_2CO_3 formed in cells run with maximum electrode temperatures of 176°F and 212°F (80° and 100°C). The quantity of K_2CO_3 attributed to the 4 ppm of CO_2 added to the oxygen supply of certain cells is not included in this data. Significantly larger amounts of K_2CO_3 were formed in the higher temperature cells. This Figure also shows the result of a P&WA sponsored open circuit test in which a cell was held at normal operating temperature but without load and without reactant flow. This cell had the same amount of electrolyte carbonation as those run with reactant flow indicating that the primary source of carbonation is material corrosion within the cell. The internal corrosion masked the effect of the variable carbon dioxide level in the oxygen supply.

Post test analysis of electrolyte has also revealed a decrease in the potassium inventory. This potassium loss contirbutes to reduction of the electrolyte volume and resultant cell voltage decay. The loss of potassium can be due to absorption of electrolyte by the cell structural materials and reaction with the PKT matrix. The possibility of expulsion of electrolyte from the cell into the reactant passages was discounted after tests of the by-product water accumulating in a condenser downstream of the cell in the hydrogen loop showed no alkalinity. In addition, no electrolyte was found during inspection of the hydrogen and oxygen lines leaving the cells and liquid traps in the oxygen purge lines.

Microscopic examination of cell frames revealed that some sections of the glass fiber laminate are not completely impregnated with the epoxy bonding agent, thereby leaving some voids within the frame which are separated from the electrolyte by thin epoxy films. A breach in the epoxy film through oxidation in the presence of electrolyte will permit electrolyte access to the glass fiber and the voids within the frame. Use of alternate structural materials in the cell should substantially reduce if not eliminate the reaction with electrolyte.

The observed loss of potassium has been greater in cells using a PKT matrix than in ones using asbestos implying that a reaction with the matrix is taking place. Reaction with PKT can be explained by a change in the chemical structure of the material. PKT can have the form $K_2Ti_6O_{13}$ or $K_2Ti_4O_9$. If the form changes from a hexatitanate to tetrantitanate in the fuel cell an absorption of potassium will take place in accordance with the following relationship:

$$2K_2O{\cdot}6TiO_2 + 2KOH \rightarrow 3K_2O{\cdot}4TiO_2 + H_2O$$

Each cell test in the program included refurbishment of the cell by flushing it with fresh electrolyte. This was accomplished without removing the cell from its test hardware by filling the reactant gas cavities with fresh electrolyte, allowing the solution to equilibrate, and draining the excess. This procedure was similar to that which would be used for refurbishing the cell stack in a fuel cell system. Because electrolyte degradation is the primary decay mode, this refurbishment technique restores cell performance and extends cell life. Refurbishment experience is summarized in Figure 59. Cell tests number 1 and 7, for example, had their initial performance fully restored and operating life doubled by refurbishment. The second refurbishment of each cell restored part of the performance lost during endurance running after the first refurbishment. The success of the second refurbishment indicates that operating life could be extended further by additional refurbishments. However, refurbishment

may not be necessary to meet the life goals of future spacecraft fuel cell systems. There are several reasons for this. Even with propulsion grade reactants, compact scrubbers can remove carbon dioxide down to less than 0.5 ppm. Hydrocarbon contamination should be less than 6 to 10 ppm experienced by all the cells in this program if the reactants are drawn from cryogenic tanks. This is due to the low vapor pressure of hydrocarbons at cryogenic temperatures. Improved cell frame materials should practically eliminate electrolyte carbonation due to internal corrosion. Finally, the high power density cell design minimizes the effect of volume reduction on performance.

Pigmentary Pottassium Titanate (PKT) matrix material was included in the program as the alternate to asbestos. This matrix material promises improved long term corrosion resistance at high temperatures and superior bubble pressure. Cells using PKT in this program, however, have decayed much more rapidly than those with asbestos matrices. Post-test analysis of a high power density cell with a PKT matrix run in conjunction with this program revealed poisoning of the anode. The test history of this cell is shown as the lower curve in Figure 60. This cell experienced voltage decay from the time it was started until the anode was oxidized after 1920 hours of operation. The anode oxidation resulted in a gain of 44 millivolts indicating a significant amount of poison was oxidized. This gain was lost almost immediately as the poisons again accumulated on the anode. The anode oxidation was repeated at 2760 load hours with similar results. It was suspected that a reaction had occurred between the PKT and the silver plating used in the electrodes. Similar interaction was observed in earlier tests of cells using PKT matrix material and silver-mercury cathodes. Titanium has been found on the electrodes of cells using PKT matrices which suggests that titanium is the poisoning agent and explains why asbestos matrices don't experience this degradation. A high power density cell with a PKT matrix and using gold in place of the silver on the electrodes and cooling plates was started to evaluate this theory. The test history of this cell is shown as the upper curve in Figure 60. This cell has accumulated over 920 hours with only a few millivolts decay indicating that the anode poisoning problem has been eliminated by using gold in place of silver.

An electrolyte fill tube, a novel device for injecting additional electrolyte into an operating cell, was suggested by NASA-LeRC to reduce the time and cost involved in electrolyte volume optimization. The fill tube concept was reduced to practice in this program and the fill tube was installed on each cell tested. Electrolyte was successfully added to an operating cell. Some difficulties were experienced, however, with weakening of the cell frame which in at least one case led to gas crossover at the area in which the tube was inserted. The electrolyte fill tube is discussed in Appendix A.

One of the variables evaluated in the program was carbon dioxide content of the oxygen. The high level of CO_2 was 4 ppm. Premixed, bottled gas for these tests would have been prohibitively expensive. NASA suggested that a mixing valve be used to blend CO_2 into the oxygen supply in the required proportions. The special mixing valve was furnished by NASA and performed in a satisfactory manner. The CO_2 level is monitored with a LIRA gas analysis device and is easily maintaining at 4 ppm. The CO_2 mixing valve is discussed in Appendix B.

Test Conditions: 500 hours

Oxygen environments

42% KOH

250°F (121.1°C)

Material	K_2CO_3 formed - grams
Asbestos - PKT	0
J. M. Asbestos	0
Epon - Fiberglas laminate	1.5
Neoprene	0
Hypon adhesive	0
Arylon	0
Electrode assembly segment including	0

- nickel sinter
- Arylon frame
- Hypon adhesive
- screen cathode
- asbestos matrix

Figure 56 Laboratory Corrosion Tests

Material	Probable Maximum Design Temperature	Status
Polyaryl Ether	250°F (121.1°C)	Used in Advanced Cells
Polyaryl Sulfone	250°F (121.1°C)	Immersion Testing
Polybutadiene	250°F (121.1°C)	Immersion Testing
Polyphenyl Oxide	200°F (93.3°C)	Experimental Cells
Polyphenyl Sulfide	250°F (121.1°C)	Immersion Testing
Polypropylene	250°F (121.1°C)	Immersion Testing
Polysulfone	250°F (121.1°C)	Experimental Cells
Abs	200°F (93.3°C)	Experimental Cells

Figure 57 Base Cell Structural Materials

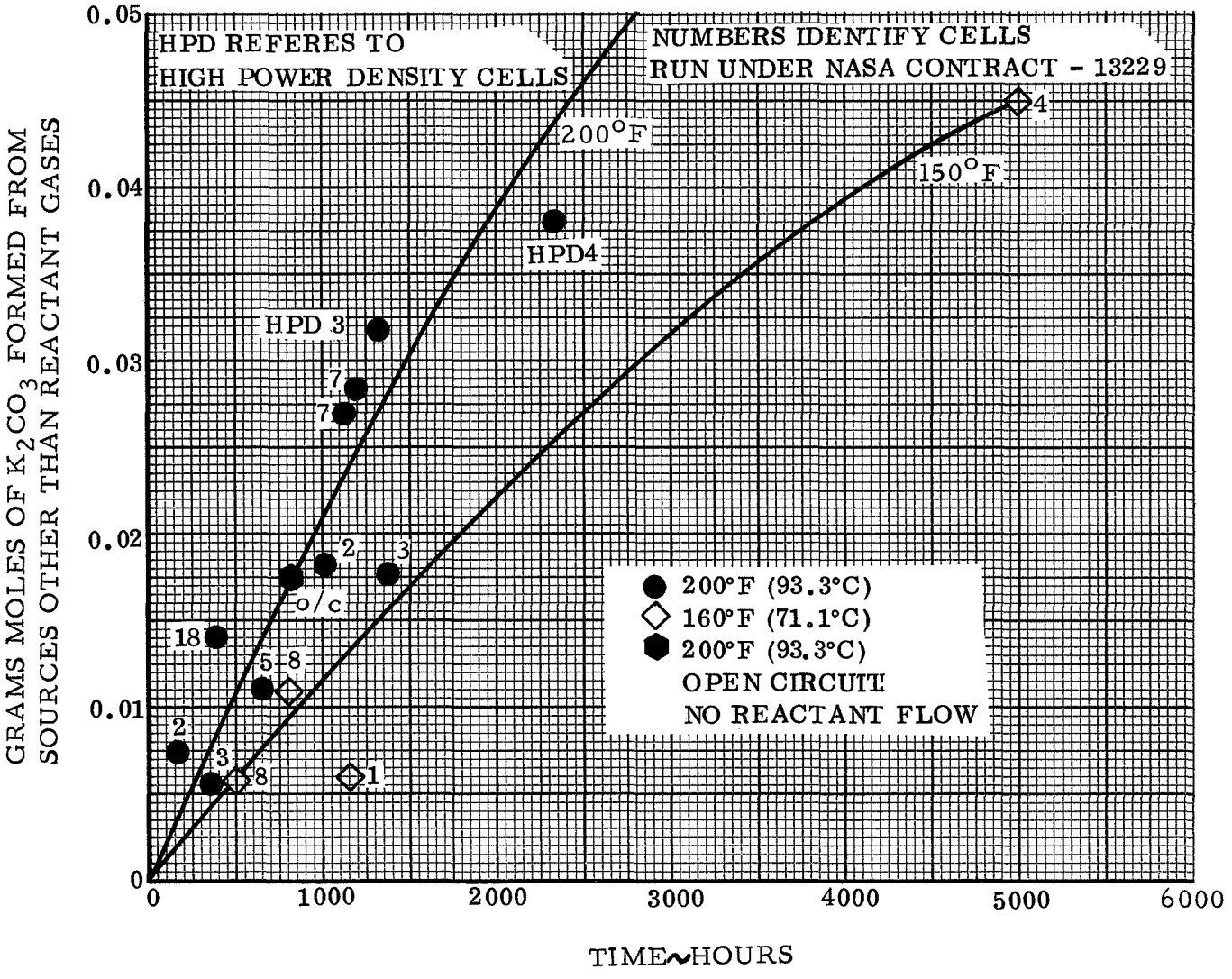

Figure 58 Effect of Temperature on Carbonate Formation in Cells With Fiberglass-Epoxy Frames

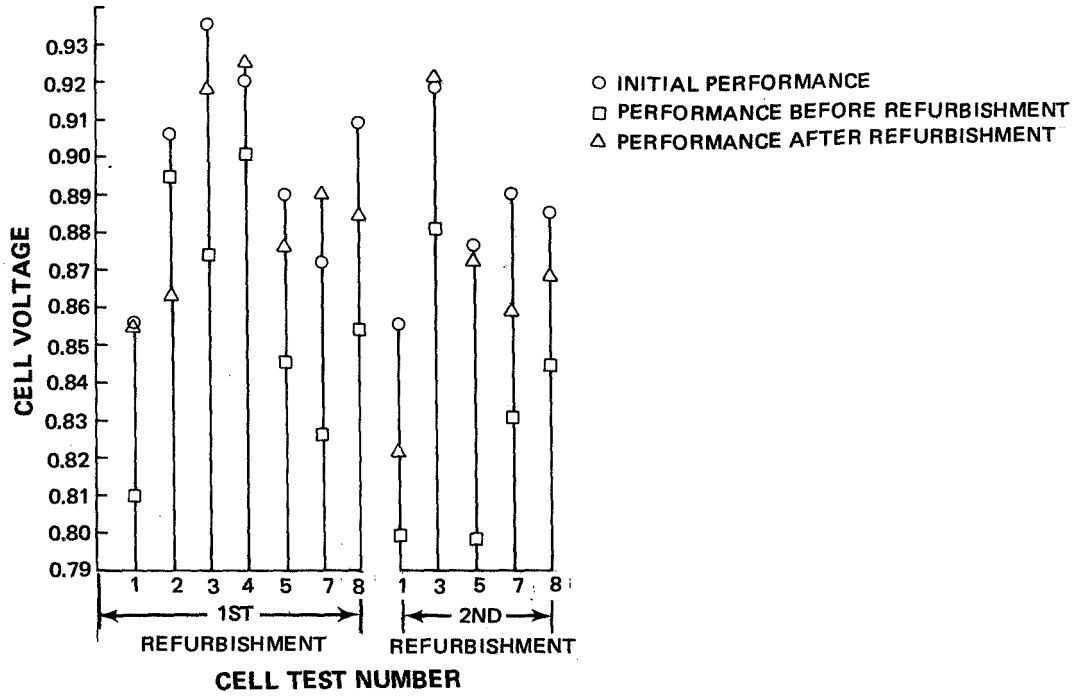

Figure 59 Refurbishment Experience

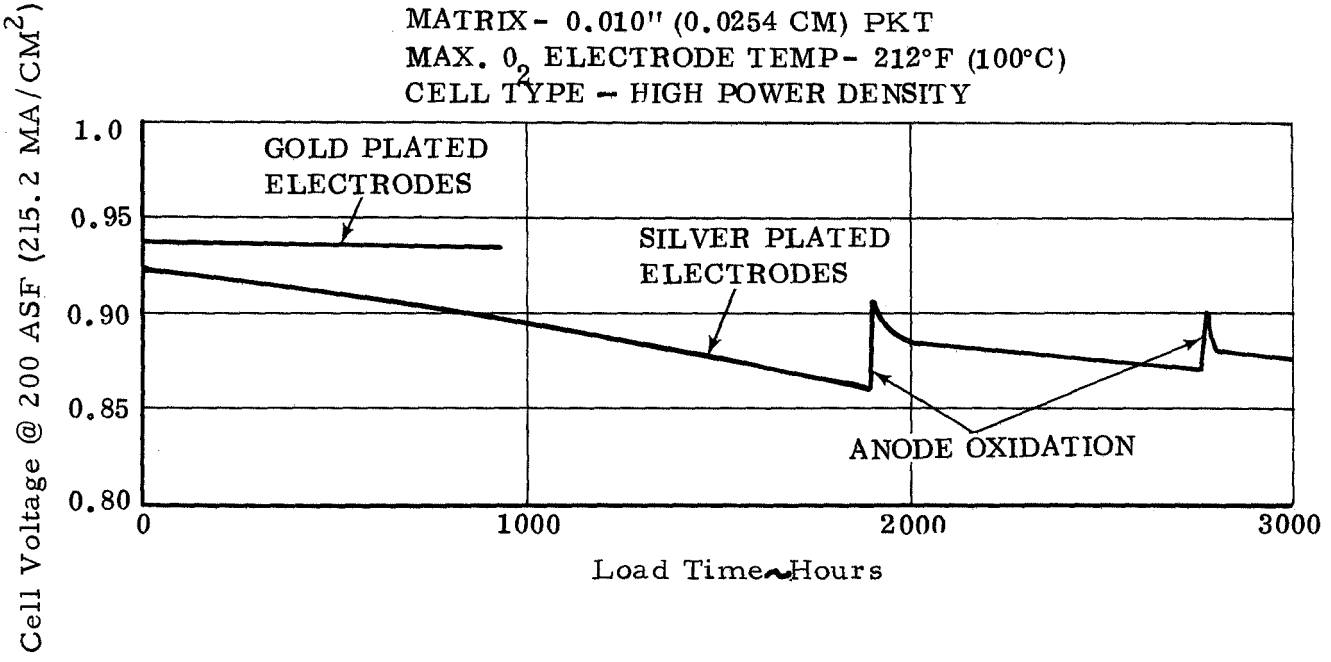

Figure 60 Cell Test History With PKT Matrix and Gold Plated Electrodes

IX. CONCLUSIONS

Alkaline electrolyte, hydrogen/oxygen, matrix-type fuel cells were tested on a simulated shuttle load cycle to investigate the effect of design and operating factors on performance and life. This experimental program provides a data base for the design of matrix-type fuel cells suitable for use in systems with nominal power output of 5 KW and an operating life of one year. Conclusions from this program are itemized below:

1. The matrix fuel cell has potential to meet the one year life goal.

2. Corrosion of the glass fiber-epoxy laminate cell frame presently used limits cell life by causing electrolyte carbonation and absorption of electrolyte into the frame. Low operating temperature reduces the frame corrosion and extends life. The use of inert frame materials such as the plastic polyaryl ether should also reduce carbonation from this source.

3. Propulsion grade reactants, if allowed to enter the cell unscrubbed, contribute a small fraction of the electrolyte carbonation.

4. Low current density is important in achieving long life with low voltage decay because the voltage loss due to a given amount of cell degradation is proportional to the current density.

5. Cell refurbishment by flushing an assembled powerplant stack with fresh electrolyte can restore performance and extend operating life.

6. The use of potassium titanate matrix material causes rapid voltage decay due to anode poisoning. This can be overcome by substituting gold for silver plating in the cell electrodes.

X. APPENDICES

APPENDIX A

Electrolyte Fill Tube Tests

Precise control of electrolyte concentration and volume in a cell requires fine adjustment of the quantity of electrolyte in the cell after initial fill. This adjustment is best accomplished by adding electrolyte to the cell while it is mounted in the test stand and operating. An exploratory test program was undertaken to evaluate the practicality of an electrolyte fill tube.

A small diameter capillary tube was inserted into the edge of a unitized electrode hardframe. A syringe was connected to the other end of the tube. This arrangement is shown in Figure 61. A close-up of the tube inserted in the cell frame is shown in Figure 62. Several additional holes are visible in this frame.

In the first fill tube test a cell with a capillary tube and syringe attached was tested at low pressure conditions. A dewpoint tolerance curve was generated with the initial electrolyte fill. Then, a known quantity of electrolyte was injected into the cell and the dewpoint excursion was repeated. The optimum electrolyte volume could not be located after the initial fill. Therefore no conclusion could be drawn as to the effectiveness of the injection. Inspection of the cell after disassembly indicated that the electrolyte had entered the electrode assembly.

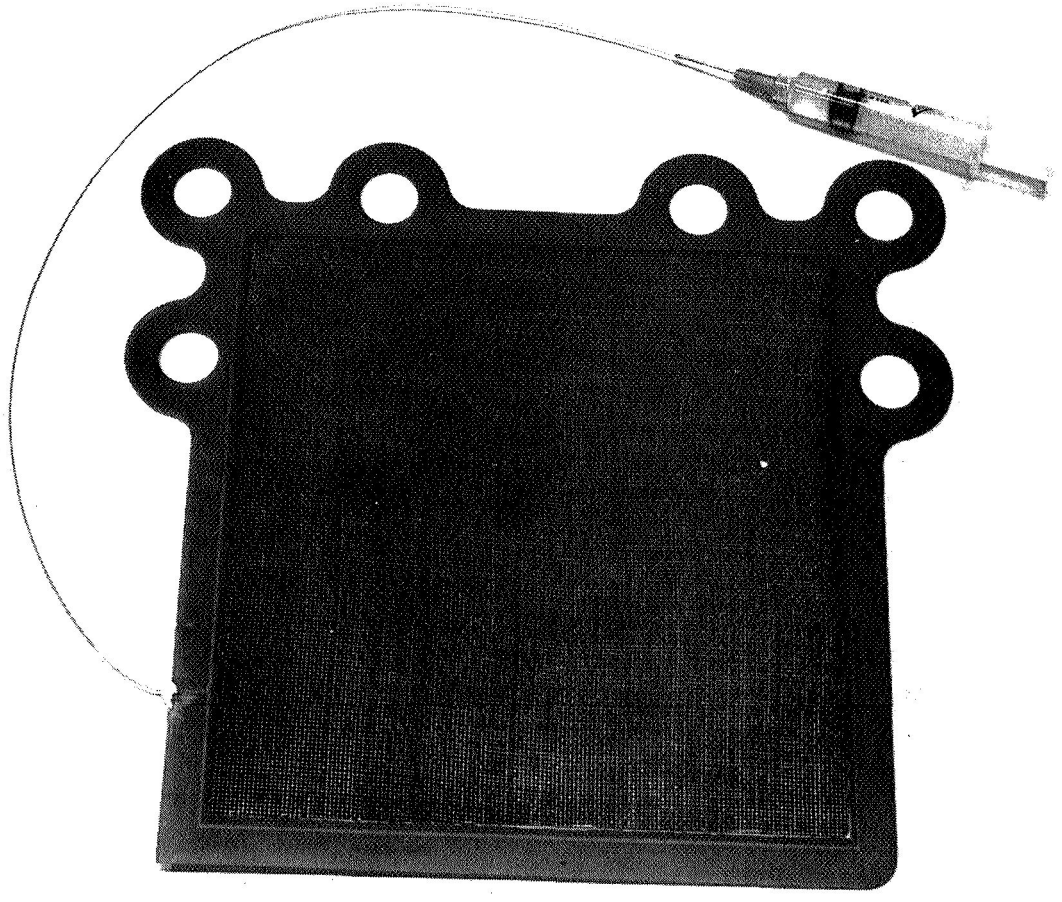

Figure 61 Electrode Assembly with Capillary Tube and Syringe, W680

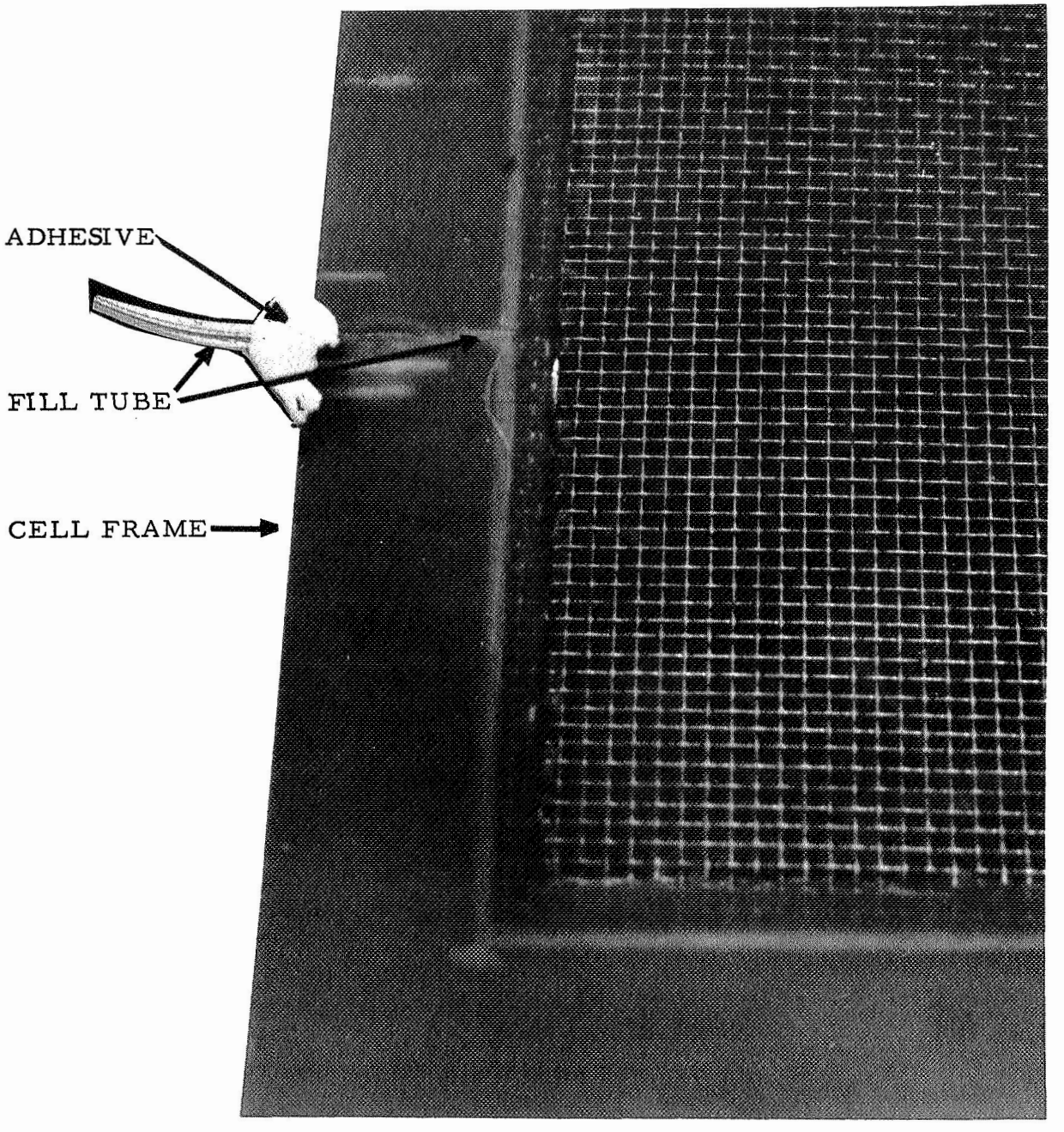

Figure 62 Corner of Electrode Assembly with Capillary Tube Inserted, W681

The second cell of the series was also tested under low pressure conditions. After running a dewpoint excursion to establish the initial optimum volume point, electrolyte was injected into the cell through a capillary tube attached to the cell. The addition of the electrolyte caused a shift in the point of optimum volume to a higher electrolyte concentration. (Figure 63). This shift was somewhat larger than the calculated value. However, the change in cell performance around the optimum volume point was very small, which makes the location of the exact point uncertain.

The third cell in the series was tested under high pressure conditions. As in the previous two cells, an initial dewpoint excursion was run to establish the optimum volume location. Then a calculated amount of electrolyte was injected into the rig which shifted the optimum volume point to a new location (Figure 64).

With the successful completion of these tests, all cells in the test program were modified to include a fill tube.

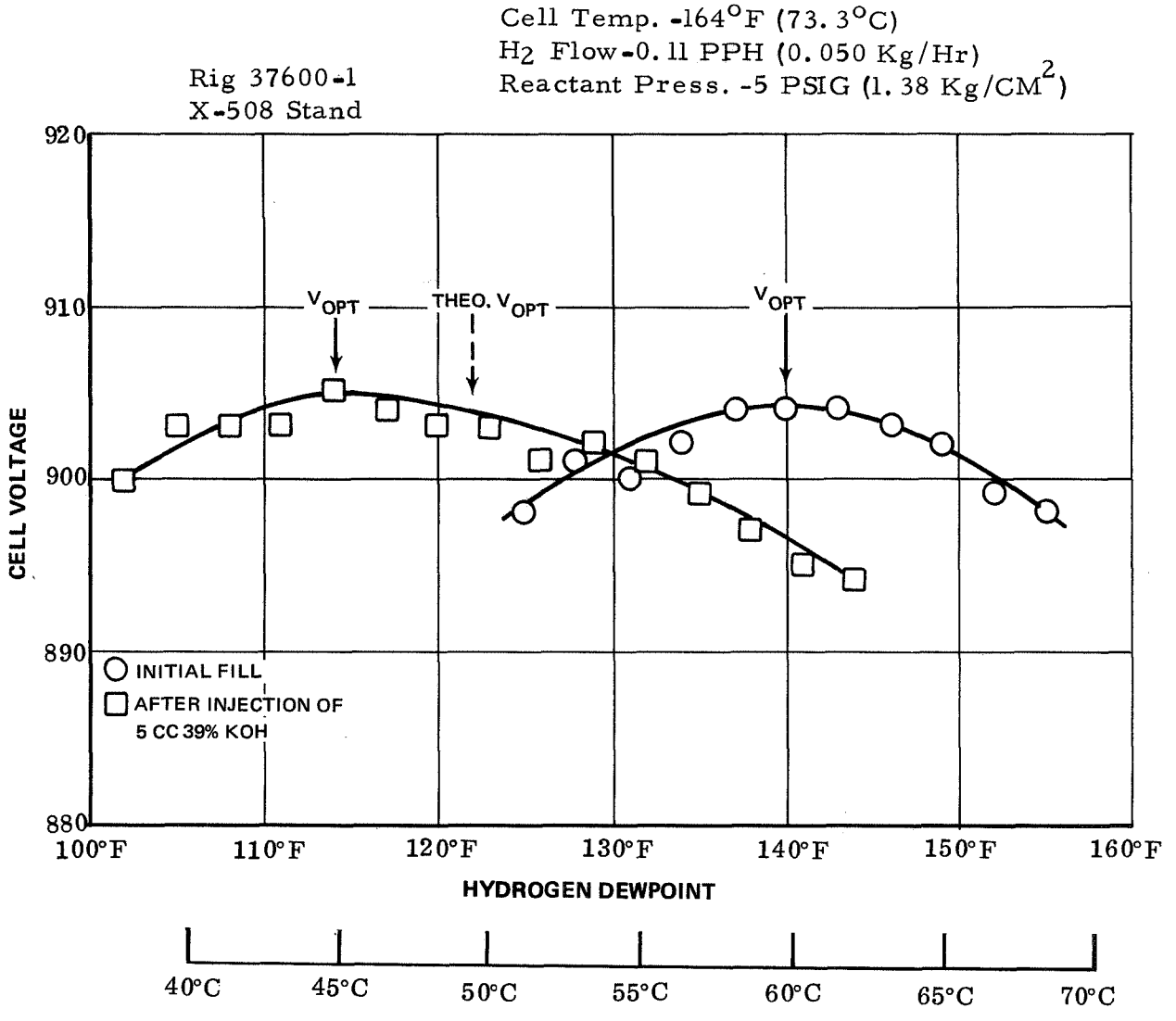

Figure 63 Electrolyte Fill Tube Test - Shift in optimum electrolyte Dew Point

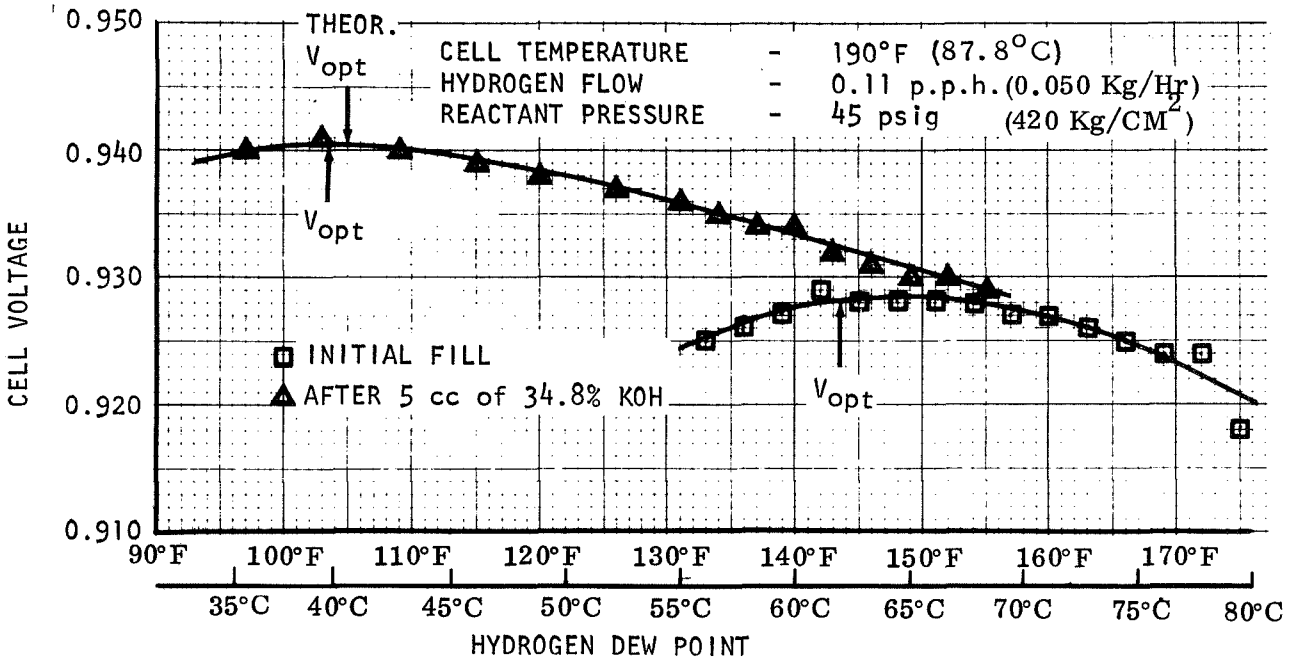

Figure 64 Electrode Fill Tube Test - Shift in optimum electrolyte Dew Point

APPENDIX B

Carbon Dioxide Mixing Valve

The high level of carbon dioxide in the test program requires that four parts per million of CO_2 be added to the oxygen supply. On-site mixing of the CO_2 and oxygen reduces cost significantly; premixed gases are very expensive. At NASA's suggestion, a government furnished special mixing valve was installed in the oxygen supply of the test stand, (Figure 65). The valve can be seen in the lower left corner of the photograph. After a period of testing and development this valve provided a controlled mixture of 4 ppm of CO_2 in the oxygen and operated faultlessly throughout the program.

The mixing valve was installed under the immediate supervision of Dr. Thaller during his visit on January 29, 1970. Initial testing revealed it was not possible to obtain a 4 ppm mixture. The valve was moved closer to the LIRA gas analysis device and eventually 5 ppm CO_2 mix for up to 12 hours without adjustment was accomplished. A skilled operator required one to two hours to adjust the valve. Both the valve setting and the CO_2 supply pressure were used to provide mixture adjustment. Small adjustments were most easily made with the CO_2 supply pressure.

All testing was done with an 80 psig oxygen supply. The pressure drop across the CO_2 mixing valve was varied from (0.1406 to 2.109 Kg/CM^2) 2 to 30 psi and the valve setting from 60 to 40. From the start of testing, it was necessary to gradually close the valve to obtain the same flow conditions.

To improve mixture control and stability, a diluted CO_2 supply was substituted for the pure CO_2 supply. A supply of premixed gas containing 1000 ppm of CO_2 in oxygen resulted in stable operation at 4 ppm of CO_2 in the oxygen supply. Only two bottles of this premixed gas have been needed for the program.

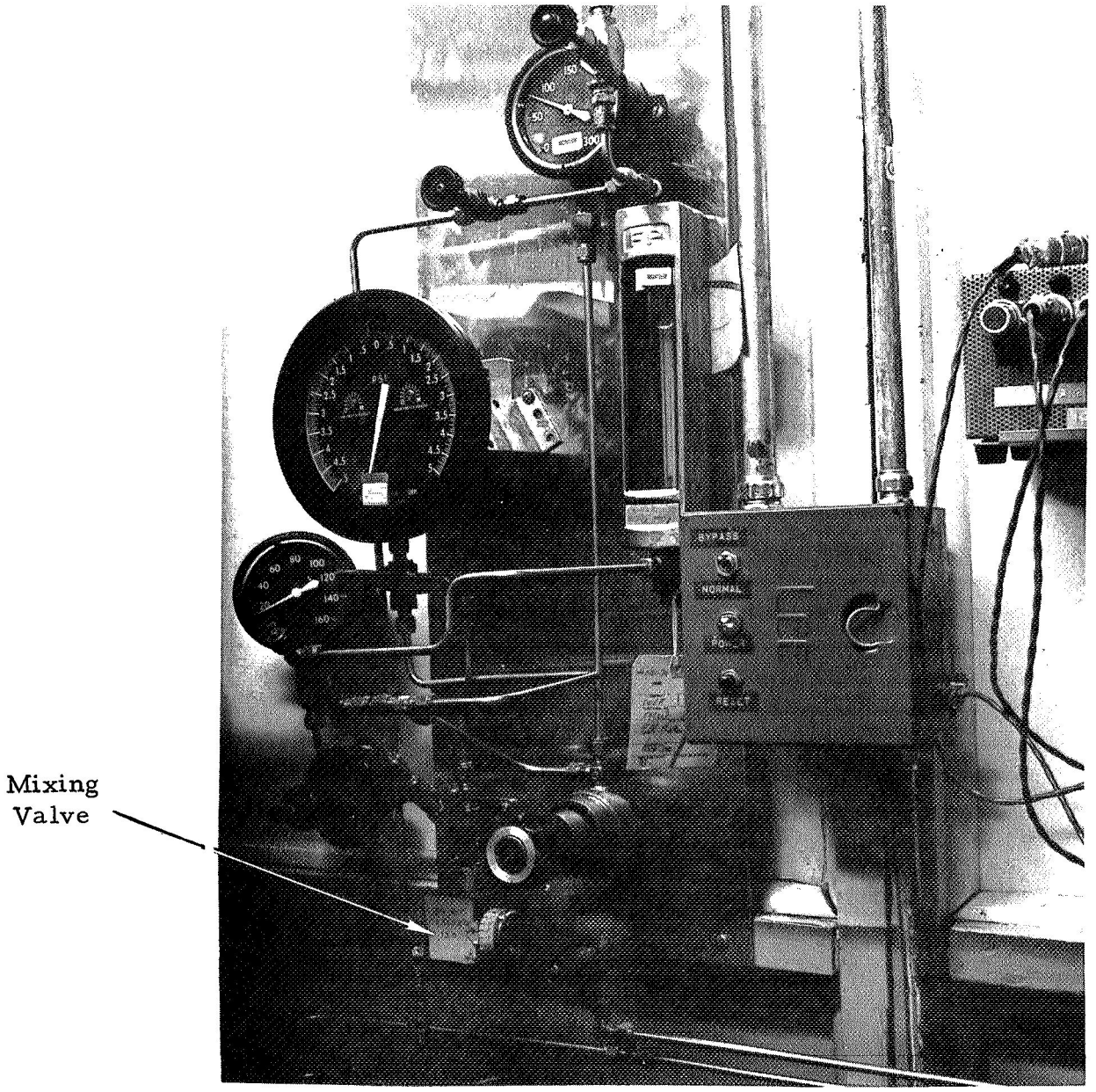

Figure 65 Carbon Dioxide Mixing Valve Installation